PENNSTATE

1855

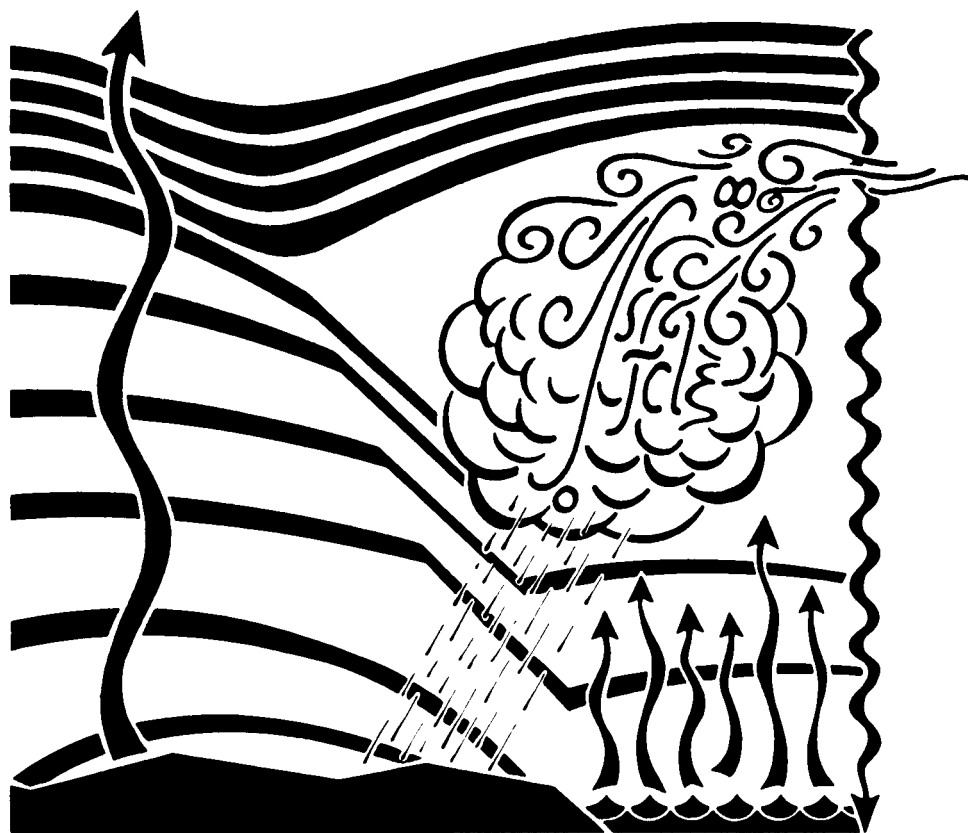## DEPARTMENT OF METEOROLOGY

Final Technical Report for NASA Grant NAG8-050

entitled

"Combined VHF Doppler Radar and Airborne (CV-990) Measurements
of Atmospheric Winds on the Mesoscale"

from

Christopher W. Fairall

and

Dennis W. Thomson

The Pennsylvania State University
114 Kern Building
University Park, PA 16802

Final Technical Report for NASA Grant No. NAG8-050

entitled

Combined VHF Doppler Radar and Airborne (CV-990) Measurements
of Atmospheric Winds on the Mesoscale

Submitted to:

National Aeronautics and Space Administration

Submitted by: *C. W. Fairall*

Christopher W. Fairall
Associate Professor
Department of Meteorology

Dennis W. Thomson
Professor
Department of Meteorology

April 1989

ABSTRACT

Hourly measurements of wind speed and direction obtained using two wind profiling Doppler radars during two prolonged jet stream occurrences over western Pennsylvania were analyzed. In particular, the time-variant characteristics of derived shear profiles were examined. To prevent a potential loss of structural detail and retain statistical significance, data from both radars were stratified into categories based on location of the jet axis relative to the site. Low-resolution data from the Penn State radar at Crown, Pennsylvania, were also compared to data from Pittsburgh radiosondes.

Profiler data dropouts were studied in an attempt to determine possible reasons for the apparently reduced performance of profiling radars operating beneath a jet stream. Increased outages were found at the level of maximum wind, where backscattered power is reduced because of the lesser shear near the jet stream maximum. But performance did not appear to be dependent upon jet stream location. Rather, cosmic interference was shown to be the major cause of reduced performance at upper levels for the Crown 50 MHz system.

Temperature profiles for the Crown site were obtained using an interpolated temperature and dewpoint temperature sounding procedure developed at Penn State. The combination of measured wind and interpolated temperature profiles

allowed Richardson number profiles to be generated for the profiler sounding volume.

Both Richardson number and wind shear statistics were then examined along with pilot reports of turbulence in the vicinity of the profiler. The calculated Richardson numbers, which depend on the square of the wind shear, were shown to be highly dependent upon the spatial resolution of the radar data. Although an empirical relation between the occurrence of clear air turbulence and profiler-derived wind shear and Richardson number statistics could not be obtained from one profiler and the less than three weeks of data, the results indicated that such might be possible. Profiler-based critical shear values could then be used for the detection of clear air turbulence and possibly for determinations of the severity of the turbulence.

TABLE OF CONTENTS

TABLE OF CONTENTS (continued)

LIST OF TABLES

LIST OF FIGURES

LIST OF FIGURES (continued)

LIST OF FIGURES (continued)

LIST OF FIGURES (continued)

ACKNOWLEDGEMENTS

I am deeply grateful for the support provided by many people during the course of the thesis research. The following list includes a few, but by no means all of the people whose suggestions, criticisms or assistance were greatly appreciated.

Special thanks are due to Dr. Dennis W. Thomson. His support was outstanding. Never was there a shortage of ideas, nor was there a lack of equipment on which to test the ideas. Dr. Thomson was largely responsible for providing an atmosphere that was conducive to academic and professional development.

I also wish to thank Dr. Gregory S. Forbes for his assistance with the synoptic aspects of this study, and his extra help during the preliminary stages of the work. Mr. Arthur A. Person, along with Dr. Forbes, provided invaluable advice concerning software development on the VAX 11/730 computer. Dr. Christopher W. Fairall, Mr. Bao-Zhong Duan and Mr. James B. Edson provided the necessary literature and critical assistance that made calculations of energy spectra possible. Dr. John J. Cahir provided suggestions that proved to be fundamental for the wind shear studies in this research.

Mr. Scott R. Williams provided critical profiler data, hands-on experience with profilers and some good advice that made the work much easier. Mr. Michael T. Moss and Mr.

Robert M. Peters kept me on the right track when research became difficult. Ms. Leslie Laskos and Mr. Theodore A. Messier patiently endured my tirades during the times when I was sure that there would be no sinners in this world if they were simply threatened with eternal life in graduate school. Their understanding is greatly appreciated.

1.0 INTRODUCTION

Meteorological investigations of the jet stream date back to some of the earliest upper-level balloon observations. Actually, there are several jet stream phenomena that have been observed in different regions of the atmosphere. Of principal interest to meteorologists are those which are evident at midlatitudes at tropopause heights: the subtropical jet and the polar front jet (Gage, 1983). "Classical" synoptic scale analyses of jet stream structure include Reiter (1963) and Palmen and Newton (1969).

The location of jet streams can vary greatly from day to day. The paths of the jet streams follow planetary waves and show varying degrees of structure. This day-to-day variation plays an important role in the structure and evolution of many tropospheric storms.

Jet streams tend to be more pronounced during the winter when meridional temperature gradients are greatest. The polar front jet is generally found between 40 and 60 degrees north latitude; it is farthest north during the winter. The subtropical jet is usually located near 30 degrees north, but both the polar front and subtropical jet streams show a pattern distorted by standing planetary waves. There is an out-of-phase relationship between the troughs and ridges of the two jet streams. Japan and the eastern United States are regions where the two tend to combine and as a consequence jet streams in these locations are particularly strong. The strength of the wintertime

case discussed in this thesis appears to be a result of such a merging of two such jet streams.

1.1 An Overview of the Jet Stream and State of Knowledge of Wind Speed, Wind Shear and Richardson Number Profiles

Thermal wind theory dictates that horizontal temperature gradients produce vertical wind shears. Globally, lower temperatures toward the poles produce increasingly strong westerlies with height. Generally the strongest winds are associated with strong horizontal temperature gradients, frontal zones, either at the surface or aloft.

Upper-level frontal zones, also known as internal fronts or upper-tropospheric fronts, slope downward from the tropopause through the middle and upper troposphere as shown in figure 1.1. These fronts are usually associated with upper-level troughs and are important because clear air turbulence develops in their vicinity due to the resulting large vertical wind shear and associated low Richardson numbers (Emanuel, 1984). Jet streams are found on the warm sides of these fronts, usually just below the tropopause, since a reversal of the temperature gradient occurs in the stratosphere.

Until recently, information about upper-level structure and wind speed profiles had been obtained primarily by aircraft and radiosondes. Figure 1.2 illustrates a "vertical" velocity profile obtained using a Sabreliner research aircraft during the descent path shown in figure 1.1.

However, serious limitations exist with both aircraft

ORIGINAL PAGE IS
OF POOR QUALITY
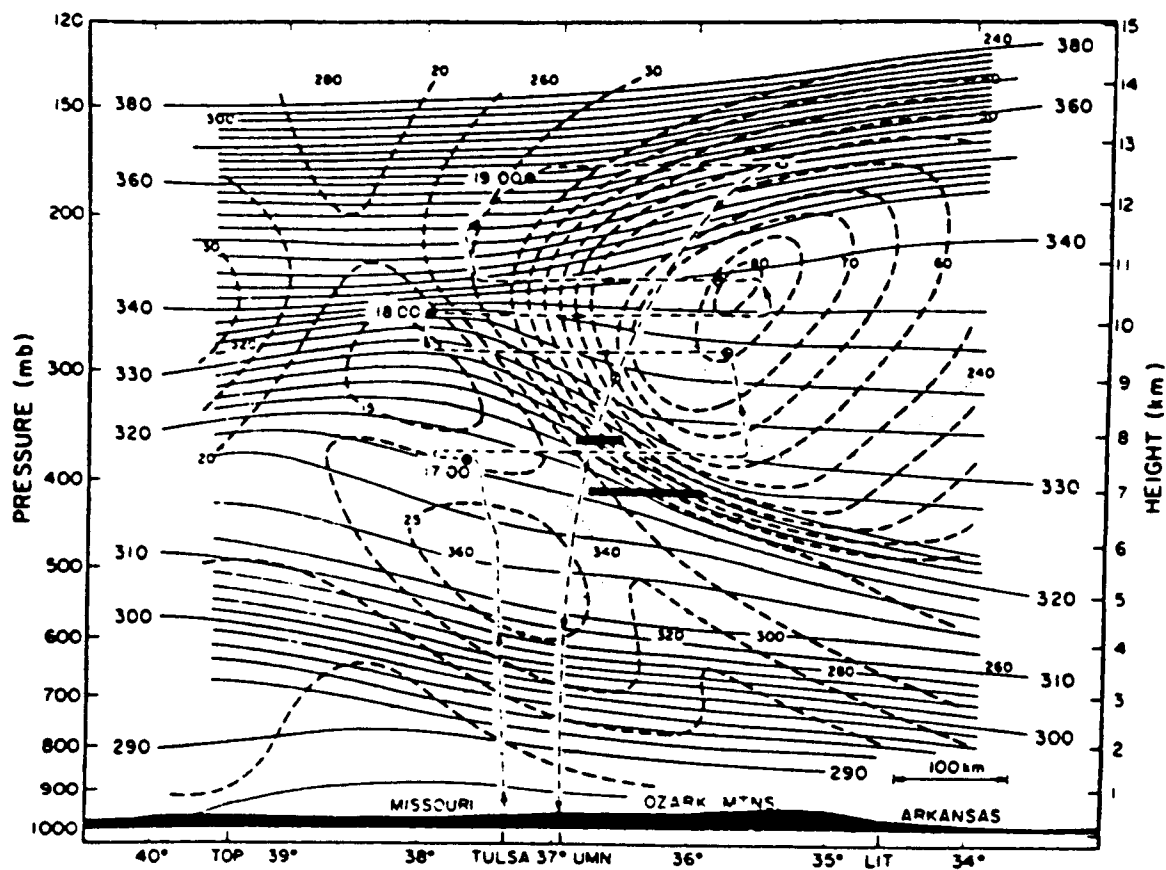
Figure 1.1.   Cross section of potential temperature (K, solid lines) and wind speed (ms^{-1}, dashed lines) (Kennedy and Shapiro, 1980). Note the descent path (light dashed line) of the Sabreliner.
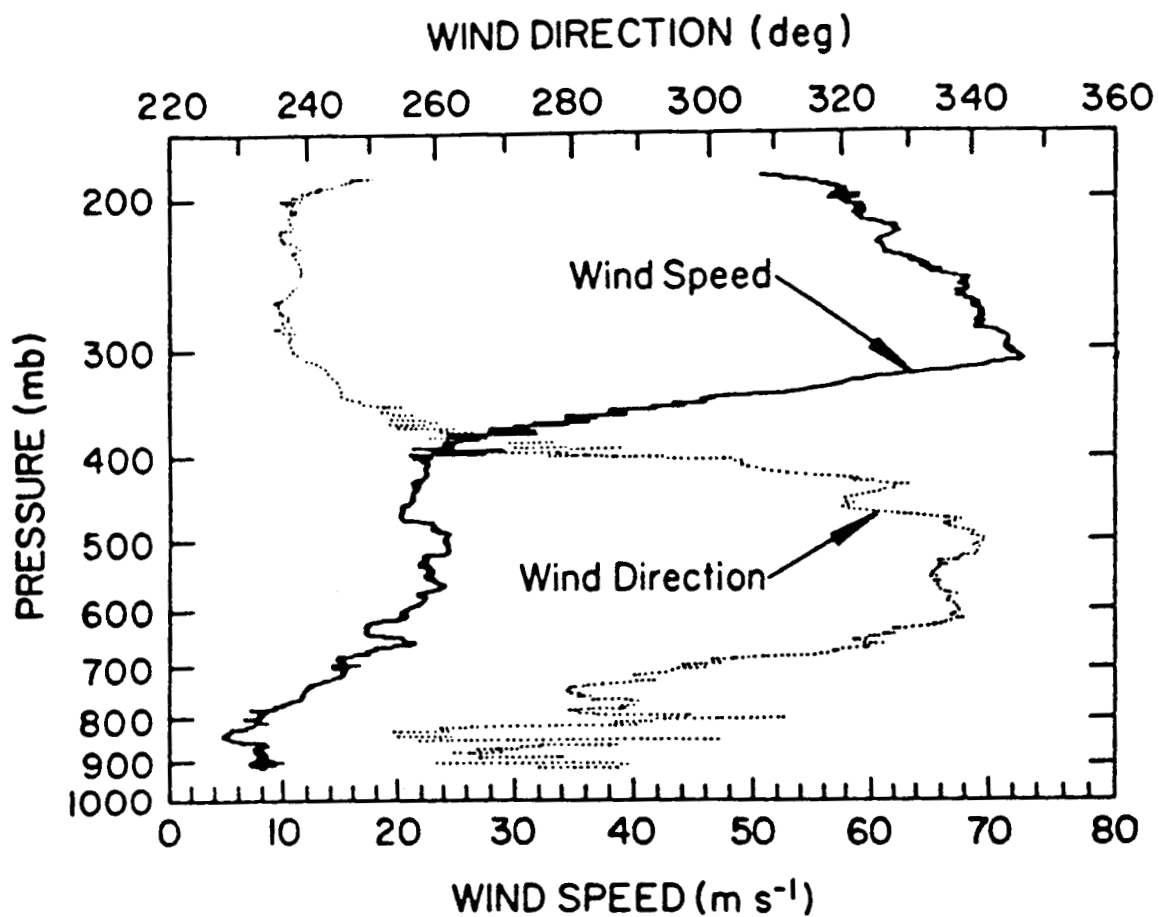
WIND DIRECTION (deg)

Figure 1.2. Sabreliner sounding of wind speed and direction obtained during the descent path shown in figure 1.1 (Kennedy and Shapiro, 1980).

and balloon data. Kennedy and Shapiro (1980) state that vertical shear measurements by aircraft in turbulent zones are quite uncertain. They found an average Richardson number of 0.71 in turbulent zones using aircraft data. Theory states (Dutton, 1976) that the local Richardson number must be less than or equal to 0.25 for turbulence to be produced. Underestimation of the vertical shear using aircraft probably occurs as a consequence of the basically "horizontal" flight path. Figures such as 1.2 are somewhat misleading. The wind profile of figure 1.1 was actually obtained over a nearly 200 km horizontal distance. Thus a true vertical wind profile was not being observed.

Balloon data is also far from ideal. A true vertical velocity profile can not be obtained using a balloon because it drifts with the wind. In fact, during strong jet stream episodes, the balloon may even be blown beyond the radio horizon before a complete sounding is obtained. Tracking errors, self-induced balloon motions, and imperfect balloon response (Keller, 1981) also detract from data quality. Turbulent layers, often only one or two hundred meters thick, are often not detected from the balloon since resolution of the processed data is generally much poorer than this. Also, since the balloon travels with the wind it will tend to "ride along" with the unstable gravity waves which may be responsible for the turbulence.

Keller states that the existence of a turbulent shear layer cannot be reliably and unambiguously inferred from an

in situ radiosonde vertical wind profile. He concludes by stating that radiosondes cannot be used to infer existence of clear air turbulence in situ, thusly they can not be used to infer its intensity. As a consequence of such uncertainties in data quality, and in the derived wind shear, Richardson number profiles are rarely produced.

Wind profiling Doppler radars have tremendous potential for examination of jet stream and turbulence structure. Hourly or even finer temporal resolution enables in-depth study of jet stream passages and mesoscale structure, especially when data from two or more profilers can be studied.

1.2 Wind Profiling Doppler Radars

"Profiling" Doppler radars measure velocities by means of the Doppler shift of the signal scattered from turbulent irregularities (on the scale of half the radar wavelength) in the atmospheric refractive index. Velocities determined by the radars have been shown to be consistent with velocities obtained by rawinsondes (see e.g., Gage and Clark, 1978). Studies at Penn State using special research radiosondes (Williams, 1986; personal communication) during light to moderate winds have clearly established that radiosonde winds are consistent with radar observations. In fact the general quality of the radar data is so good that it can now be used for quantitative studies of the limitations of conventional rawinsonde measurements.

Doppler radars operate at a wide range of frequencies. For continuous observations of "clear-air" echoes, radar frequencies from 50 MHz to 400 MHz are currently preferred. Cosmic noise and radio frequency spectrum considerations weigh heavily against frequencies below 50 MHz. Echoes from precipitation may interfere with observations of turbulence at frequencies above 400 MHz (Balsley and Gage, 1982). Williams even found substantial precipitation contamination on one of the 50 MHz Penn State profilers during a heavy thunderstorm on 26 July, 1985. However, because the duration of the heaviest rain was less than 20 minutes, the "standard" hourly averaging techniques (section 1.2.1), had they been in use, would most likely have filtered out the precipitation contamination.

The Penn State stratosphere-troposphere (ST) radars at Crown, and the "Shantytown" system sited near McAlevy's Fort, Pennsylvania, operate at a frequency of 49.8 MHz with a peak power of 30 kW. The antennas are 50- by 50-meter colinear-coaxial phased arrays. Each radar aquires data in two modes of operation with pulse widths of 3.67 and 9.67 us, respectively. The "low" mode obtains velocity profiles up to about 8 km MSL at 290 m altitude resolution, while the "high" mode obtains profiles up to just above 16 km MSL at 870 m resolution. Both modes profile down to about 1.6 km MSL; the site elevation at McAlevy's Fort is 0.25 km, and at Crown it is 0.5 km (Thomson, Fairall and Peters, 1983).

1.2.1 Hourly Averaged Wind Profiles

In the two-dimensional operating mode, twenty-four observations are made of the (u, v) wind components at each height (range gate) during a total data acquisition time of approximately 48 min. Twelve measurements are made with a 3.67 μs pulse duration, and twelve are made with 9.67 μs pulses. The 2-D wind components are measured simultaneously. Data are sampled at range intervals of two-thirds of the pulse width: 290 m resolution for the low mode, 870 m resolution for the high mode. Data acquisition and spectral computations start on the hour and last for about 48 min; about two minutes are required for spectral averaging and consensus statistical processing. The final ten minutes of the hour are set aside for telephone communication with one of the meteorology department's VAX computers. Figures 1.3 and 1.4 illustrate the time sharing between the two modes and the details of how time is spent during each mode.

As indicated above, following the 48-minute observation period, the u and v components for each height are averaged using a random sample consensus method (Strauch et al., 1983). The radial velocities of the twelve observations at each height are examined to find the largest subset of data points whose mean radial velocities are within approximately 4 ms^{-1} of each other. If the largest subset is four or more, the average of the subset is taken as the mean radial velocity during the 48-minute observation period. If the largest subset is less than 4 the data are discarded.

Calculate profiles
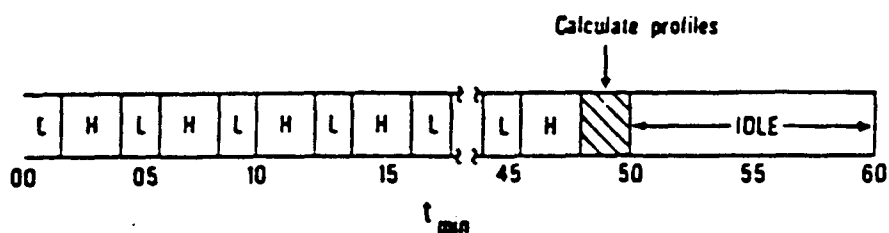
Figure 1.3. Hourly sequence of wind observations with 3-μs
pulses (L) and 9-μs pulses (H) (Strauch et al.,
1983).
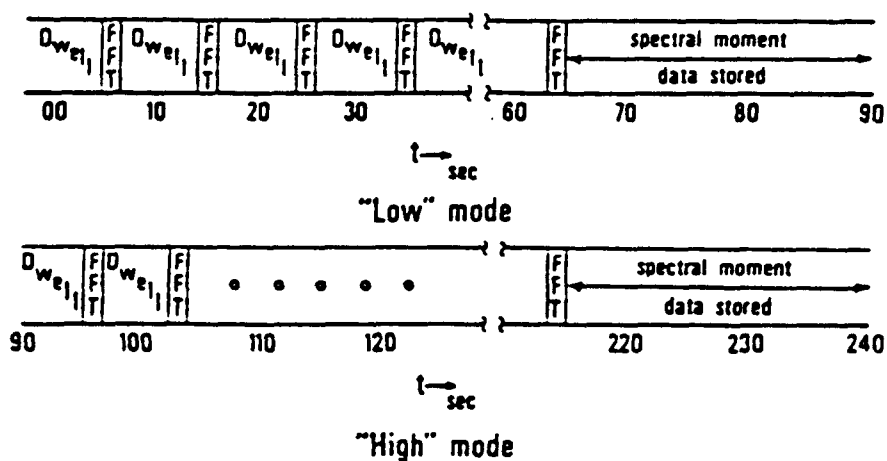
Figure 1.4. Details of temporal averaging during the 3-μs
"low" mode and the 9-μs "high" mode of
operation (Strauch et al., 1983).

Please note that this procedure was not implemented during the second case discussed in this thesis. During it the minimum consensus was set equal to 1.

1.2.2 Interference

Different kinds of interference may cause problems with the proper detection and analysis of atmospheric signals obtained using VHF (30-300 MHz) or UHF (300-3,000 MHz) radars. These may be separated into passive and active contributions.

Passive contributions are present in the receiving system even without the transmitter being switched on. These contributions include: noise from the receiver/ antenna system, cosmic noise, noise from the earth's surface, noise from the atmosphere and man-made interference. Man-made sources include signals from communication and broadcast transmitters, ignition and machine noise. Passive contributions have different effects depending on the operational frequency of the radar. For VHF radars, cosmic noise is the main problem, while man-made sources of interference are strongly dependent on site location.

Active contributions are due to scatter and reflection of the transmitted radar signal from unwanted targets, usually referred to as "clutter." Clutter can come from: fixed targets on the earth's surface such as mountains, buildings or power lines, surface waves on bodies of water, cars, aircraft, ships, satellites, the moon, planets and

sun, atmospheric turbulence and ionospheric irregularities. Several methods are used to eliminate or suppress clutter as the data are processed. It turns out that proper site selection is the first important step toward eliminating as many such problems as possible (Röttger, 1983).

1.2.3 Advantages of Wind Profilers

The combination of proper site selection, antenna and receiver design, and carefully tailored data filtering techniques can produce data of excellent quality. As will be evident to the reader, the data used for this study were clearly superior to conventional radiosonde data.

One obvious advantage of radar wind measurements is the rate at which profiles can be obtained. In as little as two minutes a wind profile can be obtained to altitudes in excess of 16 km. For this study hourly profiles were deemed sufficient.

Hourly profiles are useful for jet stream studies for at least two reasons. Temporal resolution is obviously much better than that of National Weather Service 12-hourly radiosonde launches. Also, because of the averaging procedure (discussed in section 1.2.1), hourly profiles are actually "mean" profiles. Most interference values have been eliminated. If a radiosonde profile includes bad data, there could easily be a 24-hour or greater gap before the error can be evaluated and rectified.

Detection of clear air turbulence is possible using Doppler radars because turbulent irregularities in the refractive index of the atmosphere scatter the incident radio energy. Mean profiles of the refractivity turbulence structure constant, c_n^2, can, thusly, be used to determine turbulence probabilities (VanZandt, Gage and Warnock, 1981). In this thesis, however, we focus only on wind shear and Richardson number profiles.

1.3 Clear Air Turbulence

Free air turbulence can be generated by either convection or vertical wind shear. Clear air turbulence (CAT) is defined as shear turbulence, whether it is cloudy or not (Panofsky and Dutton, 1984). It is well-established that significant CAT events are almost exclusively associated with statically stable layers possessing strong vertical shears. Keller (1981) showed that large shear is generally associated with large static stability. If static stability is large, shear can become large before dynamic instability develops. For lesser stability, vertical shear can be readily dissipated by turbulence. Keller stated that the most important factor (at the mesoscale) in determining the probability of turbulence within a given atmospheric layer appeared to be the magnitude of the shear within the layer.

Clear air turbulence is a multi-million dollar problem for the commercial air transport community. Costs of aircraft repairs after turbulence encounters, crew training

on the subject of turbulence, discomfort and injuries to passengers and crews, diversions to avoid turbulence, and implementation of ground organizations designed to detect and forecast turbulence added up to more than $20 million in 1964 alone (Lederer, 1966). Intangibles such as work missed by disgruntled passengers were not considered in Lederer's study.

The existence of CAT is usually attributed to the Kelvin-Helmholtz (K-H) instability within the shear zones which are generally associated with the jet stream. Coexistence of internal gravity waves and instabilities appears consistent with observed cases of CAT. Unstable shear zones may radiate internal gravity waves and these waves may supplement or even take the place of K-H instability in explaining CAT (Lindzen, 1974).

The growth rate of instability within a shear layer depends upon the height of the shear layer, its character- istic Brunt-Vaisala frequency and the vector shear. The magnitudes of these parameters are largely determined by the synoptic motion field, but lower troposperic gravity wave sources such as thunderstorms or mountains may provide additional sources of momentum to atmospheric shear layers (Keller, 1981).

Regions of CAT may be as much as 400 km long by 5 km deep, but in general appear to be of the order of a few kilometers long by a few hundred meters deep. Time scales of CAT apparently range anywhere from a few minutes to a few

hours. Colson (1969) indicates that CAT is more likely to be found near curved segments of the jet stream. Reiter (1969) observes that the average size of CAT patches suggests the origin of the turbulence lies in the mesostructure of the atmosphere which defies analysis and forecasting from the macroscale tool of radiosonde observations.

Internal fronts, also breeding grounds for CAT, are formed in the atmosphere when external forces deform a layer of air, across which there is a change in wind velocity and potential temperature (Dutton and Panofsky, 1970). As the front strengthens, the spacing between isotachs and isentropes is reduced (refer to fig. 1.1), thus the numerator and the denominator of the Richardson number (Ri) will be increased. The numerator is proportional to only the first power of the potential temperature gradient, while the denominator, which represents the rate of production of turbulent energy by the wind shear, depends on the square of the wind shear. It follows that the net effect is to reduce Ri. The more pronounced the front is, the smaller Ri will be.

Theory dictates that turbulent energy can grow rapidly only if Ri is less than 0.25 (Dutton, 1976). Observations seem to indicate that turbulence cannot be maintained if Ri is greater than about 0.5 to 1.0. However, the greatest difficulty lies in our ability to measure Ri in any given small layer. Values as determined by radiosondes are too coarse, actual Richardson numbers may be much smaller than

those computed from the data (Colson, 1966). Because of the virtual impossibility of measuring to vertical resolutions sufficient to achieve theoretical results, critical Richardson numbers from about 0.7 to 1.0 are considered valid for the generation of CAT (Colson, 1966; Kennedy and Shapiro, 1980).

The Richardson number may only be used qualitatively for the separation of turbulent from non-turbulent flows. The actual value is not necessarily a measure of CAT intensity. In the past the same comment has been made with respect to any critical value of wind shear. Profiler technology promises to make this statement less certain, some developments could soon make it a falsehood.

Intensity of turbulence is difficult to assess because the data to date has been so highly qualitative and subjective. Aircraft factors such as airspeed, wind loading, attitude and configuration have an effect on the handling of the aircraft in turbulent flow. Pilot factors include personal opinion and training. Severe turbulence reported by one pilot may be considered moderate by another. To help quantify turbulence, aircraft turbulence criteria were developed in May 1957 by the NACA Subcommittee on Meteorological Problems. Table 1.1 lists the criteria. These criteria eliminated some of the subjectivity of pilot reports, but did not make allowances for the aircraft factors described above.

Table 1.1 Aircraft turbulence criteria (NACA Subcommittee
on Meteorological Problems, May 1957).

Transport Aircraft Turbulence Criteria

Adjectival Class	Descriptive
Light	A turbulent condition during which occupants may be required to use seat belts, but objects in the aircraft remain at rest.
Moderate	A turbulent condition in which occupants require seat belts and occasionally are thrown against the belt. Unsecured objects in the aircraft move about.
Severe	A turbulent condition in which the aircraft momentarily may be out of control. Occupants are thrown violently against the belt and back into the seat. Objects not secured in the aircraft are tossed about.
Extreme	A rarely encountered turbulent condition in which the aircraft is violently tossed about, and is practically impossible to control. May cause structural damage.

1.4 Radiosonde Measurements During Strong Winds

Although radiosondes are adequate for many meteorological applications, significant errors can occur for wind measurements in the upper troposphere and above. These errors are related to the low-elevation angles that result when the radiosonde balloon is carried down range in strong wind conditions. In instances where wind speeds exceed 70 or 80 ms^{-1}, and the measurements become more uncertain, observers often report missing winds. This deficiency of the observing/analysis system may also contribute to wind profiles that eliminate high-frequency wind variations, and result in underestimations of the magnitude of maximum winds in jet cores and reduced values of the vertical wind shear (Ucellini et al., 1986).

It will be shown that while missing data is a problem with radiosondes during high winds, profilers actually perform quite well under these conditions. Results from a study of profiler data dropouts are presented in chapter 4.

1.5 Statement of Purpose and Chapter Summary

Hourly wind speed and direction observations taken by the wind profiler located at Crown, Pennsylvania, during two jet stream passages are compared to conventional rawinsonde data. Properly filtered profiler data is shown to be of quality superior to that obtained by radiosonde. The high temporal resolution of the profiler allows detailed observation of wind profiles in the vicinity of the jet

stream. It appears that the finer temporal resolution and improved quality of data obtained by wind profilers can be used for the development of critical wind shear criteria for the detection of clear air turbulence.

Chapter 2 contains the details of a synoptic classification scheme used to arrange the data from the two case studies in this thesis according to the location of the jet axis relative to the wind profiler. This data stratification was necessary for the determination of statistical differences in data values and quality brought about by jet stream location relative to the site. Specifics of each case such as the number of hours of data, amount of time that Crown and Pittsburgh were near the jet stream, and general wind patterns are also discussed.

Chapter 3 contains descriptions of a profiler data filter designed by the author and an interpolated temperature and dewpoint temperature sounding process, chiefly designed by A. L. Miller. An interpolated sounding was produced at Crown to facilitate the calculation of Richardson numbers above the site. The procedures used to calculate wind shears and Richardson numbers are also detailed in chapter 3.

Results of the data analyses are presented in the fourth chapter. The final chapter contains a brief summary of results and some suggestions for future research.

2.0   CASE SELECTION

Initially, the scope of this thesis research project was far more broadly defined than may be evident from the emphasis and organization of this thesis. It was not obvious that "cases" would be as well defined as they were and, hence, it was necessary to begin compiling a large data base. In the end the most essential part of that data base consisted of four hundred sixteen hours of data taken during jet stream passages in mid-November 1986 and mid-January 1987 at Crown, Pennsylvania. Radiosonde observations from Pittsburgh taken every twelve hours during those periods were also archived for later analysis.

Southwesterly flow was desired in order to perform comparison studies on Crown and Pittsburgh data. Because Crown is located to the northeast of Pittsburgh, southwest flow would place both stations in similar locations relative to the jet axis. This is advantageous for the stratification scheme implemented for the data. More than 300 hours of data were identified during the periods when wind direction satisfied this criterion.

2.1   Stratification of the Data Sets

Each case contained at least 200 hours of data. Because fluctuations in jet stream position occurred during that time it was necessary to further stratify the data set. Cases were chosen for the purpose of grouping the data on

the basis of the jet stream location relative to the site. We believed that treatment of the data sets as single homogeneous ensembles could lead to loss of resolution and erroneous interpretation of the governing physical processes. Thus, observations taken north of, south of, under, and far away from the jet stream, as it moved with respect to the radar, were averaged and compared to establish whether or not statistically significant differences would be evident.

The classification scheme used stems from an extensive one which had been earlier designed by the author to enable evaluation of radar performance with respect to meteorological conditions. In the original scheme twelve categories were used to classify the meteorological conditions. Four surface, five upper-air, two cloud, and a mesoscale influence category provided the basis for the stratification. One category, "position relative to jet stream axis," was the basis used for the stratification of the data analyzed for this thesis. Table 2.1 contains the complete classification scheme used by the author to evaluate meteorological conditions for four Colorado profilers and the Shantytown site for much of the period from May 1984 through April 1986. The scheme consisted of 14 columns of numeric data, with values in any column of "0" representing missing data or "9" representing data which was not applicable.

Table 2.1 Complete weather classification scheme used for
          profiler performance studies.

Classification Scheme

Column 1: Surface circulation type
           1 = low (cyclonic), 2 = high (anticyclonic), 3 =
           neither

Column 2: Location relative to surface circulation center
           1 = NW, 2 = SW, 3 = SE, 4 = NE, 5 = circulation
           center

Column 3: Surface frontal type
           1 = warm, 2 = cold, 3 = occluded, 4 = no front
           present, 5 = low pressure trough

Column 4: Location relative to surface front
           1 = warm side, 2 = cold (dry) side, 3 = within
           frontal zone, 4 = not within 300 km of front, 5 =
           ahead, 6 = behind (occlusion or trough)

Column 5: Upper-level wave category
           1 = northerly wind maximum, 2 = trough, 3 =
           southerly wind maximum, 4 = ridge, 5 = zonal
           flow, 6 = split flow center (very weak height
           gradient), 7 = cutoff low within 300 km (two or
           more closed contours at 200 or 300 mb), 8 = light
           and variable flow

Column 6: Position relative to jet streak
           1 = left front, 2 = right front, 3 = left rear,
           4 = right rear, 5 = no streak present

Column 7: Upper-level front type
           1 = cold, 2 = warm, 3 = occluded, 4 = no front
           present

Column 8: Location relative to upper-level front
           1 = ahead, 2 = behind, 3 = within frontal zone,
           4 = not near front

Column 9: Position relative to jet axis
           1 = left (0-150 km), 2 = right (0-150 km), 3 =
           left (150-300 km), 4 = right (150-300 km), 5 =
           greater than 300 km, 6 = under jet axis, 9 = jet
           streams of equal strength to right and left of
           station, neither dominates

Table 2.1 (continued)

Column 10: Cloud type
1 = clear, 2 = shallow convection, 3 = deep convection (Cb), 4 = low stratiform, 5 = middle, 6 = high, 7 = layered

Column 11: Position relative to solid, large cloud area
1 = NW (0-150 km), 2 = NE (0-150 km), 3 = SE (0-150 km), 4 = SW (0-150 km), 5 = NW (150-300 km), 6 = NE (150-300 km), 7 = SE (150-300 km), 8 = SW (150-300 km), 9 = no cloud areas within 300 km of station or station under cloud area of type determined from column 10, 11 = no cloud area within 300 km of station (if clouds reported at station), 22 = cloud areas in two or more quadrants within 300 km

Column 12: Mesoscale influences
1 = cold air damming, 2 = mesoscale convective complex, 3 = squall line, 4 = tropical disturbance, 5 = none detected, 6 = mesohigh, 7 = mesolow (indicates presence of a thunderstorm complex of undetermined type- no satellite data)

Column 13: 200 mb wind direction (nearest 10 degrees)

Column 14: 300 mb wind direction (nearest 10 degrees)

2.2 Case Specifics

Both cases analyzed consisted of very strong jet stream
events. Wind speeds in excess of 200 miles per hour were
measured during peak hours by both the Crown profiler and
the Pittsburgh radiosonde. As figures 2.1 and 2.2
illustrate, the January 1987 jet stream occurrence was
stronger and better-defined than the one in November 1986.

Specifically, the first case occurred during a 200-hour
period from 7 through 14 November 1986. Peak wind speeds
were slightly greater than 80 ms^{-1}; the most common
direction was southwesterly. The second passage covered a
216-hour period from 15 through 23 January 1987. Peak wind
speeds exceeded 90 ms^{-1}; the wind direction was generally
from the west to southwest. Data was stratified into five
categories based upon station location relative to the jet
axis. Jet axis position was estimated by evaluation of the
300 and 200 mb upper-air maps in conjunction with potential
temperature cross sections taken perpendicular to the mean
wind, when they were available. Sometimes the wind fields at
300 and 200 mb differed substantially and potential
temperature cross sections were either missing or
inconclusive. At these times it was not possible to fix the
exact jet axis locations. Figure 2.3 illustrates the 200
and 300 mb isotach analyses for 12 UT, 16 January 1987.
Note that it is essential to watch for missing observations
during high wind conditions. The isotach analyses may be in
error when substantial balloon data losses occur at upper
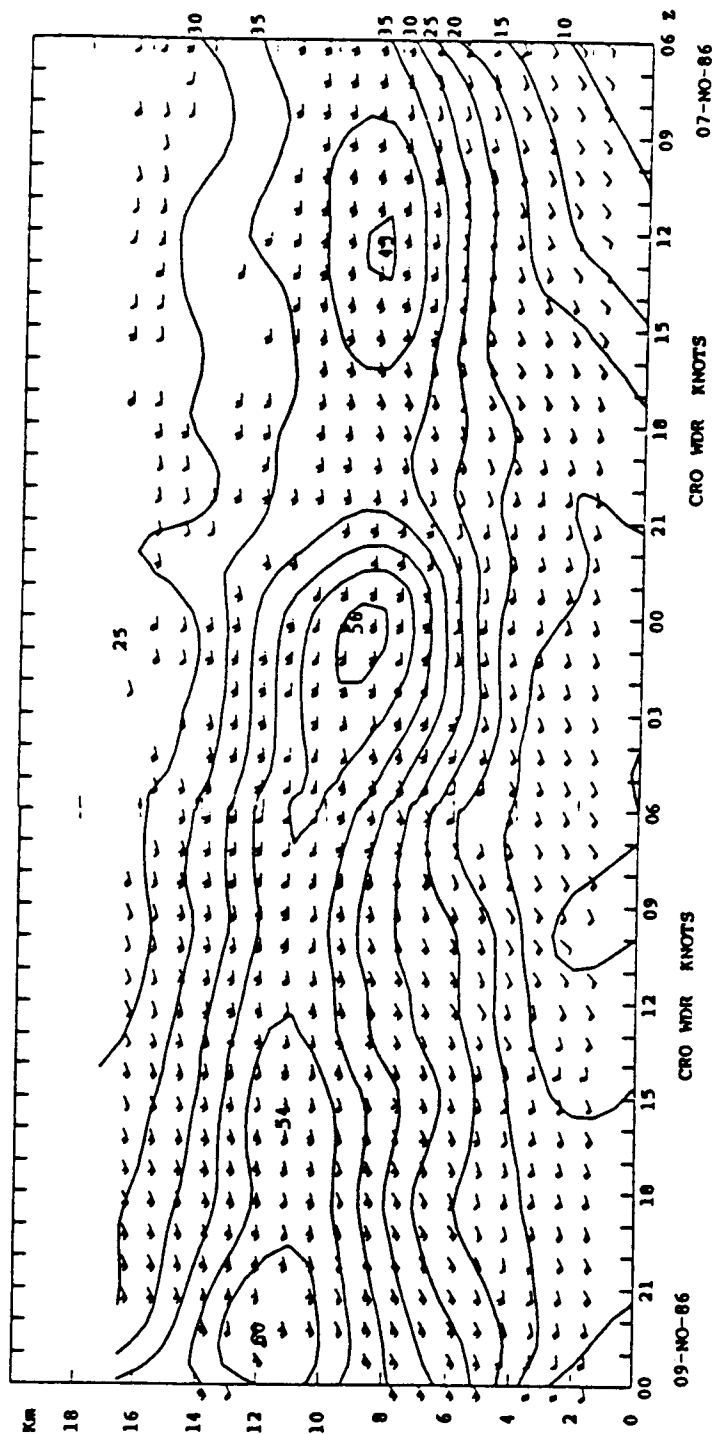
(a) November 7, 8, 1986

Figure 2.1. Time-height cross sections of hourly wind speed
and direction above the Crown profiler during
case 1. Time passes from right to left.
Contour interval is 5 ms^{-1}.
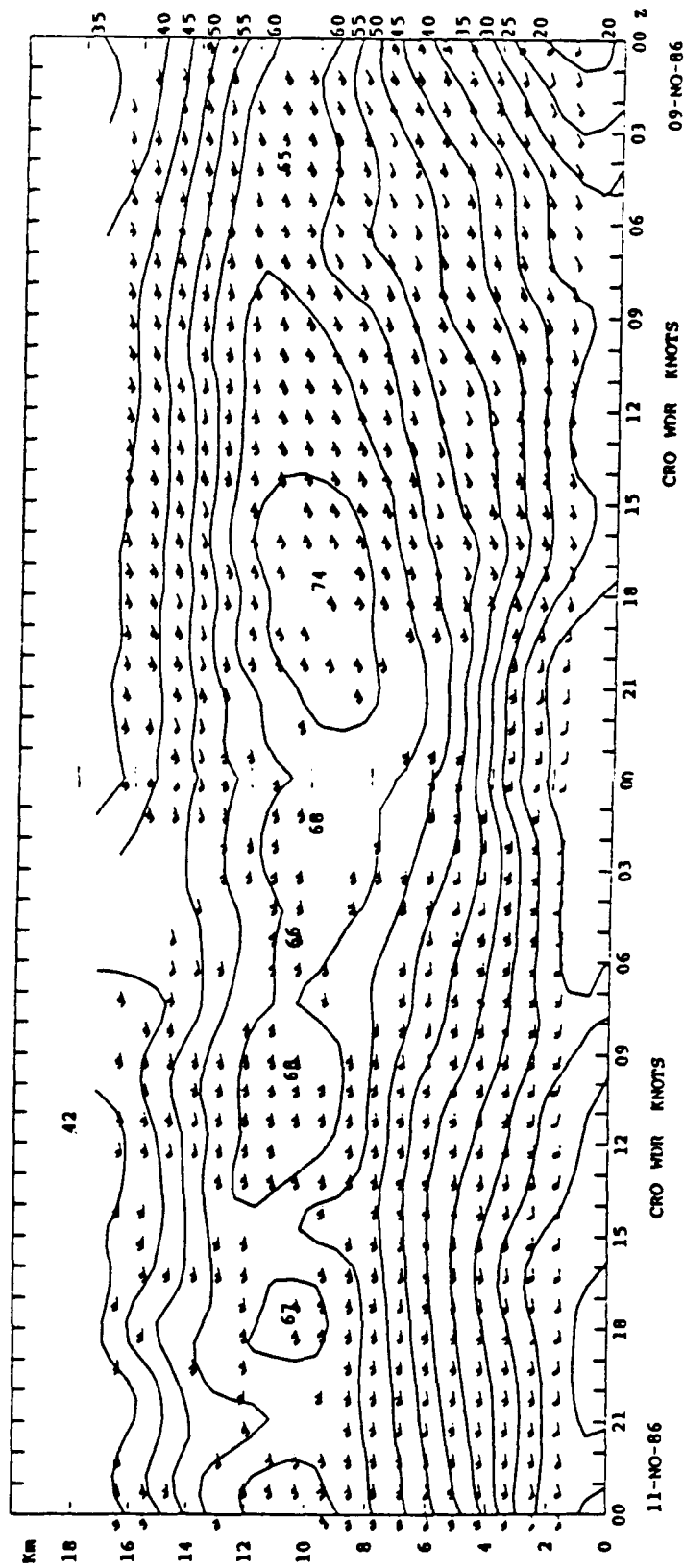
(b)   November 9, 10, 1986

Figure 2.1 (continued).
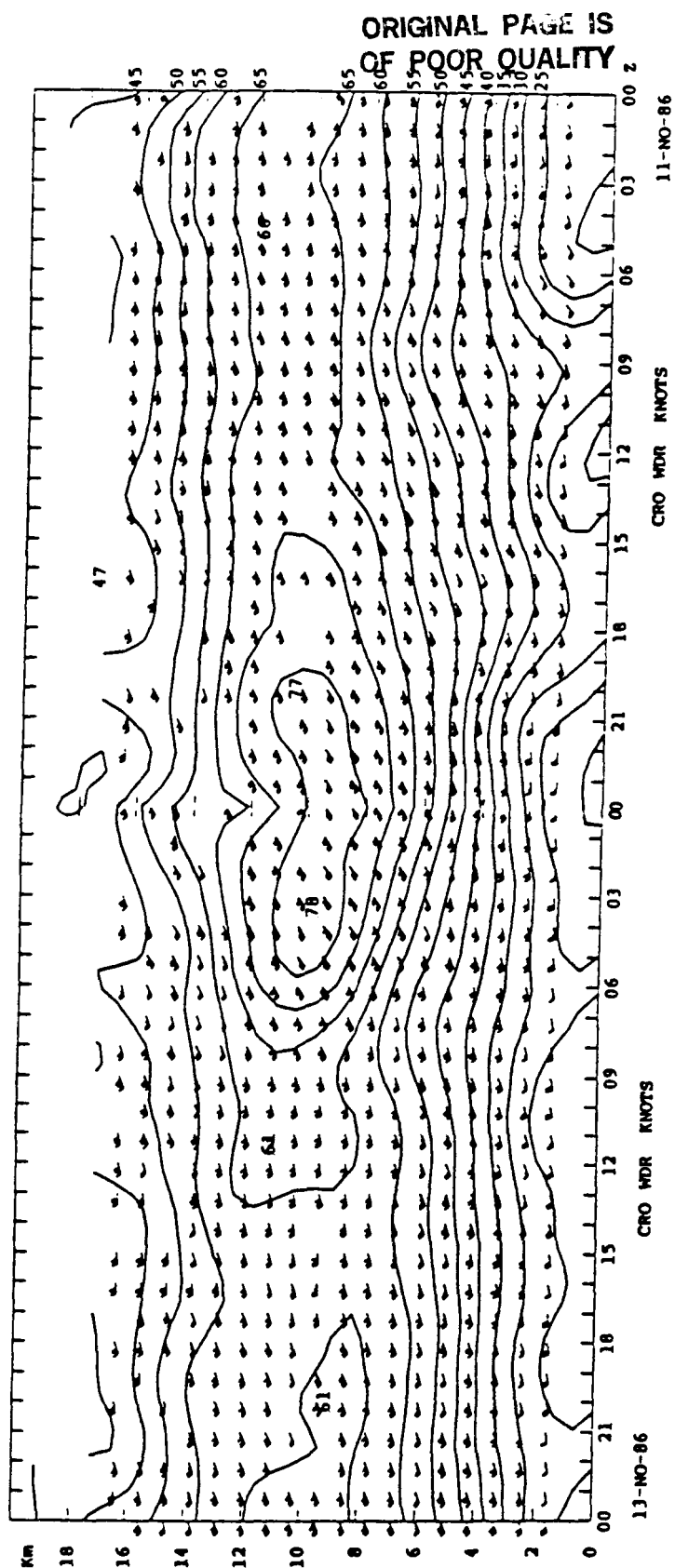
(c) November 11, 12, 1986

Figure 2.1 (continued).
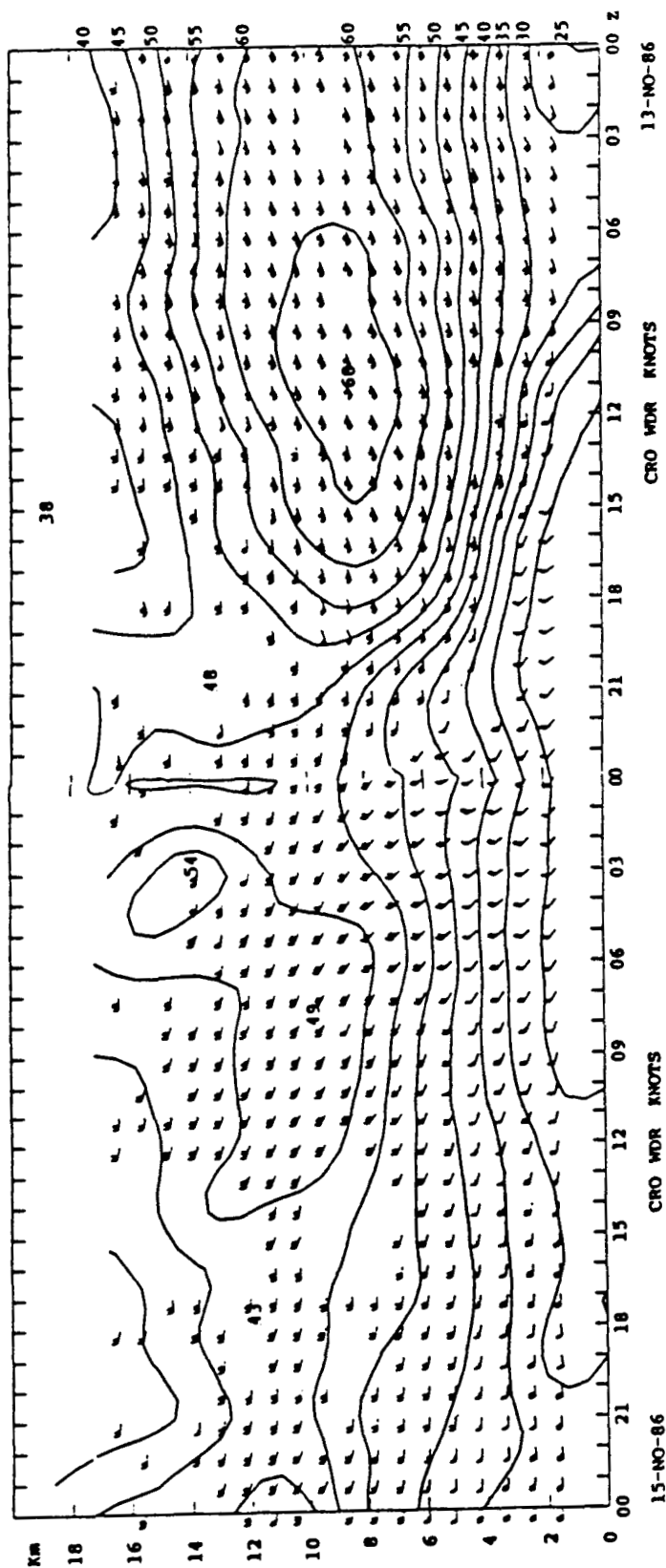
(d) November 13, 14, 1986

Figure 2.1 (continued).
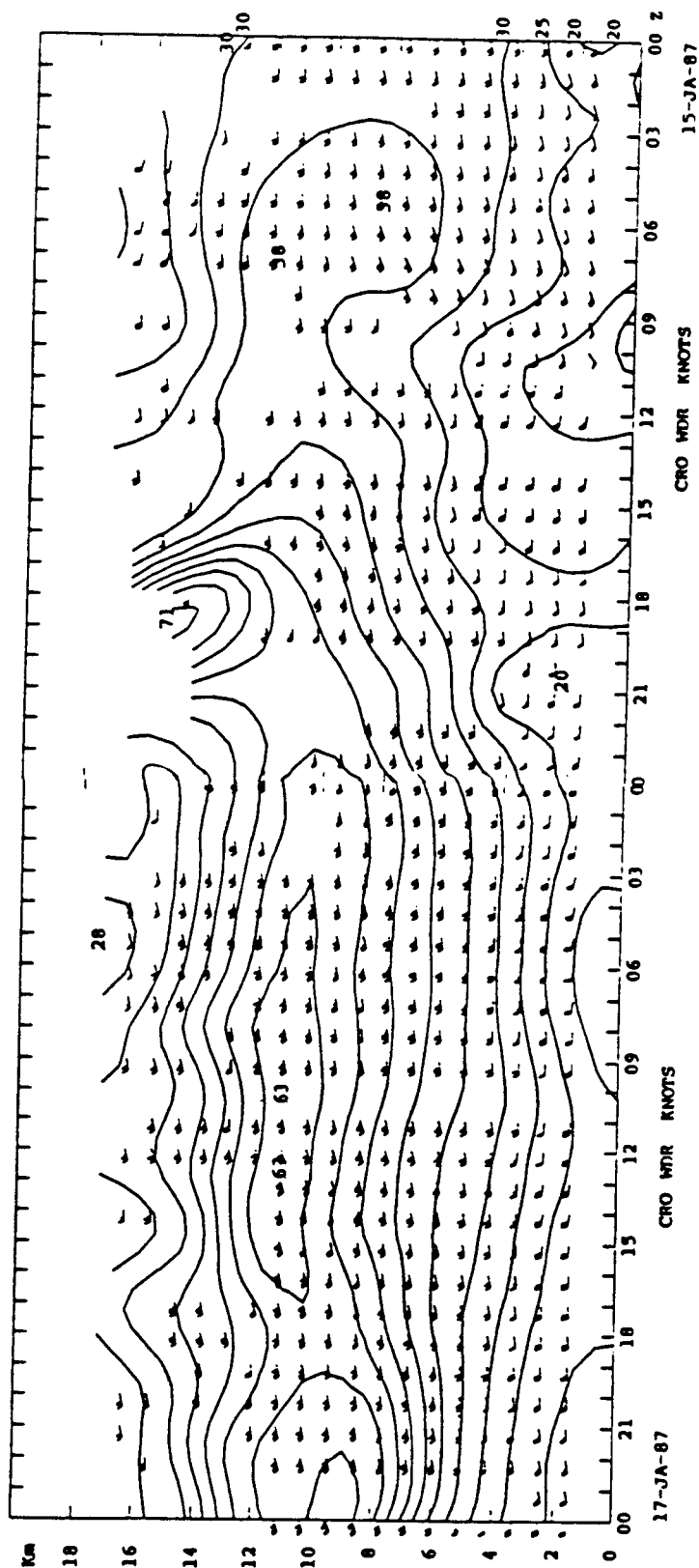
(a) January 15, 16, 1987

Figure 2.2. Time-height cross sections of hourly wind speed and direction above the Crown profiler during case 2.
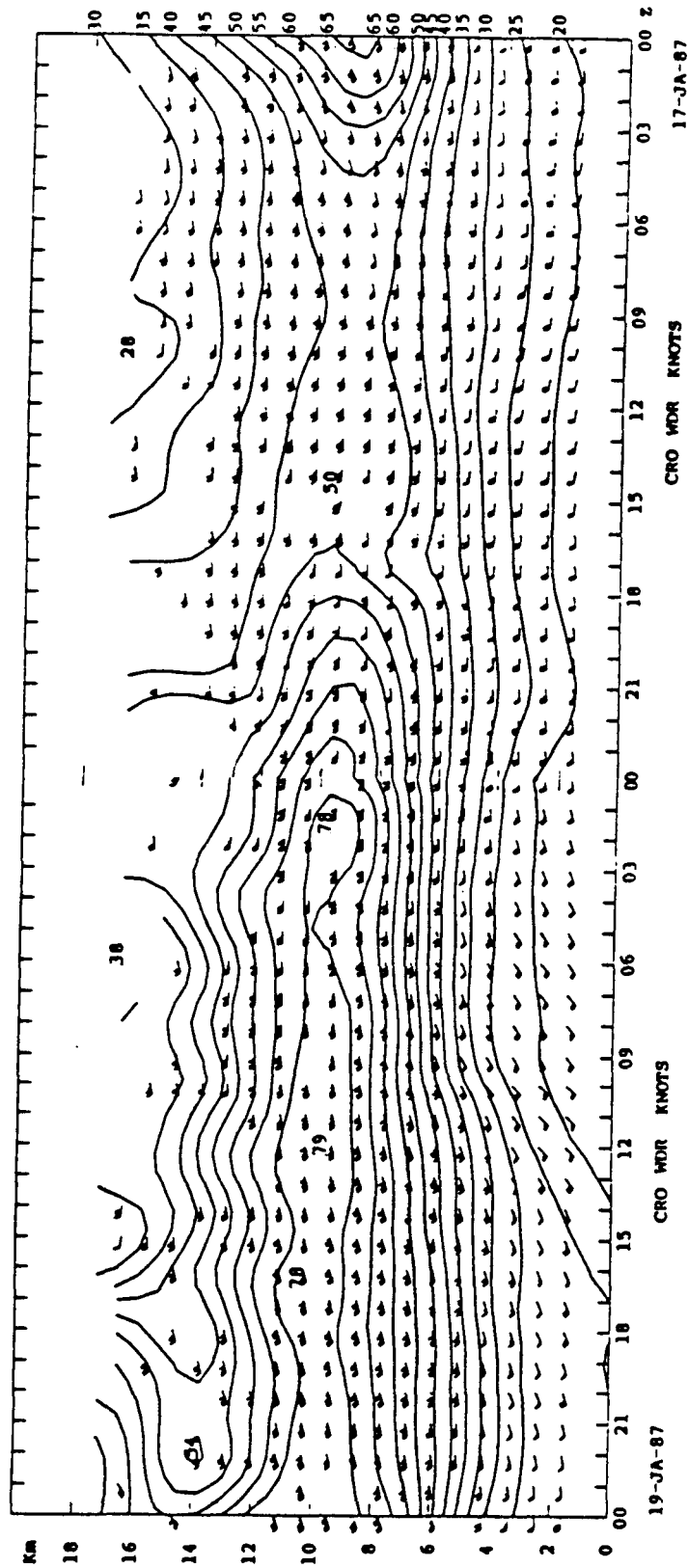
(b) January 17, 18, 1987

Figure 2.2 (continued).
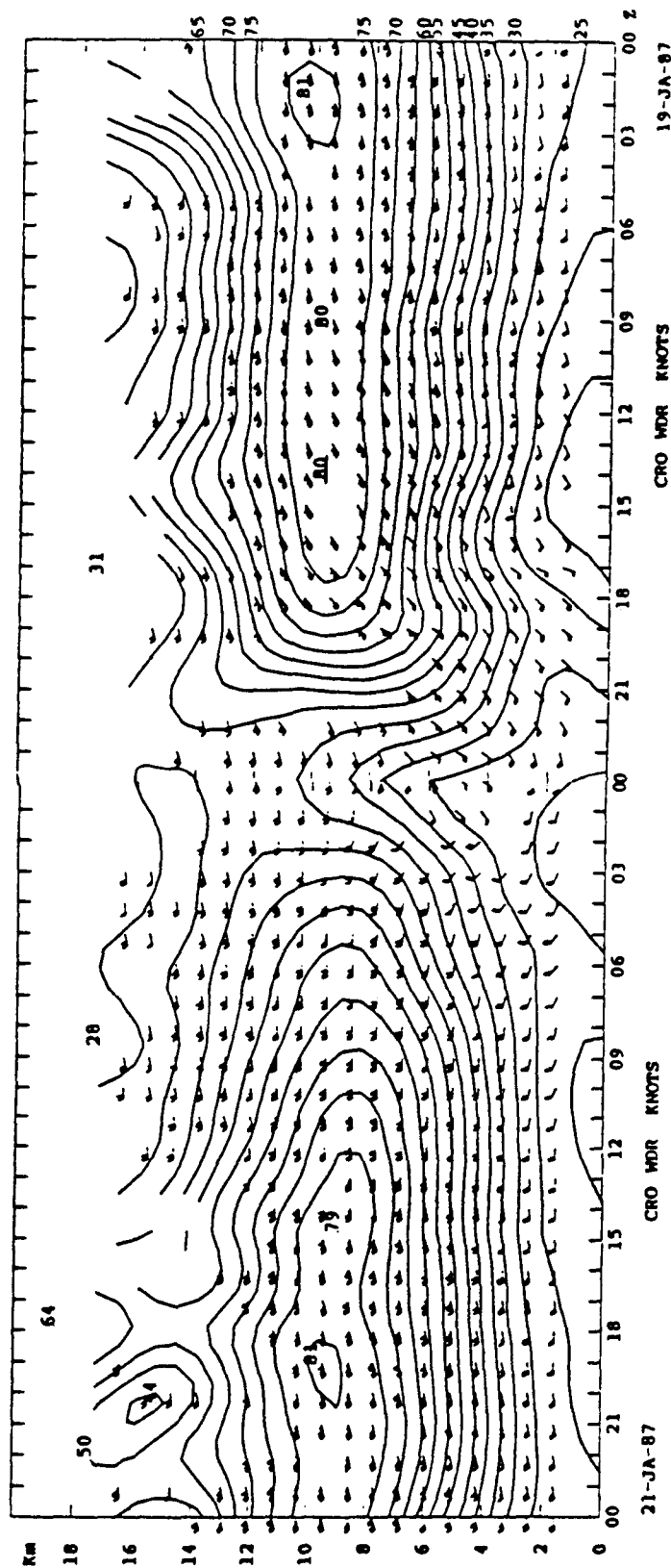
(c) January 19, 20, 1987

Figure 2.2 (continued).
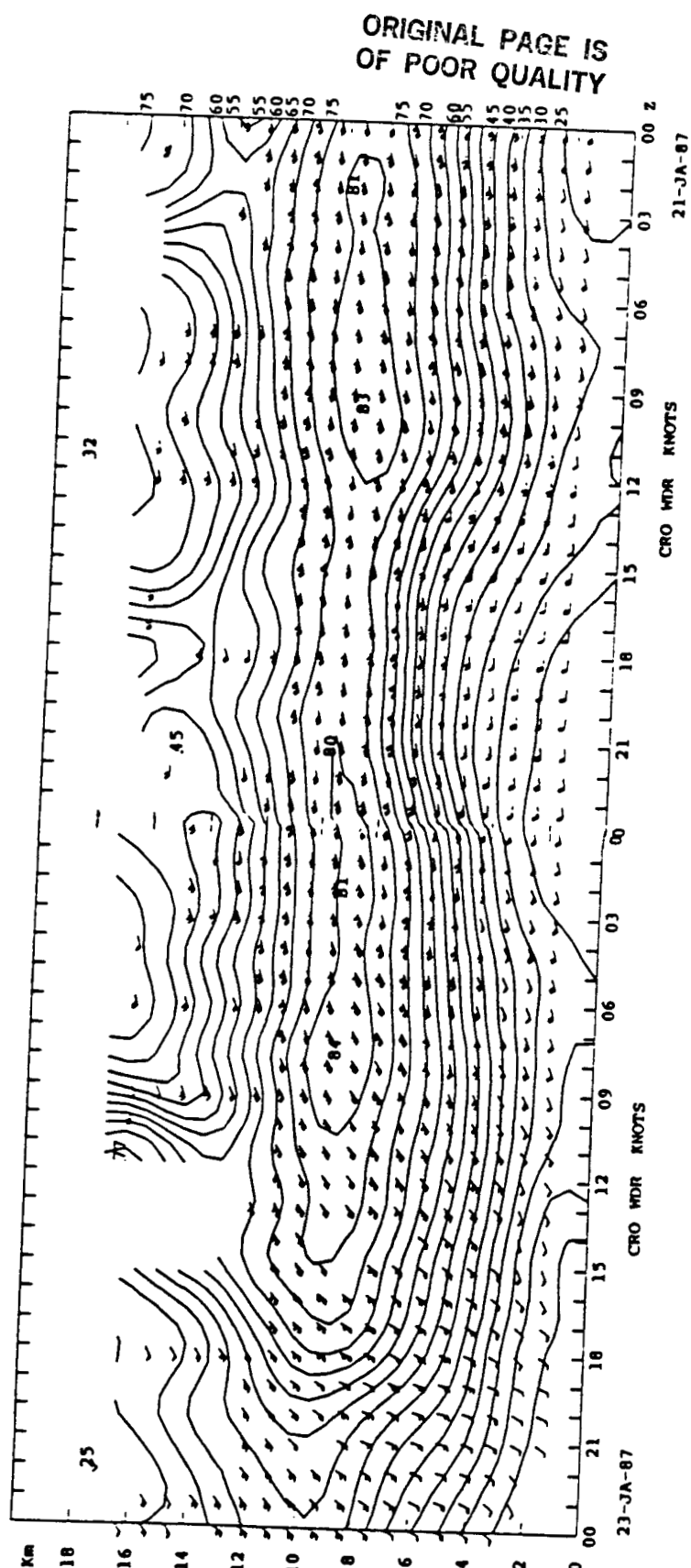
(d) January 21, 22, 1987

Figure 2.2 (continued).
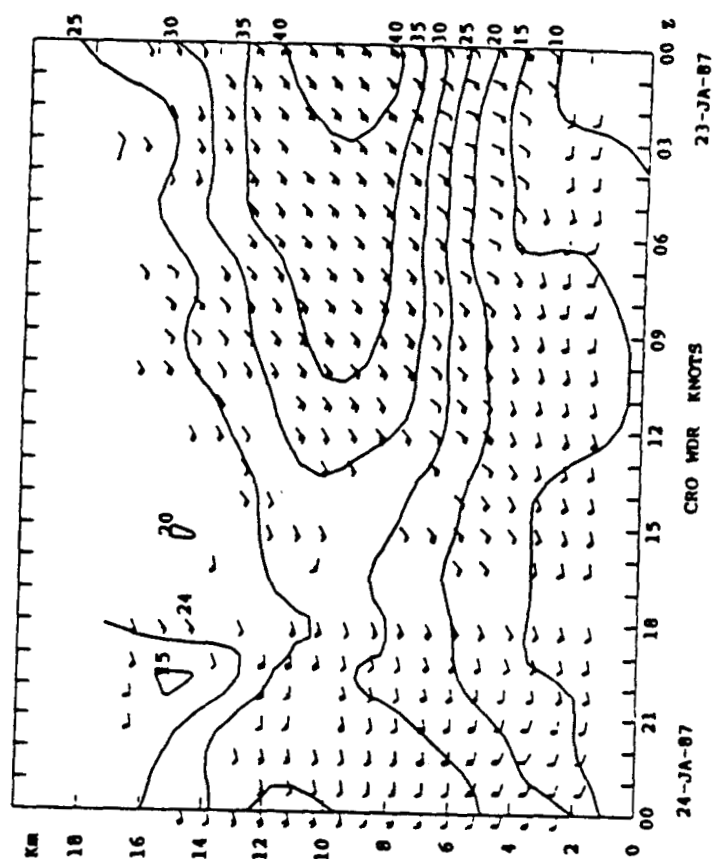
(e)   January 23, 1987

Figure 2.2 (continued).
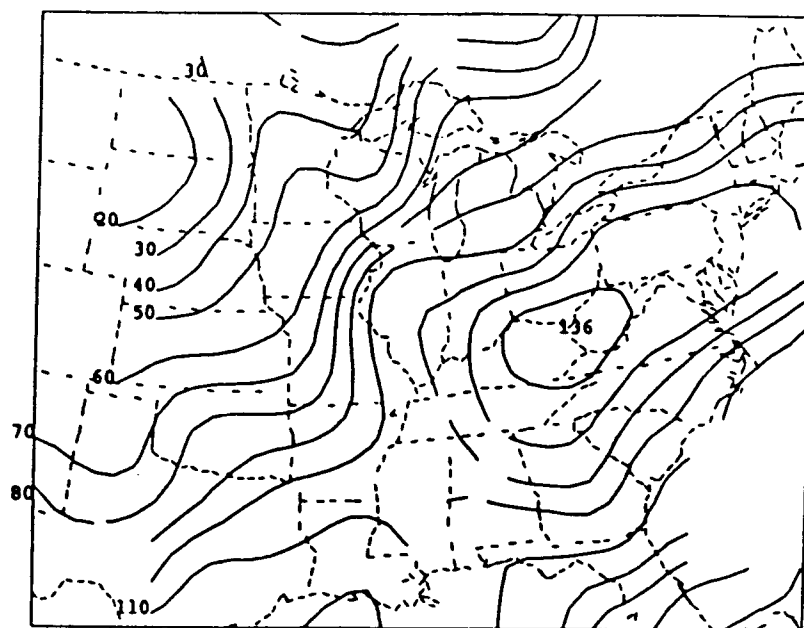
200 WSP
FRI 12Z 16-JA-87
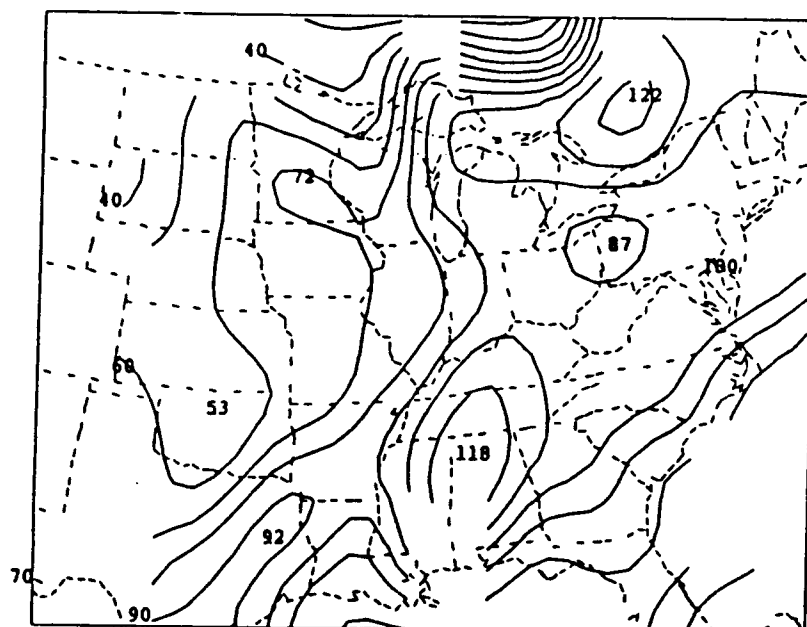
300 WSP
FRI 12Z 16-JA-87

Figure 2.3. Isotach analyses for 200 and 300 mb derived
from radiosonde data, 16 January 1987, 12 UT.
Wind speed in knots.

levels. The data stratification scheme reflects this uncertainty.

The five categories used were chosen to produce the smallest, most consistent data sets possible, considering both the resolution of the radiosonde network and the frequency of occurrence of missing data. Observations were classified as being greater than 300 km north or south of the jet axis, 100 to 300 km north or south of the jet axis, or within 100 km of the jet axis, which is referred to as "under the jet." Table 2.2 lists the categories and number of hours of observation for each at Crown and Pittsburgh.

Table 2.2. Number of observations per data category.
            Category 1 represents observations taken greater
            than 300 km north of the jet axis, 3 represents
            observations taken under the jet stream and 5
            represents observations taken greater than 300
            km south of the jet axis. Categories 2 and 4
            are for observations taken from 100 to 300 km
            north and south of the jet axis, respectively.

Number of Observations

| | Pittsburgh | | Crown | |
Category	Case 1	Case 2	Case 1	Case 2
1	3	4	26	54
2	1	2	20	56
3	3	9	61	79
4	4	0	74	0
5	3	2	19	22

3.0 DATA ACQUISITION AND PROCESSING

In order to do a statistical characterization of jet stream variables such as wind speed and shear and parameters such as Richardson number, a large volume of good quality data is required. Data from either numerous jet stream occurrences of short duration or from jet stream passages that last a week or more are necessary to build a sufficient data base. The latter option was chosen so that power spectra could be computed and therefore energy distributions calculated for different altitudes. Recall that the two jet stream passages chosen for this study consisted of a 200-hour period in mid-November 1986 and a 216-hour period during mid-January 1987. The second case was the stronger one, but both cases involved peak wind speeds in excess of 75 ms^{-1}. The quality of wind data was ensured by using a data filter that was developed specifically for use in jet stream conditions.

Temperature profile data was acquired for the Crown, Pennsylvania, wind profiler by using a routine for interpolating soundings to sites located between the National Weather Service launch stations. Crown is located approximately between the Buffalo and Pittsburgh launch sites.

3.1 The Interpolated Temperature and Dewpoint Temperature Sounding

A method for creating a temperature and dewpoint temperature sounding for the wind profiling radar site near McAlevy's Fort, Pennsylvania, was initially developed by A. Miller (1985), G. Forbes, J. Cahir and the author. This method has since been revised so that it can be used to produce an interpolated sounding at any arbitrary location across the country.

The sounding is created by a command file, written in FORTRAN 77, containing several programs and subprograms that run on the VAX 11/730 computer. Depending upon the computer workload, the entire procedure requires seven to twenty minutes to run.

3.1.1 The Procedure

Significant level radiosonde data from across the country, averaging approximately 90 stations per data set, at midnight or noon Greenwich mean time is read and stored in a large array. The data is then standardized so that temperature and dewpoint temperature readings are available at 50 mb intervals above all stations.

The standardization procedure involves the creation of mean-level profiles of temperature and dewpoint temperature above every reporting radiosonde station. Mean-level profiles are created by calculating the average values of temperature or dewpoint temperature for the layers between significant levels and then weighting the values by the

difference of the logarithms of pressure at the significant levels. The sum of all the weighted averages in each 50-millibar layer is then divided by the sum of the differences of the pressure logarithms.

The readings begin at the first level above the surface evenly divisible by 50 and continue up to 100 mb, if data exists to that level. For example, the values at 700 mb represent the mean of data found in the 725 mb to 675 mb layer. The 100 mb temperature value (dewpoint temperature is not computed above 300 mb) is obtained by assuming isothermal conditions from 100 mb to 75 mb.

When the dividing line between two 50-millibar layers does not coincide with a significant level, values of temperature and dewpoint temperature are linearly interpolated to the boundary from significant levels both above and below it. Average temperature and dewpoint temperature values for the layers between the boundary and the lower and upper significant levels are then calculated. This is done to ensure that all 50-millibar layers between the reported bottom and top values contain data.

Upon completion of the 50-millibar grouping the data is set onto a grid. Values are obtained for all grid points using a nearest neighbor approach. Final values for each level of the sounding are obtained by linear interpolation of the four nearest grid points. Surface values of pressure, temperature and dewpoint temperature are manually entered as replacements for the first data level. Potential

temperature is calculated at profiler range gate heights by linearly interpolating between the 50 mb mean values, and the interpolated temperature sounding is plotted by the VAX on a skew T, log p diagram. Figure 3.1 shows an example of an interpolated sounding for the Shantytown radar site.

3.1.2 Advantages and Disadvantages of the Interpolated Sounding

The sounding is a mean-level profile, therefore rapid fluctuations in the data with height are smoothed. This smoothing can be an advantage or a disadvantage, depending upon the quality of balloon data received and the atmospheric conditions. If the radiosonde passes from a very moist layer to a much drier one, evaporative cooling of the hygristor can create a steeper reported lapse rate than actually exists. This process can create a ficticious superadiabatic layer. In cases such as these, mean-level smoothing reduces the reported lapse rate so that it will, in fact, correspond to a more realistic situation.

Another advantage of the mean profile is the smoothing of unnaturally fluctuating dewpoint temperature reports during very dry conditions. Known as "motorboating," this fluctuation occurs when the frequency of the audio signal through the monitoring speaker of an audio-modulated radiosonde becomes so low that it resembles the sound of a motorboat.

One disadvantage of the mean-level processing is that the rapid changes of dewpoint temperature that commonly

P	T	TD	RH
100	-59		
150	-58		
200	-56		
250	-51		
300	-46		
350	-39	-67	3
400	-34	-56	8
450	-28	-38	36
500	-22	-35	29
550	-17	-32	25
600	-13	-29	24
650	-9	-24	27
700	-6	-15	48
750	-5	-7	85
800	-4	-6	85
850	-3	-8	68
900	-2	-14	39
950	-1	-12	42
989	-3	-8	68

STATION: 0
12Z 05-12-85
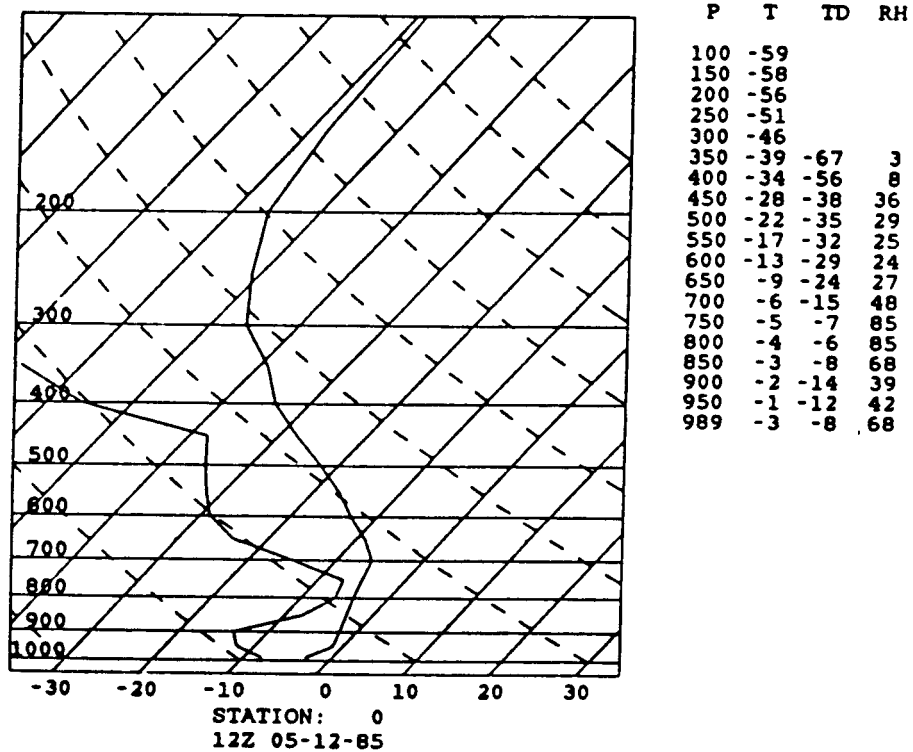
Figure 3.1.   Interpolated sounding at Shantytown, 5
December 1985, 12 UT.

occur at cloud boundaries are somewhat smoothed. This loss of detail is, perhaps, the major drawback to the mean-level smoothing technique.

One other disadvantage results from the procedure used in creating the sounding. Unrealistic lapse rates are often created between the surface and first level above that is divisible by 50 mb. A possible remedy is weighting the lowest one or two interpolated levels as a function of the surface values of temperature and dewpoint. This is not, however, a problem if the user is only interested in levels above 850 mb, as was the case for this thesis.

The process could be expedited by eliminating the reading and gridsetting of data outside a certain radius from the site of interest. For example, it is not necessary to use data from Grand Junction, Colorado, when one is computing an interpolated sounding for Crown, Pennsylvania.

Sensitivity analyses show that a Cressman objective analysis scheme performs somewhat better than the nearest neighbor approach (refer to Haltiner and Williams, 1980, for an explanation of objective analysis procedures), but the former scheme does require more computer time. It was felt that for most users the faster run-time of the nearest neighbor approach was more important than the slight increase in precision provided by use of the Cressman objective analysis.

3.2 A Filter for Wind profiler Data

As discussed earlier, bad data warrants filtering of wind profiler output speeds and directions. Unfortunately, the meteorological community is apparently not yet sufficiently sensitive to this issue as is evidenced by figures 4, 5, 9 and 12 in Augustine and Zipser (1987). Wind data of good quality is crucial for obtaining precise wind speed, and thus wind shear and Richardson number profiles. A data filter was developed primarily for use during high wind speed episodes, that is, jet stream passages over the profiler site. It was used for the two case studies discussed in this thesis.

The wind profiler data filter was developed primarily from extensive observations of profiler output. A suitable amount of common sense combined with thermal wind theory can be used to justify the procedures followed in the data filter.

The filter was designed to remove bad data from profiler observations during jet stream occurrences. This implies strong winds and use of high-mode data since the jet stream is a core of high winds and it is generally found above altitudes profiled during low-mode measurement. Consensus statistics are insufficient as constraints because a low consensus value is no guarantee that data is bad. Data processing software at each radar site was set to omit data if the consensus fell below four on either beam during much of case one, before filtering could be done. For case

two there was no omission of data before the filtering subroutine could be used, as the minimum acceptable consensus was set to one. Due to this lowered acceptance criterion, additional bad data was entered into the filter, but, as hoped, the data filter did adequately remove the additional poor quality data.

Observations show that interference most often appears as abnormally light winds. A five meter per second value was chosen as to eliminate as much bad data as possible before comparison filtering commenced. The comparison filtering constraints, as well as the minimum speed and ground clutter warning values were empirically deduced from approximately 800 hours of data, much of which was taken when the jet stream was relatively strong and close to the profiler site.

Observations show that the highest average returned power and thus best quality data occur at range gates one through five. This is one justification for the initialization procedure described below. We believe it gives the highest confidence practical for obtaining a starting value.

Directional constraints are tightened with increasing height. This can best be explained by using thermal wind theory, but can also be justified simply by looking at surface weather maps and comparing them with upper-air maps. One can readily see that the complicated flow patterns at the surface become smoother with height.

Analytically, consider a streamline drawn parallel to the wind vectors in a horizontal flow. This streamline will have a slope in (x,y) coordinates of: $S = dy/dx = v/u$. Assuming the thermal wind represents the actual wind shear, the slope of the streamline aloft will be: $S = (v+V)/(u+U)$, where U and V are the components of the thermal wind. If U is greater than zero, and if the magnitude of U is much greater than that of V, as is the case when cold air is found to the north and warm air to the south, then there is a reduction in slope of the streamline with increasing altitude (Dutton, 1976).

A bad data flag value of -999 was chosen because the VAX computer plotting routines recognize this value as bad. Thus if bad data is reported it is not entered into the various plotting routines.

3.2.1 General Overview of the Wind Profiler Data Filter

Post-processing wind profiler data filtering was performed in a FORTRAN subroutine containing roughly 400 lines of code. Input data consisted of wind speed and direction, the number of levels (range gates), number of hours of observation, and the particular profiler site. The site is input so that site-specific ground clutter parameters can be determined in the subprogram. Output data are wind speed and direction for each range gate for the number of hours of observation specified. Wind speeds and

directions deemed "bad" by the filter are, as stated earlier, flagged with a value of -999.

Wind speeds of less than five meters per second are considered bad data, since the majority of interference appears as abnormally light winds. During jet stream passages this is a safe estimate, but if the same filter were applied to light wind conditions adjustments would have to be made so that good data would not be lost.

Data filtering is accomplished by first establishing a good data point and then by comparing the good data with surrounding values in height and time. The order of filtering is from lowest to highest altitudes and first to last hours of observation. Data is defined as "good" if direction and speed fluctuations are smaller than the chosen constraint values. The values chosen depend upon altitude of the observation, wind speed and wind direction.

Interference has been observed to be preferentially oriented along site-specific angles, thus a ground clutter check is instituted in order to screen out interference that shows up at speeds greater than five meters per second. Notice the light northwest winds in figure 3.2 at roughly the level of maximum wind. Figure 3.3 illustrates unfiltered versus filtered data. The contours depict wind speed in 2 ms^{-1} intervals.
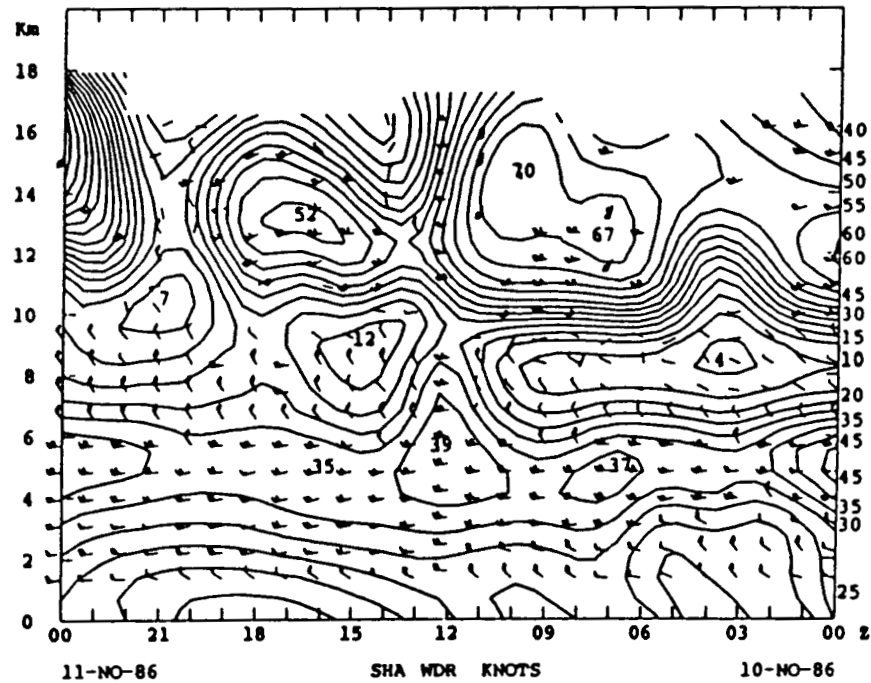
Figure 3.2. Unfiltered time-height cross section of hourly wind speed and direction above the Shantytown profiler, 10 November 1986.
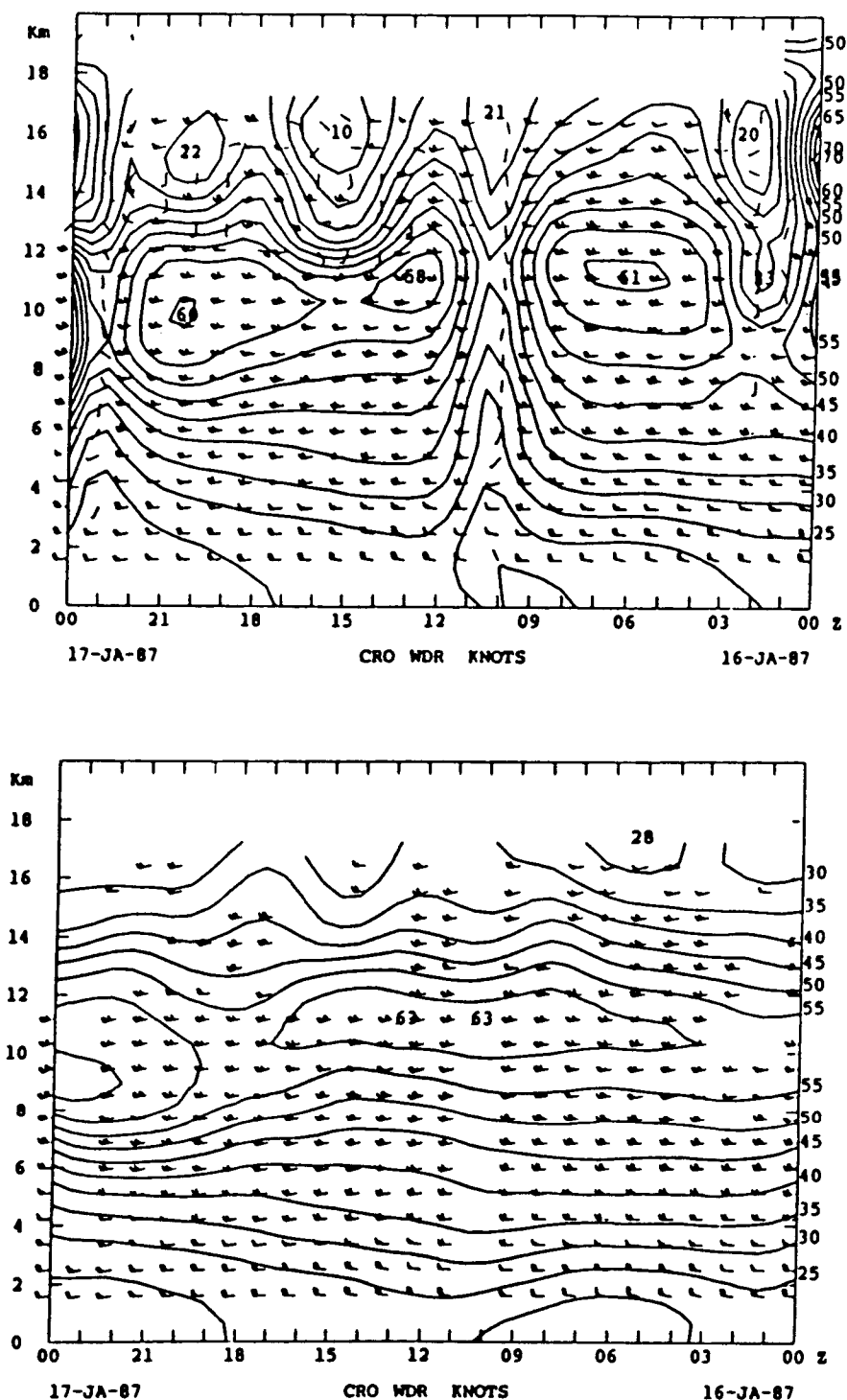
Figure 3.3. Unfiltered versus filtered time-height cross sections of hourly wind speed and direction above the Crown profiler, 16 January 1987.

3.2.2 The Filtering Procedure

The wind profiler data filtering subroutine consists of six major data quality checks. Abnormally light wind speeds are looked for and then direction is examined for each level in the order stated above. Next, comparison filtering begins. For all hours except the first and last, temporal consistency is looked for in the first five range gates, then the remaining gates are similarly examined. Finally, vertical consistency of the first five, and then the remaining range gates is judged. The consistency checks in height are done for every hour. They are stricter than the temporal checks and are the guidelines that ultimately decide which data will be used to initialize the filter.

The data filter is initialized if two or more of the lowest five range gates are found to contain good data. Twelve vertical comparison checks are performed on the data, in order of decreasing confidence, to ensure that data used to initialize the filter is good. The comparison checks are shown in the following list:

- First four values good
- First value bad, next three good
- First, second, fourth, fifth values good
- First three values good
- First two values bad, next two good
- First, third, fourth values good
- First, second, fourth values good
- Second, fourth values good
- First three values bad, next two good
- First, third values good
- First value bad, next two good
- First two values good

If none of these criteria are satisfied, the data for the hour is considered bad and all gates are flagged with the -999 value for speeds and directions. Notice that a tendency for interference to affect the first two range gates has increased confidence in data for gates three, four and five. At this point and before going further, let us return to the beginning.

Following the initial five meter per second data check, wind direction is compared to site-specific ground clutter angles. If the reported wind direction is close to any one of the critical angles, warning flags are set and the data is filtered more strictly than unflagged data. There are three warning categories, based upon how close the direction is to a critical angle. A very small difference in wind direction from a critical angle warrants the most strict filtering of data. Allowances are made for climatological averages in wind direction. For example, west winds are far more common than those from the east, therefore a reported wind with an easterly component that is ten degrees off of a critical angle has a higher likelihood of being interference than a westerly wind that is ten degrees off critical.

Filtering with respect to time is done next for all but the first and last hours of observation. If interference has been determined to be at least moderately possible, that is, if either of the two most severe warning flags are set off, temporal consistency is examined for each range gate up to gate five that triggers a warning. Should the previous

and next hours at the same height contain data set to -999, then this step is omitted. Above range gate five, filtering with respect to time is done for any wind direction, providing that potentially good data, data not set to -999, is found on both sides of the target data point.

For the first and last hours of observation, filtering with respect to height follows the ground clutter warning procedure. For all other hours, vertical filtering is performed after the temporal consistency check. As previously stated, filtering is performed first on the lowest five range gates. Data from the lowest five gates is typically better in quality than higher level data. Thus if good data is lacking at the lower levels poor data is expected aloft and the filter will flag all data for the hour as bad.

If at least two good data points are found, as determined by the twelve quality checks listed above, filtering is performed on the remaining range gates, building upon good data below to check data aloft. Filtering constraints tighten with increasing altitude as upper-level wind flow patterns are normally less variable than those near the surface. Allowances are made for missing data. The allowances and justification for tightening the constraints with increasing altitude are explained above.

3.2.3 Specific Challenges of Profiler Data Filtering

The first, and most important, challenge concerns choosing a good starting value upon which to judge remaining data. The initial decision-making process has already been detailed and it is considered to be a sound one.

Other difficulties arise when missing data is encountered. Missing data can be either data previously flagged as "bad" by the filter or data omitted due to minimum consensus processing at the site prior to the filtering procedure. When missing information is noted during comparison filtering, constraining values must be altered to allow for the gaps in the data.

If missing data is encountered during temporal consistency checks it is possible that only vertical data quality checks will be performed and the temporal checks will be bypassed. This occurs if data is missing from both sides of the target data point during filtering of the first five range gates or if data is missing from either side of the point in question above range gate five.

Since filtering with respect to height is done on all potentially good data points, the constraint values must be relaxed if missing data occurs. This is logical because 890 meters of space is added between observations for each missing value encountered.

Construction of the data filter was a constant compromise to find the highest ratio of good data kept to bad data kept, or bad data thrown out to good data thrown

out. It was no small task and certainly in the future more permutations are likely to be discovered for initial vertical data filtering. For the cases discussed in this thesis the present data filtering subroutine appeared in all respects to be more than adequate. Perhaps some future filter will be implemented using AI (artificial intelligence) methods (Campbell and Olson, 1987).

3.3 Wind Shear Calculations for Crown and Pittsburgh

Wind shear calculations were performed after filtered wind data was obtained from the Crown profiler. Data from the Pittsburgh radiosonde was used for altitudes between the first and last range gates of the Crown radar.

Data from both sites were then splined to 250-meter intervals starting at the height of the first range gate containing good data and continuing up to the last good gate. Maximum data range in the vertical is from 1620 to 16440 meters above mean sea level, thus 60 data points can be splined from 1620 m to 16370 m when good data is found at least in the first and eighteenth range gates.

The 250-meter interval was chosen so that a resolution of 500 m could be obtained for Richardson number calculations and then compared to lower resolutions. This interval created the necessary data base while being nearly equal to the best resolution obtainable by the Pittsburgh radiosonde and the Crown profiler.

Calculations of the wind shear were done at 250-meter height steps with the height interval, "dz," used to compute the shear equal to 500 m. Thus, a maximum of 58 shear values could be computed each hour. Wind shear was calculated by taking account of both wind speed and direction changes over the 500-meter intervals. The magnitude of the velocity change was computed by using the following equation: $dV^2 = v_T{}^2 + v_B{}^2 - 2(v_T * v_B)\cos(r)$, where v_T is the wind speed at the top level, v_B is the speed 500 m below and r is the directional difference. This value was then divided by the 500-meter height interval to obtain the wind shear. For the entire data set, this calculation was performed nearly 20,000 times.

3.4   Richardson Number Calculations

Potential temperature values were necessary at the same vertical and temporal resolution as wind data in order to create an adequate Richardson number data base. Because temperature data were only collected at 12-hour, 50-millibar intervals, values were linearly interpolated to one-hour time steps and then splined to 250-meter height resolution.

Richardson numbers were computed for three different resolutions of data. As stated earlier, the best resolution examined was 500-meter, with 1000- and 2000-meter resolution completing the data set. Thus, the value of "dz" varied from 500 to 2000 m for the computations of the Brunt-Vaisala frequency and the wind shear. Specifically, Richardson

number, $Ri = N^2/(dV/dz)^2$, where the denominator is simply
the square of the wind shear and N^2 is the square of the
Brunt-Vaisala frequency: $N^2 = (g/T)*(dT/dz)$, where g is the
acceleration due to gravity and T is potential temperature.

After inspecting Crown radar Richardson number data, it
was determined that variations in the Richardson number
field were caused primarily by variations in wind shear.
Changes of potential temperature gradient with respect to
time were slight. Therefore, calculations of Richardson
number were not performed on the Pittsburgh data.
Comparisons of wind shear data from Crown and Pittsburgh
were deemed sufficient. Figure 4.22 (pages 91, 92) shows
surface plots of the temperature gradient, wind shear and
Richardson number from 16 January 1987 to illustrate the
point. Note the inverse relationship between shear and
Richardson number.

4.0   EXAMINATION OF THE DATA

A total of 411 hourly observations obtained with the Crown profiler were examined in this study. During mid-November 1986, 200 consecutive hours of data were gathered and referred to as "Case 1." A 216-hour period during mid-January 1987 produced the 211 hours of data that comprise "Case 2." Figures 4.1 and 4.2 provide the details of data availability versus height in relation to jet stream location for the Crown profiler and the Pittsburgh radiosonde, respectively.

Note that an individual radiosonde launch is referred to as an "hour" of data simply for comparison to the profiler data, perhaps "observation" would have been a better term. The profiler performs continuous, fixed measurements while the radiosonde drifts with the wind and takes about an hour to complete a sounding up to 16 km. There were 31 reported radiosonde launches from Pittsburgh during the two periods of observation.

Balloon data quality appeared to decrease with increasing wind speed, as was expected, but profiler performance could not be so easily correlated with the meteorological conditions. Based upon a study of Colorado wind profiler outages (Frisch et al., 1986), data dropouts of the Crown profiler were studied in the hope of finding a cause, whether meteorological or not, for reduced profiler performance.

NUMBER OF OBSERVATIONS PER HEIGHT
CASE 1   CROWN, PA

> 100KM SOUTH (74 HOURS)

UNDER JET (61 HOURS)

> 300KM NORTH (26 HOURS)
> 100KM NORTH (20 HOURS)
> 300KM SOUTH (19 HOURS)

HEIGHT M

NUMBER OF OBSERVATIONS PER HEIGHT
CASE 2   CROWN, PA

UNDER JET (79 HOURS)

> 100KM NORTH (56 HOURS)
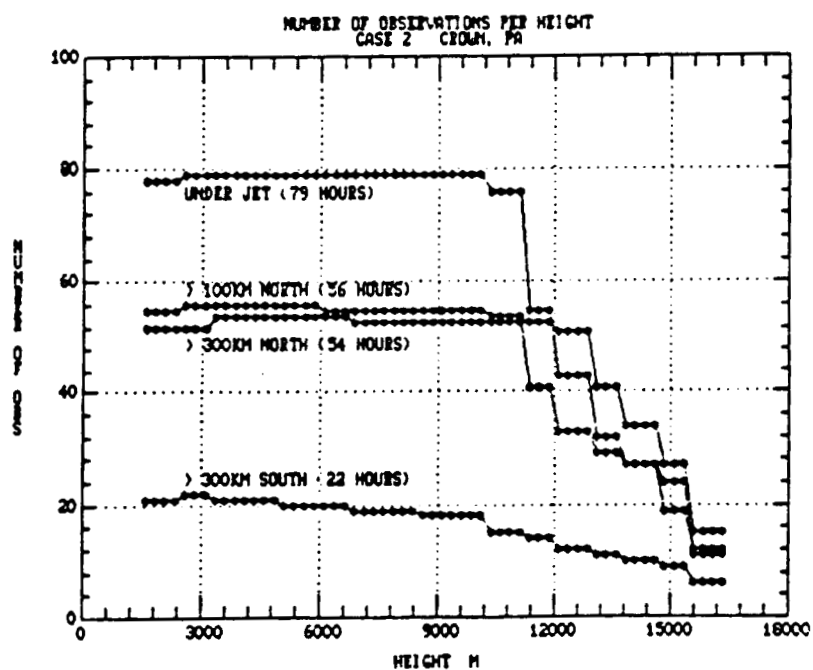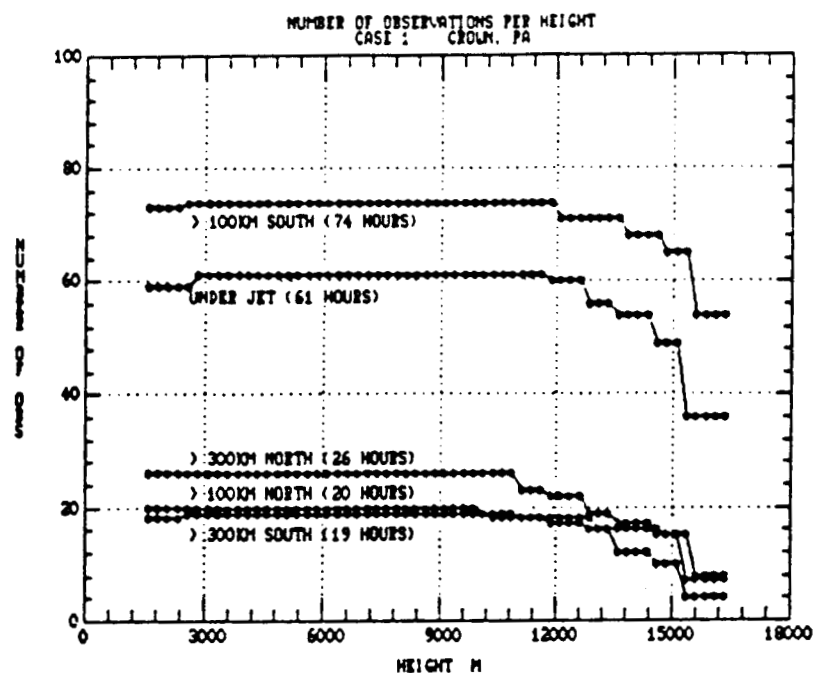> 300KM NORTH (54 HOURS)

> 300KM SOUTH (22 HOURS)

HEIGHT M

Figure 4.1.   Number of splined data values accepted for each
height at the Crown profiler during the first
and second cases, respectively.

**NUMBER OF OBSERVATIONS PER HEIGHT
CASE 1   PITTSBURGH**

) 100KM SOUTH (4 HOURS)

) 300KM NORTH (3 HOURS)

UNDER JET (3 HOURS)

) 300KM SOUTH (3 HOURS)

) 100KM NORTH (1 HOUR)

HEIGHT M

**NUMBER OF OBSERVATIONS PER HEIGHT
CASE 2   PITTSBURGH**

UNDER JET (9 HOURS)

) 300KM NORTH

) 300KM NORTH (4 HOURS)

UNDER JET

) 300KM SOUTH (2 HOURS)

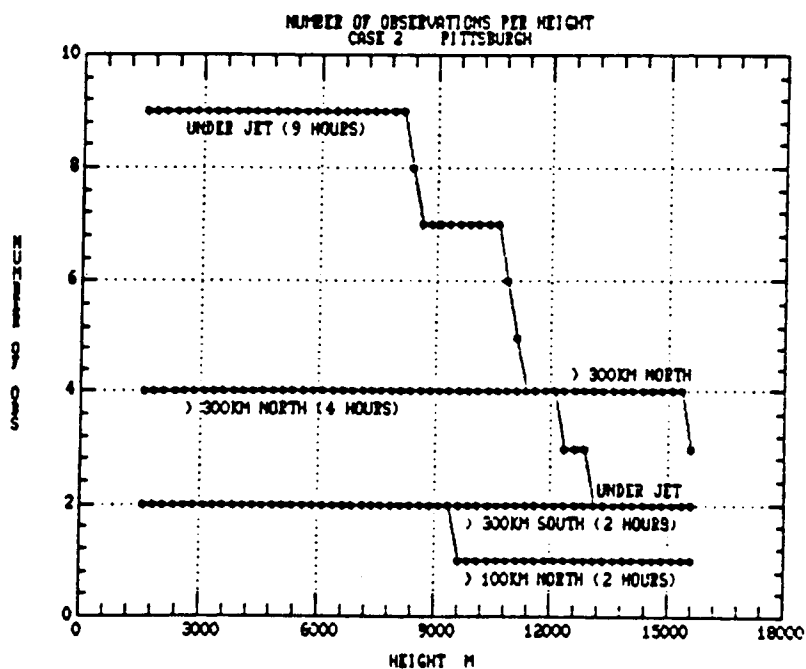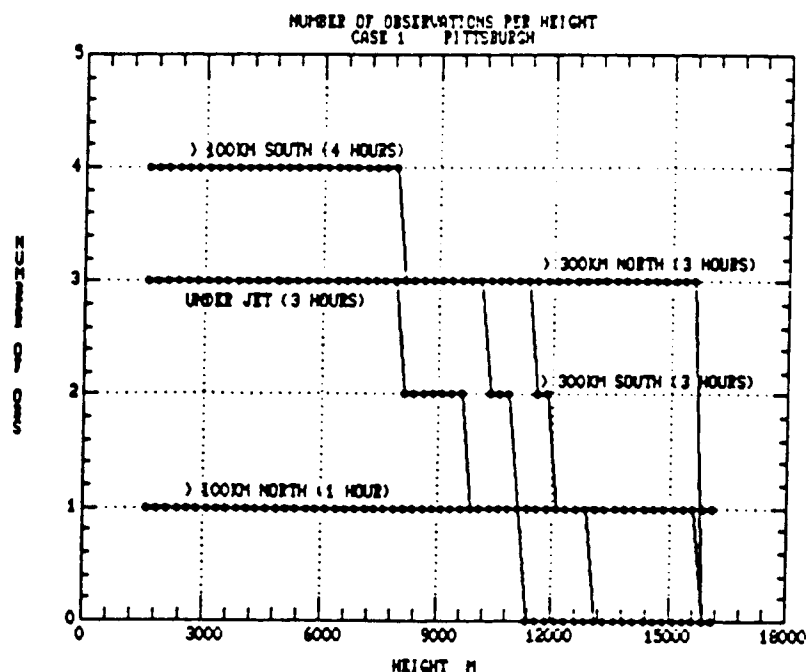) 100KM NORTH (2 HOURS)

HEIGHT M

Figure 4.2.   Number of splined data values accepted for each
height at Pittsburgh during the first and
second cases, respectively.

4.1 Profiler Performance

The performance studies done for the Crown radar differed in several ways from the Colorado study. Wind data accuracy, unaddressed in the Colorado study (although it will be in a forthcoming paper), was examined for the hourly averaging and filtering techniques previously discussed. Data were considered "accurate" if they produced meteorologically consistent wind profiles in height and time. Because only filtered data was analyzed, accuracy of hourly averaged data was not established. However, filtered data was nearly 100 percent accurate and outage statistics along with past experience indicated that hourly averaged data sets are less accurate than filtered data sets.

4.1.1 Profiler Performance and Jet Stream Location

The term "outage" refers to a one-hour period when hourly averaging or filtering techniques deemed a measurement as bad.   Tables 4.1 and 4.2 show the percent of time when "acceptable" (not necessarily accurate) data was obtained from the profiler by both techniques, as related to jet stream location. Several interesting results may be obtained through analysis of the tables.

If one assumes radiosondes are launched every twelve hours and that each balloon obtains a profile up to 16 km, in 100 hours only 9 profiles can be obtained. This translates to only 9 percent of total possible profiler data, and is worse than the lowest percentage (11) found in

Table 4.1 Percent of time case 1 data was considered
          acceptable (hourly averaged/filtered).

	Site Location Relative to the Jet Axis				
Gate	>300 km S	>100 km S	UNDER	>100 km N	>300 km N
1	100/ 95	100/ 99	100/ 97	100/100	100/100
2	100/100	100/100	100/100	100/100	100/100
3	100/100	100/100	100/ 97	100/ 70	100/100
4	100/100	99/ 99	100/ 85	100/ 90	100/100
5	100/100	100/ 99	100/ 95	100/100	100/100
6	100/100	100/ 99	100/ 93	100/ 95	100/100
7	100/100	99/ 99	95/ 89	100/ 95	100/ 96
8	100/100	100/100	85/ 84	90/ 95	100/ 81
9	100/100	95/ 99	84/ 80	100/100	92/ 69
10	95/ 95	80/ 86	72/ 70	95/ 95	65/ 62
11	89/ 89	82/ 85	74/ 74	95/ 95	100/100
12	63/ 53	82/ 81	84/ 80	90/ 90	96/100
13	37/ 37	93/ 95	84/ 84	70/ 75	58/ 65
14	37/ 32	92/ 86	90/ 77	65/ 60	50/ 42
15	16/ 11	86/ 84	77/ 70	40/ 35	42/ 38
16	47/ 37	81/ 80	77/ 74	30/ 25	46/ 35
17	79/ 79	77/ 74	69/ 69	40/ 30	54/ 46
18	42/ 42	64/ 73	48/ 61	40/ 20	42/ 27

Table 4.2   Percent of time case 2 data was considered
            acceptable (hourly averaged/filtered).

	Site Location Relative to the Jet Axis				
Gate	>300 km S	>100 km S	UNDER	>100 km N	>300 km N
1	100/ 95		100/ 99	100/ 96	100/ 96
2	100/100		100/100	100/100	100/ 96
3	100/100		100/ 99	100/ 98	100/ 87
4	100/ 91		100/100	100/ 98	100/ 98
5	100/ 95		97/ 97	100/ 98	100/100
6	100/ 91		99/ 99	100/ 98	100/ 96
7	100/ 86		97/ 96	100/ 96	96/ 91
8	100/ 77		99/ 97	98/ 95	98/ 89
9	100/ 82		96/ 95	98/ 96	91/ 89
10	100/ 77		89/ 94	93/ 88	94/ 93
11	100/ 77		95/ 97	93/ 88	93/ 87
12	91/ 59		99/ 96	82/ 86	87/ 87
13	86/ 45		94/ 62	77/ 65	78/ 85
14	73/ 27		87/ 48	54/ 39	94/ 83
15	55/ 23		72/ 23	72/ 35	74/ 59
16	55/ 18		56/ 27	70/ 27	52/ 43
17	64/ 36		47/ 16	61/ 37	48/ 39
18	77/ 27		25/ 15	46/ 18	28/ 28

the tables. Because of the splining procedures used, no
less than 15 percent of the profiler measurements reach the
16 km level in any one synoptic category, with a maximum of
73 percent found in one case. Comparison of figures 4.1 and
4.2 shows that radiosondes, as well as profilers, suffer
increased data losses with height. Notice the total number
of observations involved: 411 from the profiler to 31 from
the radiosonde. Thus, there are only 7.5 percent as many
balloon soundings from the start.

A clear relationship between performance and jet stream
location could not be established. However, comparison of
outage statistics with wind speed and shear profiles
indicated reduced performance at the level of maximum wind,
where shear and turbulence are reduced.

Figures 4.3 and 4.4 more clearly show the reduction in
performance just above 9 km, the level of the jet core in
both cases. Notice also that filtering generally reduces
the number of data points accepted. This means that a
minimum consensus of 4 still allows acceptance of some bad
data. But during case 2 at the level of the jet core,
percent time down was greater for hourly averaged data,
indicating a loss of critical jet core data because good
data was found with consensus values less than four. Thus,
the number of jet core observations was increased by
ignoring minimum consensus testing and developing a filter
based on meteorological observations.

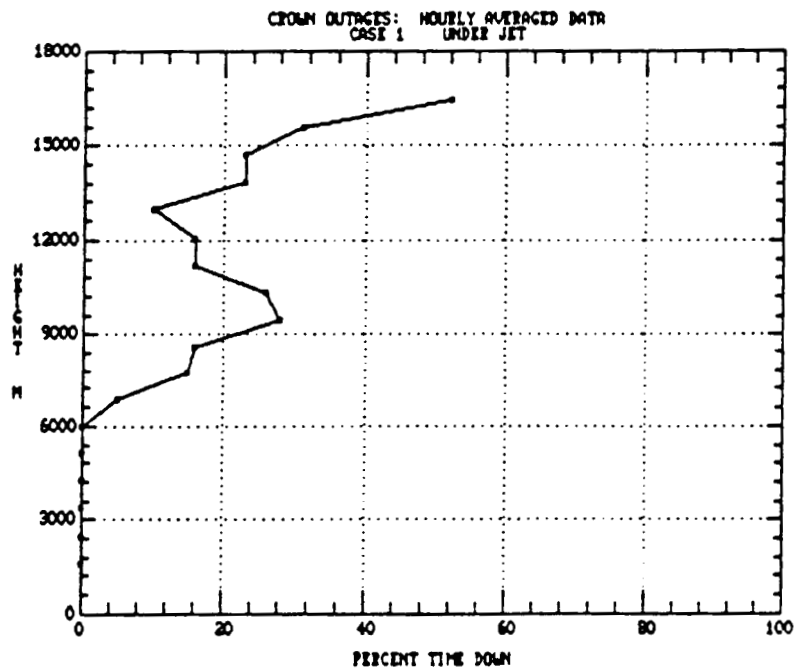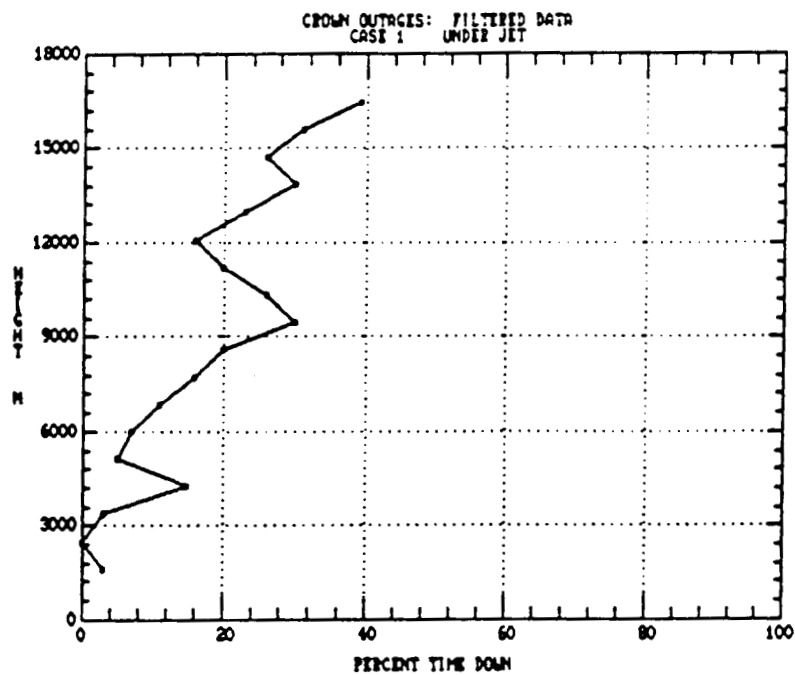Crown outage statistics indicate a rapid loss of good

Figure 4.3. Percent of time during the first case that the
Crown profiler failed to report winds while the
jet axis was within 100 km of the site. The
statistics are for filtered and hourly averaged
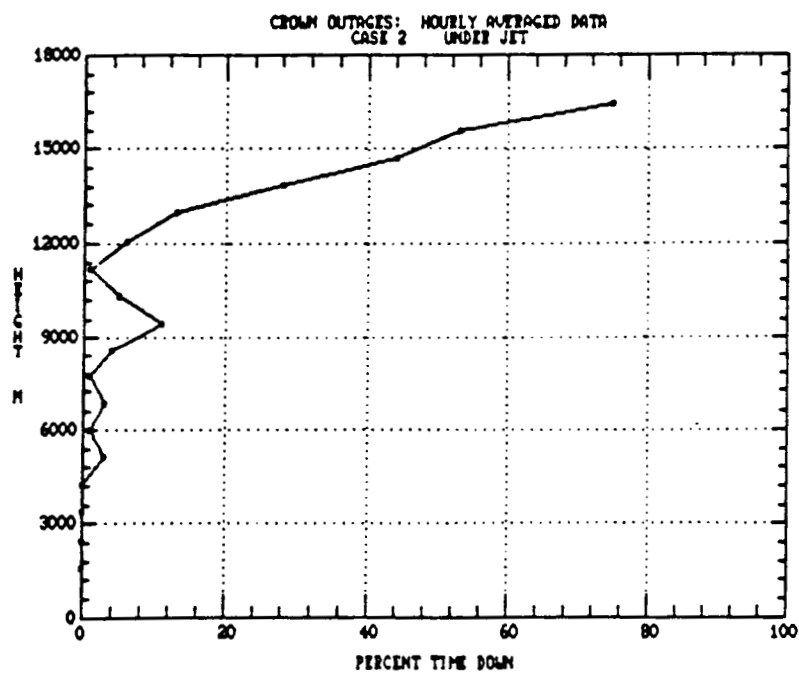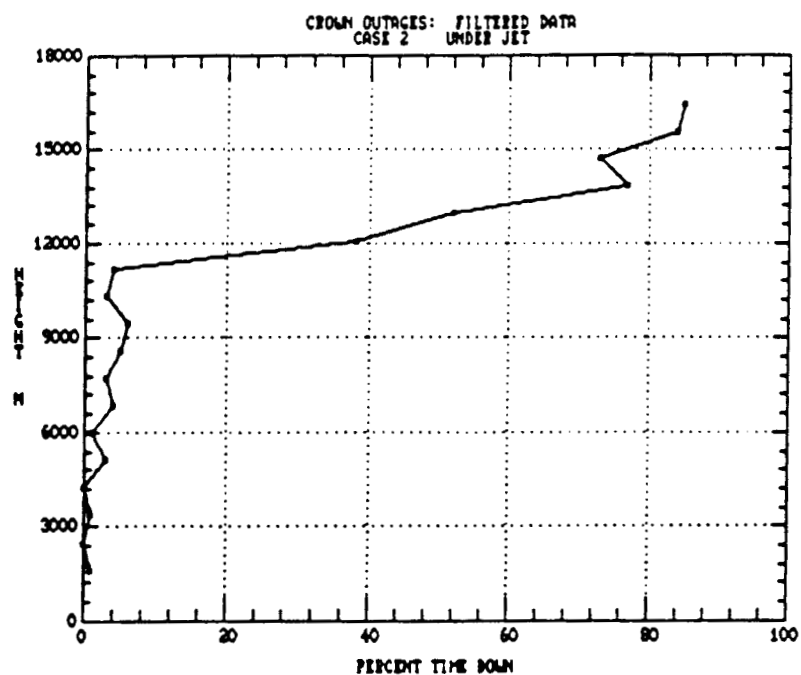data, respectively.

CROWN OUTAGES: FILTERED DATA
CASE 2   UNDER JET

CROWN OUTAGES: HOURLY AVERAGED DATA
CASE 2   UNDER JET

Figure 4.4.   As in figure 4.3 but for the second case study.

data near or above 12 km similar to that of the Colorado
profiles from January 1985. Both Crown and Colorado
profilers show reduced performance near 10 km, implying a
minimum of backscattered power at this level probably due to
the level of maximum wind. Note that an "outage" in the
Colorado study had to last at least 3 hours. If Crown data
had been judged in the same way, performance would have
appeared to have been significantly better.

Apart from the reduction in profiler performance due to
wind shear minima and the resulting reduction in
backscattered power, meteorological effects on data quality
were found, as will be seen in the following section, to be
relatively unimportant when compared to the effect of cosmic
interference on profiler performance.

4.1.2 Cosmic Noise

When Doppler radars are used to measure wind in clear
air, noise contributions are of major importance since the
echo power may be smaller than the noise power. The noise
power has contributions from several sources, one of which
is radiation from space, also known as cosmic noise (Doviak,
1984).

The contribution to receiver noise from the sky
temperature is a function of the direction in which the
antenna points because cosmic radiation is nonuniformly
distributed over angular space. The frequency of the radar

is also important since cosmic interference has a greater effect on lower frequency radars as figure 4.5 illustrates.

Based upon measurements taken with the Shantytown east beam and a map of brightness temperature of the radio sky similar to figure 4.5a, Moss (doctoral research, 1986) developed a program that estimated brightness temperatures for that site. Several factors facilitated the use of this data for the Crown studies.

First, because of the earth's rotation, the times of the Shantytown observations did not exactly match Crown observations. The Crown radar detected the same sky features approximately 6 minutes later than the Shantytown radar. However, since we dealt with hourly averaged data, this time lag was insignificant.

A potentially more serious problem arose due to the different beam pointing angles for each site. The Shantytown east beam actually is directed towards 60 degrees while the Crown east beam looks toward 90 degrees. Because we correlated data dropouts defined if either the Crown east or north (pointing toward 360 degrees) beams failed the minimum consensus test, use of the Shantytown data was considered valid as 60 degrees falls between 360 and 90 degrees. It was also considered valid since only a relative measure of cosmic noise was required for this study, and cross-correlations of data dropouts with cosmic noise support this claim.
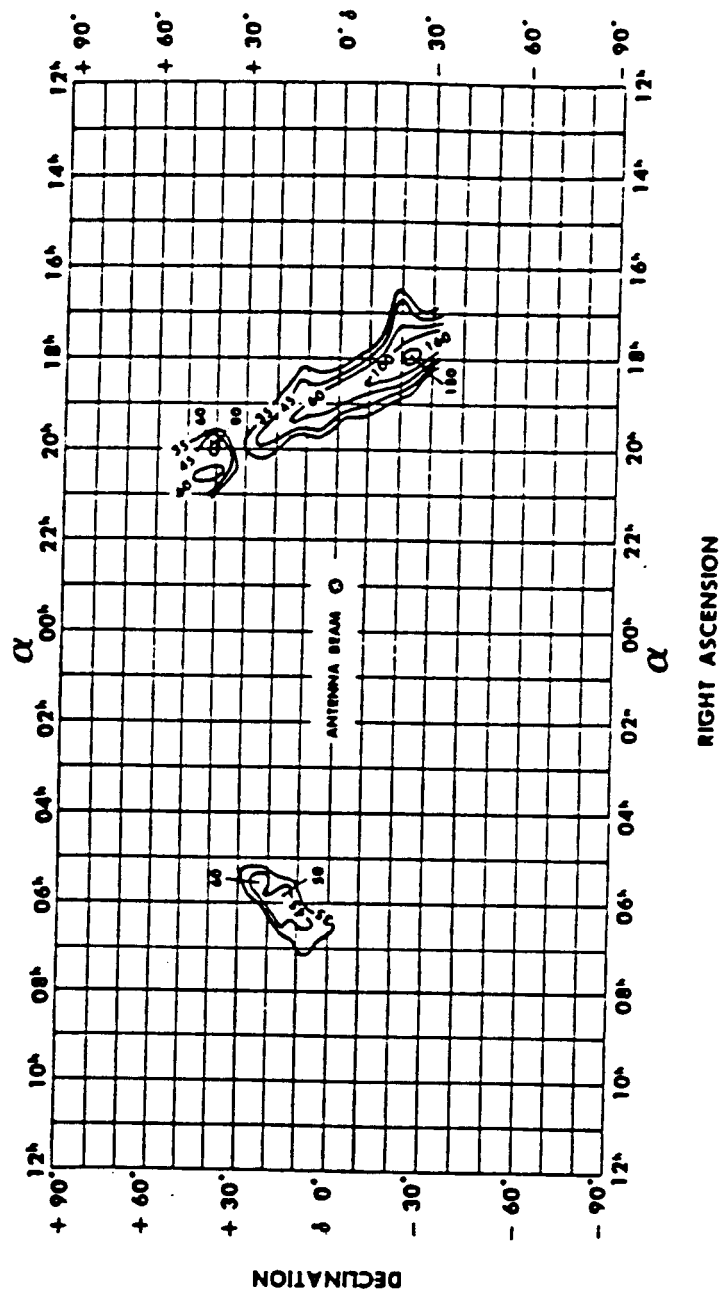
64 MC MAP
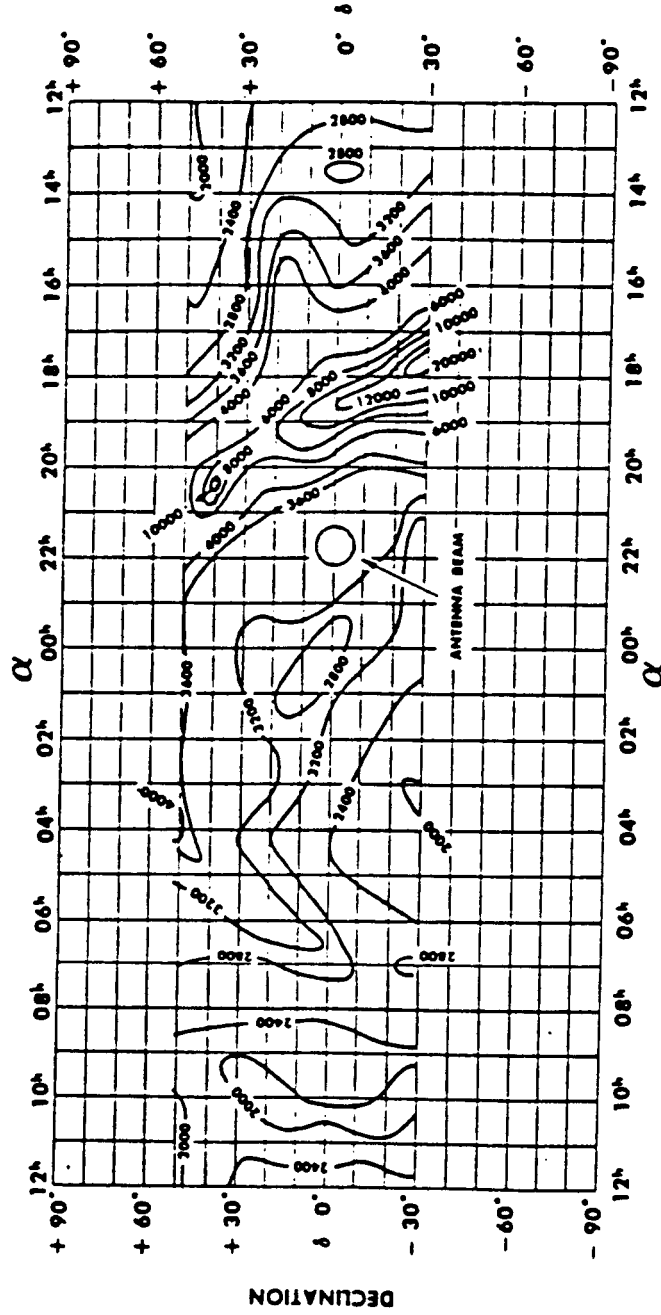
(a)

Figure 4.5. Absolute brightness temperatures of the radio sky in degrees Kelvin for (a) 64 MHz and (b) 480 MHz.

480 MC MAP

Figure 4.5 (continued).

(b)

The relative cosmic noise values were plotted on the same scale as the total number of profiler data dropouts above gate 7 for Crown hourly averaged data. Cosmic noise was not considered a problem at or below gate 7 because signal-to-noise ratios are generally high at low levels. In fact, data dropouts by hourly averaging techniques at low levels were practically nonexistent. Figure 4.6 shows the diurnal variation of cosmic noise and the strong tendency of data dropouts to occur when cosmic interference is high. Estimated cross-correlations between cosmic noise and data dropouts are shown in figure 4.7. Note that the highest correlations are found with no time lag, as was expected, and notice the diurnal variation in the cross-correlations.

The data is quite well correlated when considering that an effective sky noise temperature contains contributions from radiation emitted from the earth and atmosphere, as well as cosmic noise. Thus, although the main lobe may point at a relatively cool sky, side lobes are directed at a relatively warm and reflecting earth.

In conclusion, it is evident that there is a strong correlation between cosmic noise and profiler performance. It is also evident that even with radar data dropouts wind speed and shear profiles in and around the jet stream can be obtained far more frequently by profiling radars than by radiosondes. It also clear that radar data quality is better than that from balloons during high wind speed episodes such as jet stream passages.
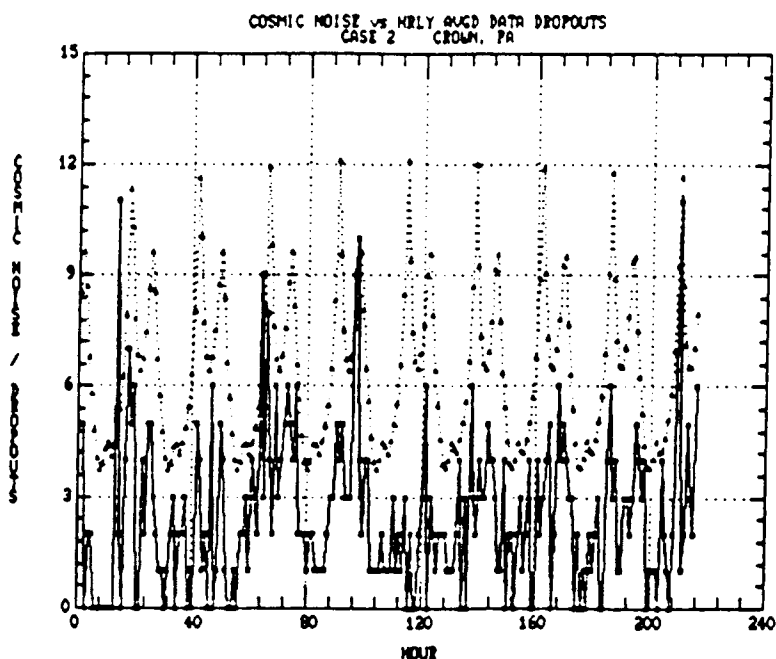
COSMIC NOISE vs HRLY AVGD DATA DROPOUTS
CASE 2   CROWN, PA

Figure 4.6.   Plot of hourly averaged profiler data dropouts (solid line) for case 2 versus relative cosmic interference.

ESTIMATED CROSS-CORRELATIONS
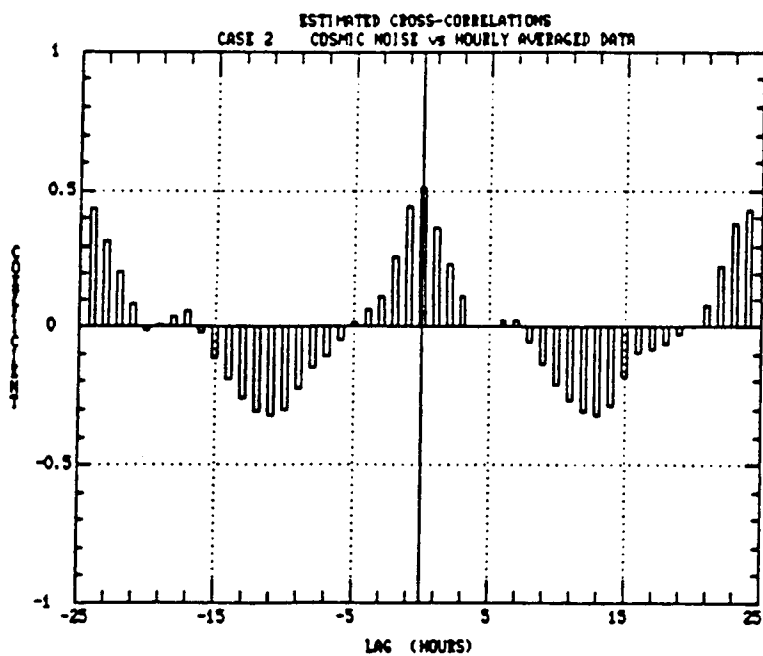CASE 2   COSMIC NOISE vs HOURLY AVERAGED DATA

Figure 4.7.   Estimated cross-correlations of the data presented in figure 4.6.

4.2 Wind Speed

Detailed observations of the wind were made by the Crown profiler and grouped according to the location of the jet axis in relation to the site. In addition, Pittsburgh radiosonde wind measurements were also stratified in this manner for direct comparison to the profiler-observed winds.

The low frequency of radiosonde observations limited the effectiveness of a statistical study on that data. However, revealing intercomparison studies could still be done between the Crown and Pittsburgh data.

Figures 4.8 through 4.12 show Crown mean wind speed profiles with standard error bars for the five categories discussed in section 2.1. The width of the error bars indicated principally whether or not trends existed in the stratified data. Narrow bars indicate relatively steady-state conditions. For example, case 2 data from figures 4.11 and 4.12 show large standard deviations at the level of maximum wind speed. This either means that the altitude of maximum wind speed changed, the maximum speed itself changed or a combination of both occurred. Observations of time-height cross-sections of wind speed indicated that speed variations with time coupled with changes in the level of maximum wind caused the apparent large error bars in both figures. Notice that the intensity and altitude of the jet stream during case 2 (figure 4.10) were very consistent for the 79 hours of observation.
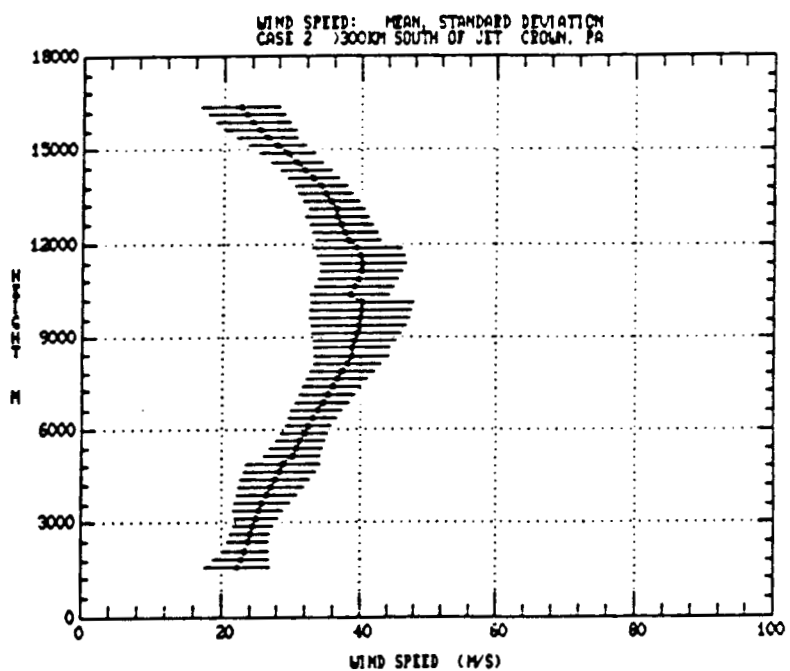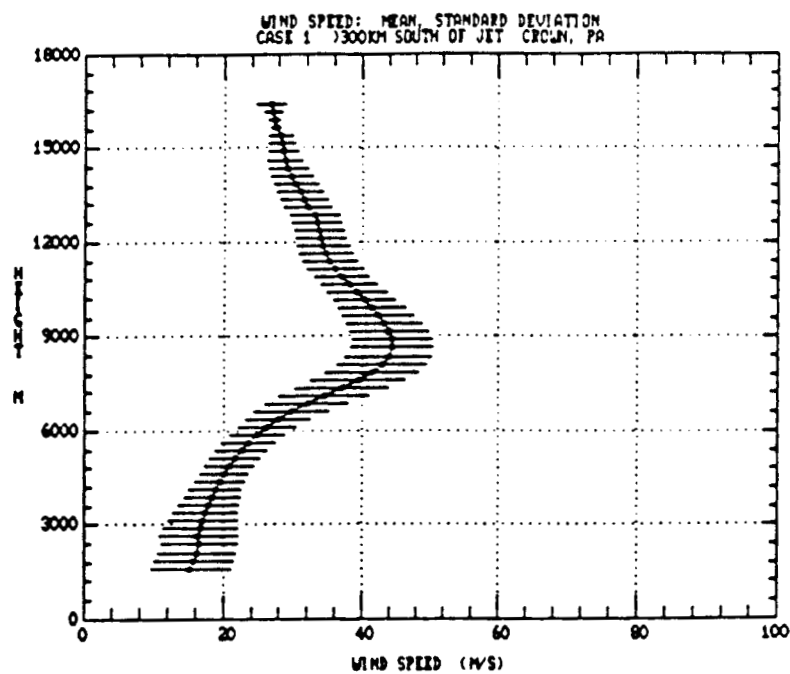
Figure 4.8.   Crown mean and standard deviation profiles of
wind speed far to the south of the jet axis for
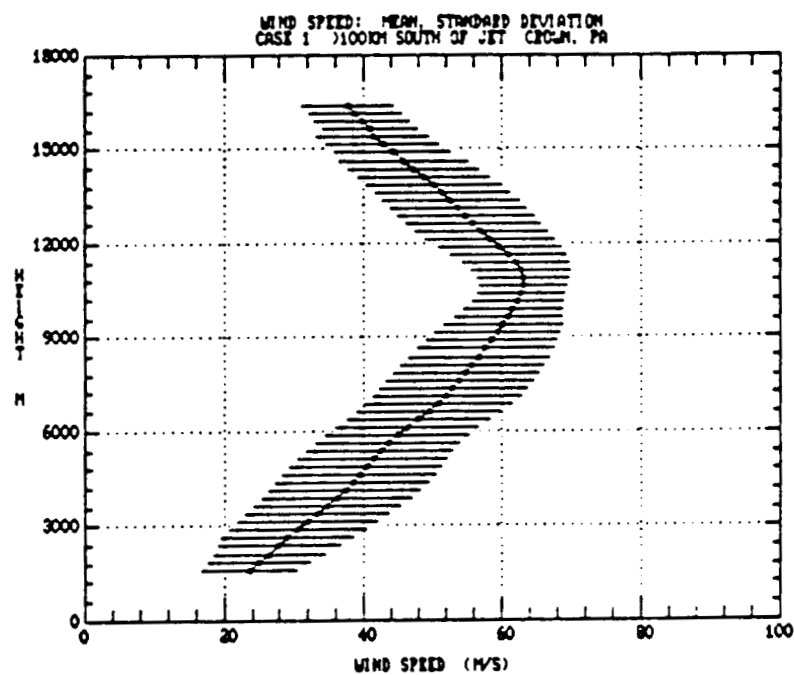cases 1 and 2, respectively.

Figure 4.9.   As in figure 4.8 but 100 to 300 km south of the jet axis. Only for case 1 since jet stream location never satisfied this criterion during the second case.
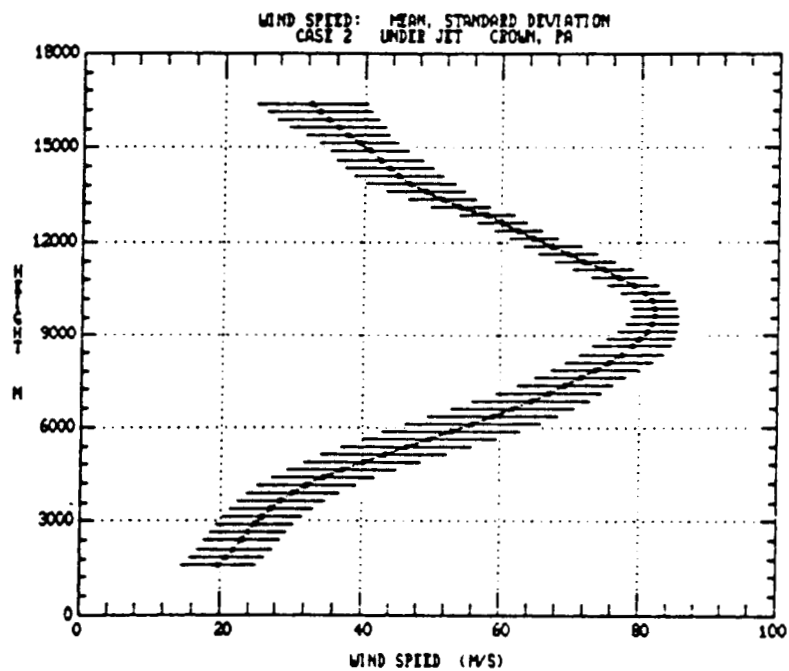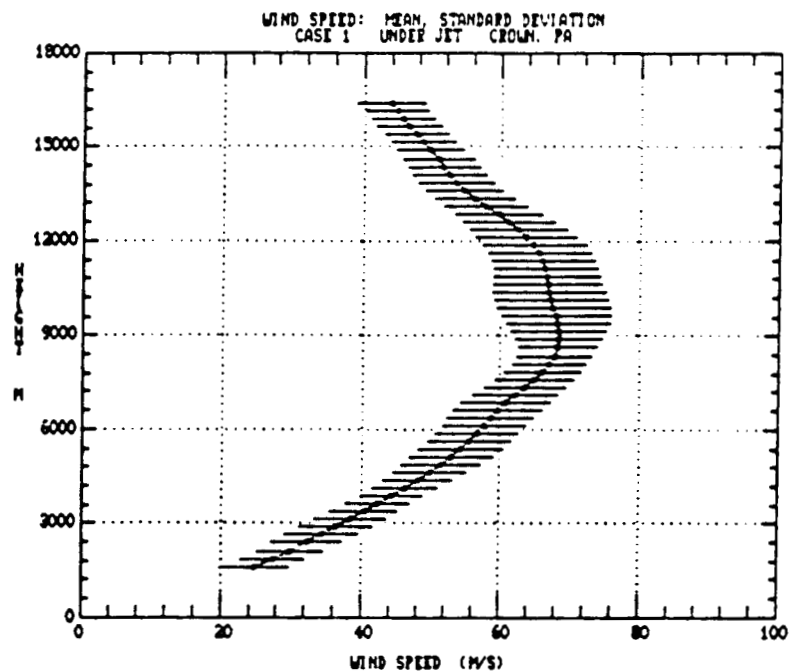
WIND SPEED: MEAN, STANDARD DEVIATION
CASE 1   UNDER JET   CROWN, PA

WIND SPEED: MEAN, STANDARD DEVIATION
CASE 2   UNDER JET   CROWN, PA

Figure 4.10.   As in figure 4.8 but within 100 km of the jet axis.

WIND SPEED: MEAN, STANDARD DEVIATION
CASE 1 >100KM NORTH OF JET CROWN, PA

WIND SPEED: MEAN, STANDARD DEVIATION
CASE 2 >100KM NORTH OF JET CROWN, PA
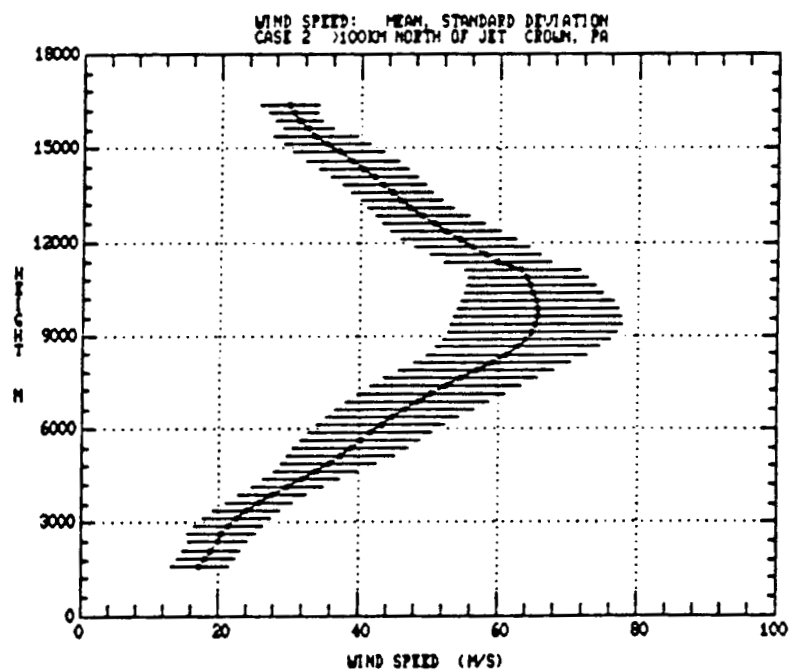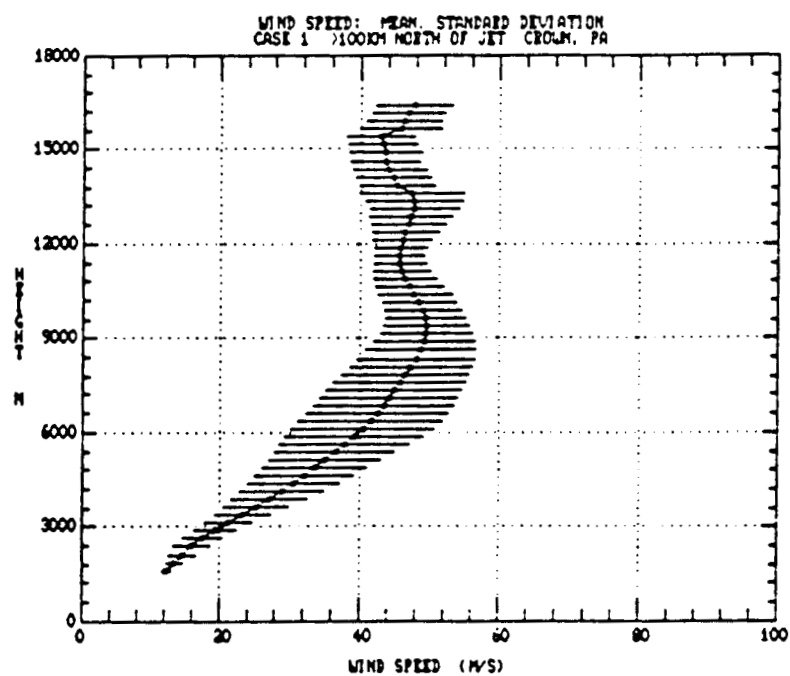
Figure 4.11. As in figure 4.8 but 100 to 300 km north of the jet axis.

WIND SPEED: MEAN, STANDARD DEVIATION
CASE 1 >300KM NORTH OF JET CROWN, PA

WIND SPEED: MEAN, STANDARD DEVIATION
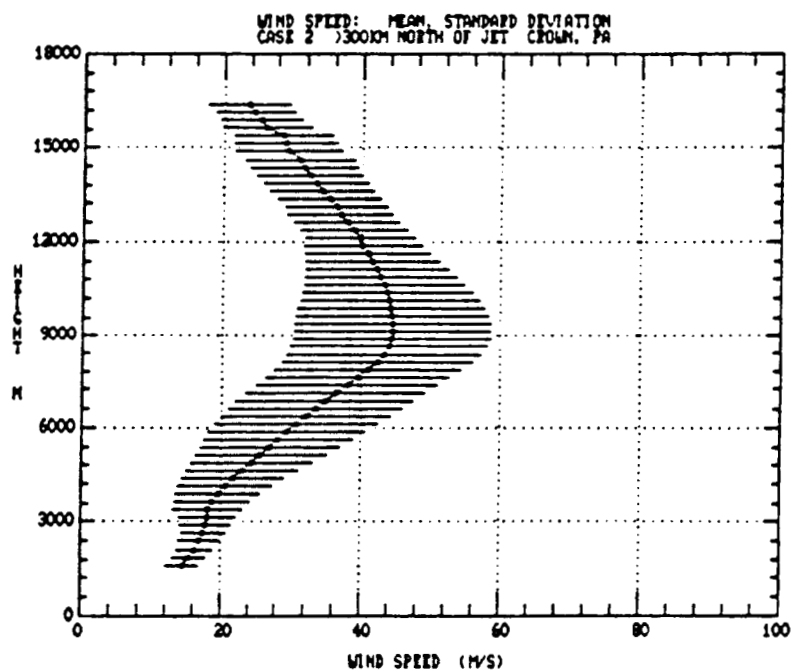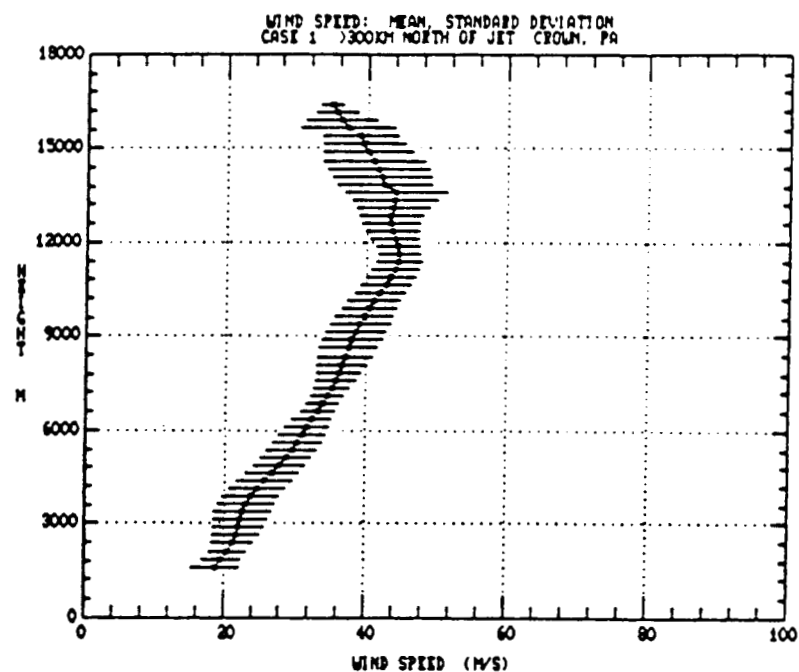**CASE 2 >300KM NORTH OF JET CROWN, PA**

Figure 4.12.   As in figure 4.8 but far to the north of the jet axis.

The shape of the profiles is also important. As a profile becomes more "peaked," the change in wind speed with height, the wind shear, increases. Notice that slopes both above and below the level of maximum wind are similar, but there is an indication that greater shear occurs below the level of maximum wind. Wind shear will be discussed in more detail in the next section.

It is also seen that slopes lessen with increasing horizontal distance from the jet axis, with the notable exception of the top plot in figure 4.8. Upper-air maps showed the jet stream to be far to the north over Canada during 7 November, but the time-height cross section of wind speed (figure 2.1a) indicated that a wind maximum did pass over Crown during the day. The level of maximum wind varied from 8.5 to 12 km with a preferred height of 9 to 10 km.

Pittsburgh profiles differed in several ways from the radar data recorded at Crown. The level of maximum wind averaged a full 2 km higher than at Crown and the "slopes" of the Pittsburgh profiles were much more variable. The variability was due to the smaller sample size and probable tracking difficulties resulting from the strong winds (section 1.4).

The most important difference between the Pittsburgh and Crown profiles was the increase in shear reported above the level of maximum wind at Pittsburgh. Figure 4.13 shows the Pittsburgh jet stream profile for case 2. Notice the higher level of maximum wind and the increased shear aloft.
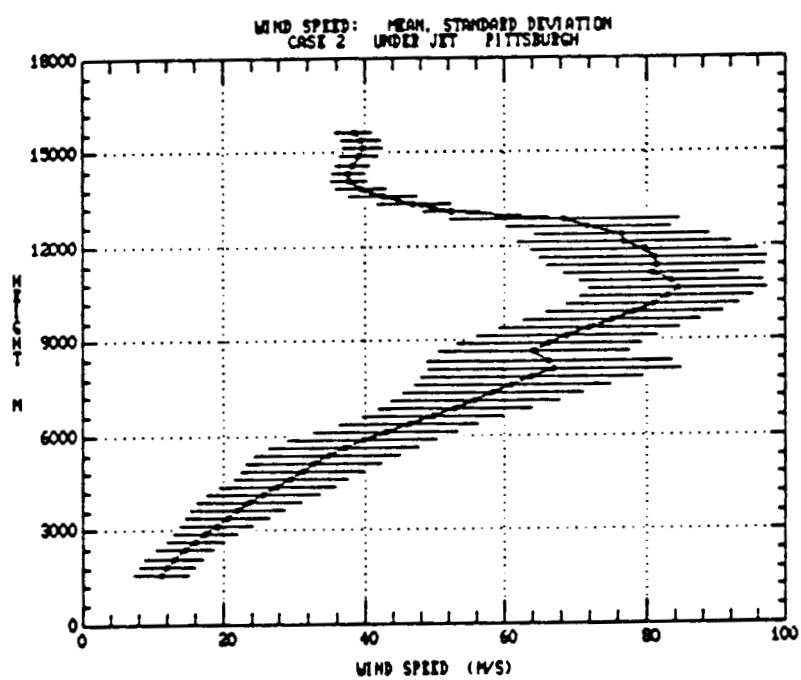
Figure 4.13.   Pittsburgh mean and standard deviation
               profile of wind speed during case 2, within
               100 km of the jet axis.

It is probable, based upon radar data and the previously

mentioned tracking difficulties, that the increased shear is

ficticious. It should also be noted that maximum wind speed

values were in good agreement between the two sites in all

cases.

4.3 Wind Shear

Following analysis of the wind speed (and direction)

profiles, wind shear statistics were compiled. The units of

measure were $ms^{-1}/500m$, chosen so that centered values could

be found every 250 m at the same heights as the speed

values, minus the endpoints, of course.

Two types of shear statistics were collected. Mean and

standard deviation profiles, similar to the speed profiles

of the previous section, were compiled along with frequency

statistics in the form of cumulative frequency diagrams and

frequency histograms. Shear data were compiled for both

cases and both sites; all values were grouped according to

jet axis location.

4.3.1 Mean and Standard Deviation Profiles

Figures 4.14 through 4.18 show Crown mean and standard

deviation profiles of wind shear for the five jet axis

location categories. As in the wind speed profiles, error

bar width indicates whether or not trends existed in the

data. Small standard deviations denote steady conditions.

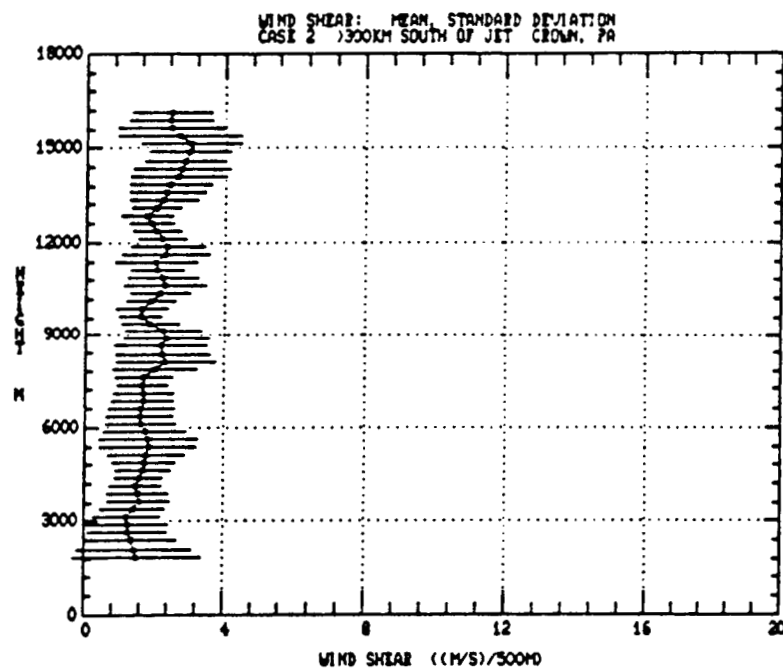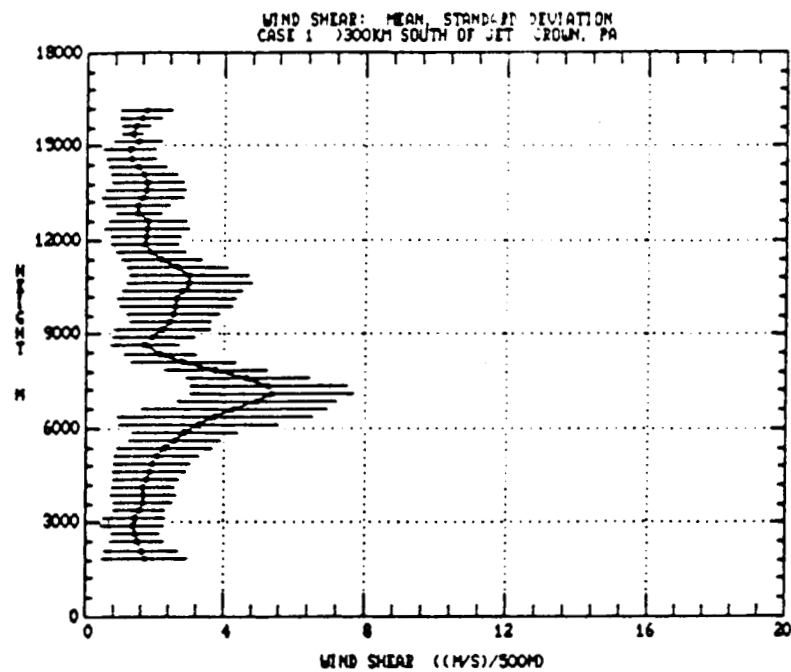Notice the reduction in shear at the level of maximum

WIND SHEAR: MEAN, STANDARD DEVIATION
CASE 1)300KM SOUTH OF JET CROWN, PA

WIND SHEAR ((M/S)/500M)

WIND SHEAR: MEAN, STANDARD DEVIATION
CASE 2)300KM SOUTH OF JET CROWN, PA

WIND SHEAR ((M/S)/500M)

Figure 4.14.   Crown mean and standard deviation profiles of
wind shear far to the south of the jet axis
for cases 1 and 2, respectively.

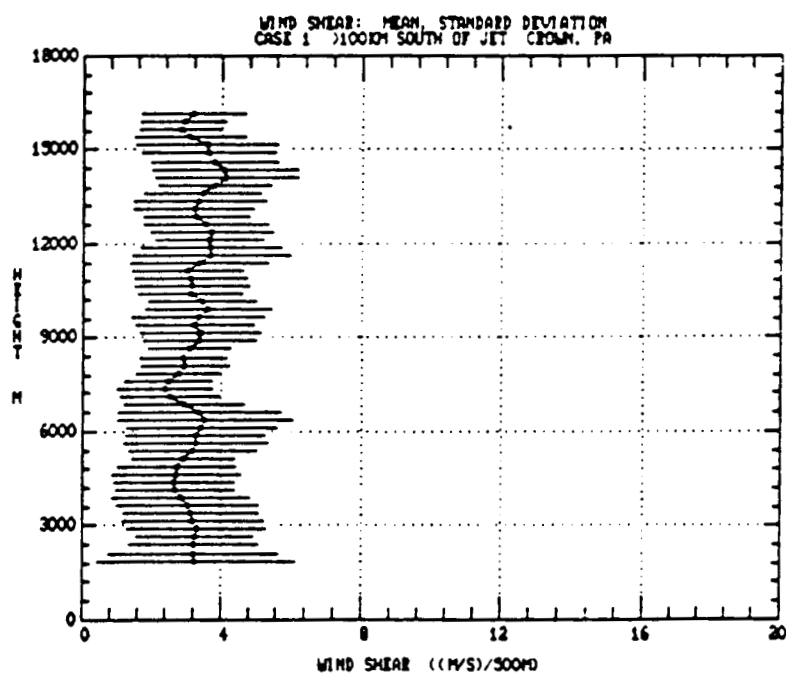WIND SHEAR: MEAN, STANDARD DEVIATION
CASE 1   >100KM SOUTH OF JET   CROWN, PA

Figure 4.15.   As in figure 4.14 but 100 to 300 km south of
the jet axis. The jet axis was not found in
this location during case 2.

WIND SHEAR: MEAN, STANDARD DEVIATION
CASE 1   UNDER JET   CRCLN, PA

WIND SHEAR: MEAN, STANDARD DEVIATION
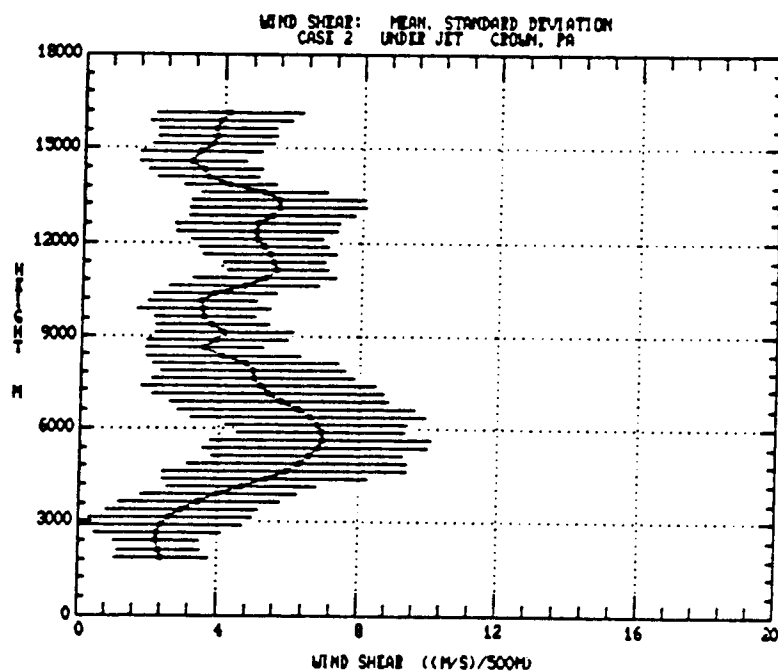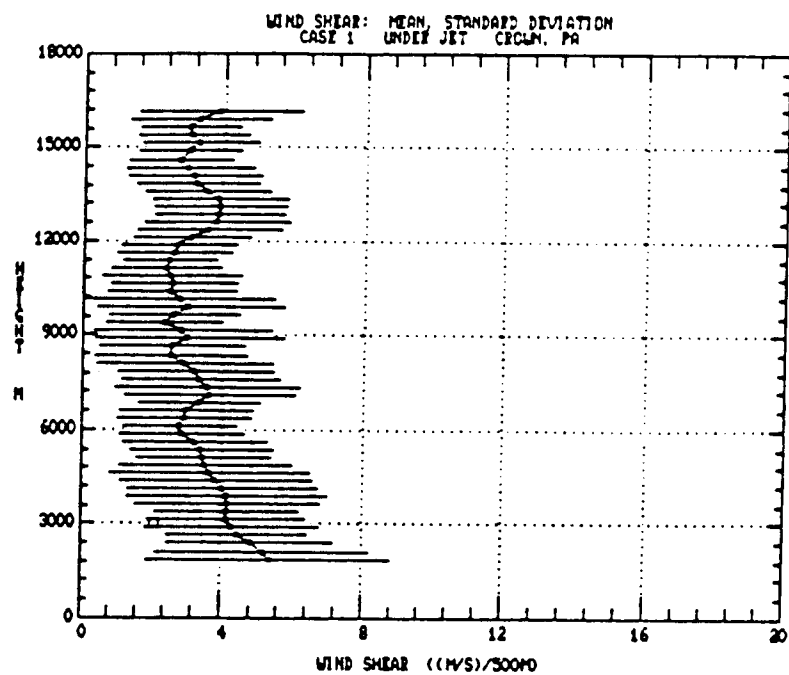CASE 2   UNDER JET   CRCLN, PA
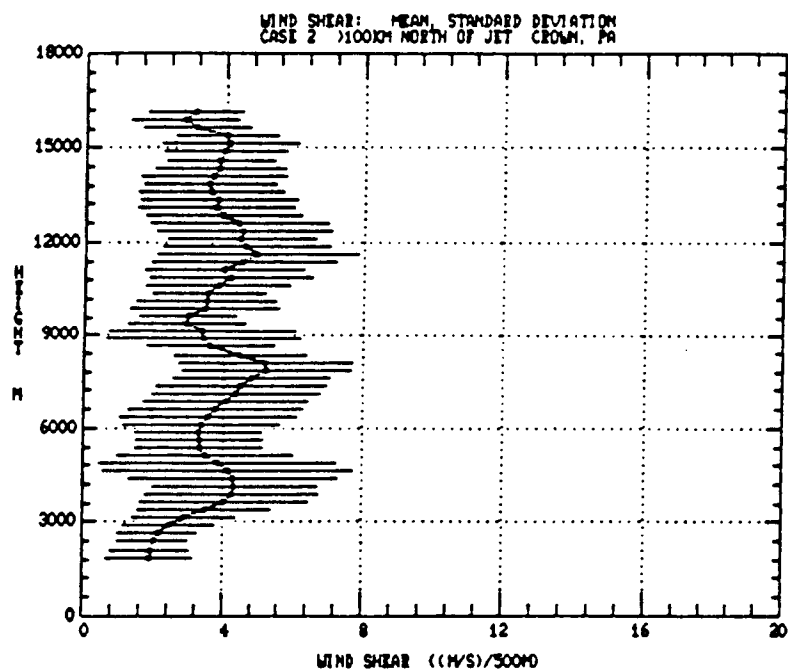
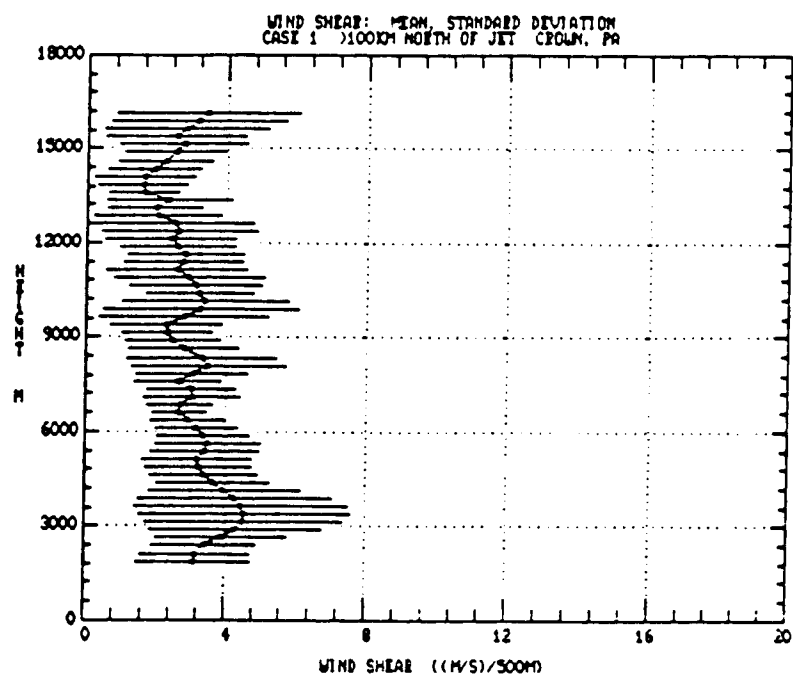Figure 4.16.   As in figure 4.14 but within 100 km of the jet axis.

Figure 4.17.   As in figure 4.14 but 100 to 300 km north of
               the jet axis.

WIND SHEAR: MEAN, STANDARD DEVIATION
CASE 1 >300KM NORTH OF JET CECUN, PA

WIND SHEAR ((M/S)/500M)

WIND SHEAR: MEAN, STANDARD DEVIATION
CASE 2 >300KM NORTH OF JET CECUN, PA
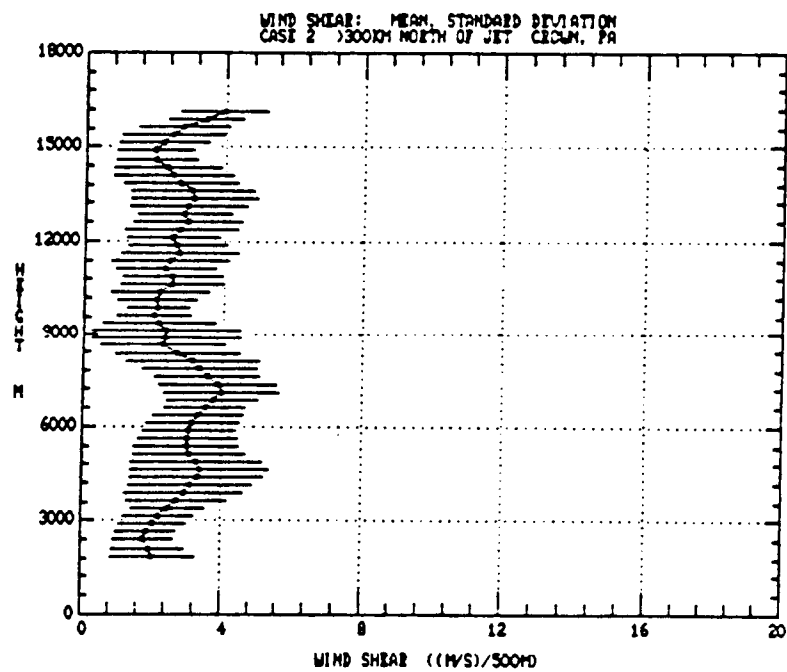

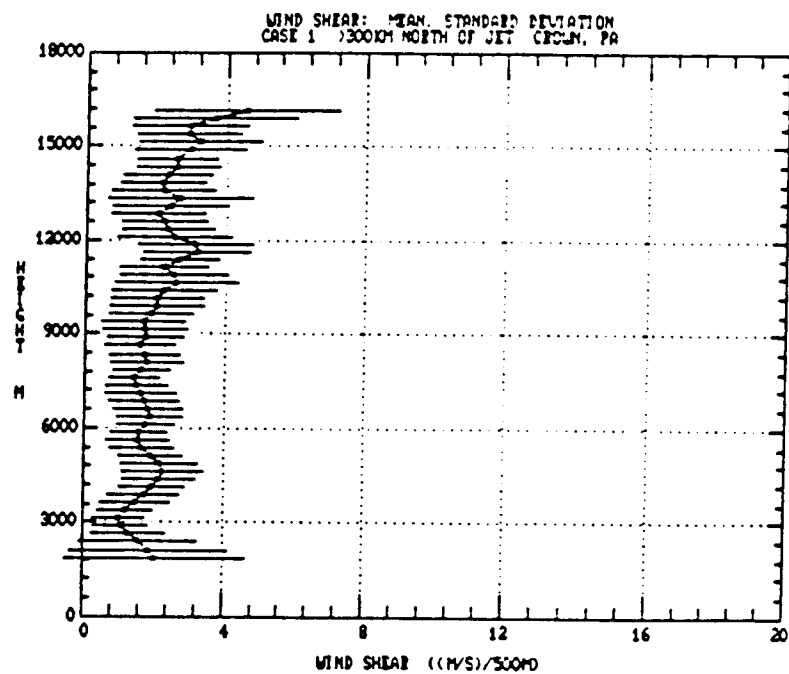
WIND SHEAR ((M/S)/500M)

Figure 4.18.   As in figure 4.14 but far to the north of the
jet axis.

wind in all figures. The minimum is especially noticeable
in the case 2 data. Also observe that the peak shears are
nearly always below the maximum wind level at about 6 to 8
km above sea level. During the first case when the jet axis
was found over or 100 to 300 km to the south of Crown, the
maximum shear values were found below 5 km, while when the
axis was far to the south, maximum shears were found above
15 km.

From this we conclude that the maximum shear level will
generally be found at a height nearly 3 km below the level
of maximum wind, but occasionally will be far-removed from
this feature. It was also found that shears are maximum
when the jet axis is located near the radar site, as was
expected. Finally, it appears that shears are more
consistent through the entire profile as the jet axis moves
farther from the site (the profiles are less bumpy).

Pittsburgh shear profiles were extremely variable.
Figure 4.19 shows the shear profile corresponding to the
speed profile in figure 4.13. Notice the very wide error
bars due to extreme variability in reported winds. A
curious feature is the small variation above 13 km. This is
easily explained by noting (figure 4.2, bottom plot) that
only two observations were made at these altitudes, thus
they must have been in good agreement with each other. The
small sample size, however, obviously precludes error
analysis of Pittsburgh data.

Some distinct differences are evident between mean

WIND SHEAR: MEAN, STANDARD DEVIATION
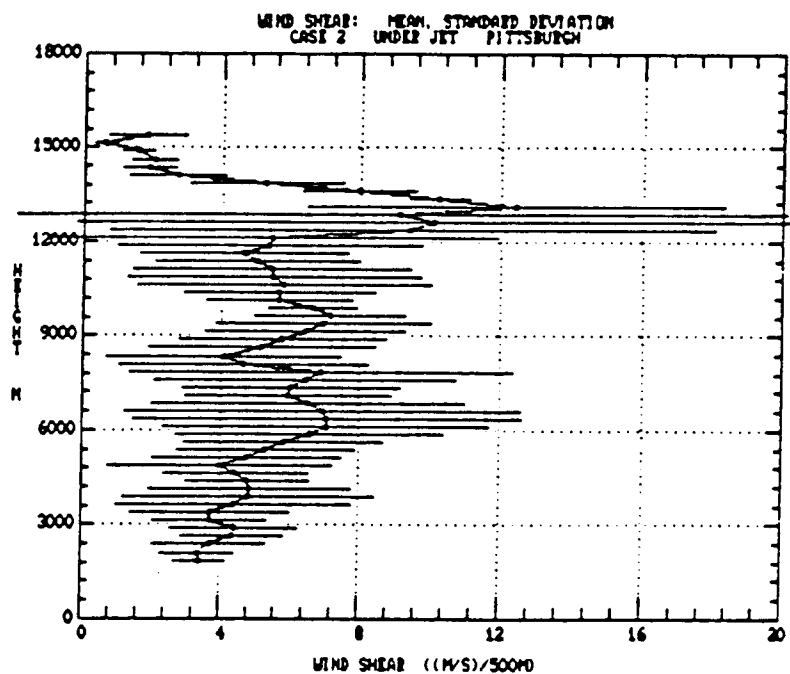CASE 2   UNDER JET   PITTSBURGH

WIND SHEAR ((M/S)/500M)

Figure 4.19.   Pittsburgh mean and standard deviation profile
of wind shear during case 2, within 100 km of
the jet axis.

profiles derived from the radiosonde and radar data. First, two-thirds of the Pittsburgh profiles show a peak in the wind shear above the level of maximum wind. It appears that radiosonde measurements tend to yield overestimates of the wind shear when the balloon is at high altitude and far down range. The resulting low elevation angles make the resulting shear measurements highly sensitive to tracking errors. From a signal processing point-of-view, a noisy signal has been twice differentiated, a risky procedure.

The wind maximum that was observed at Crown (figure 4.8, top plot) during case 1 was not as evident in the Pittsburgh data. Since the maximum value occurred at a launch time (12 UT), it is possible that the wind maximum passed to the north of Pittsburgh. This may well be the case, but a more likely explanation is that because only three observations comprised that particular Pittsburgh data set, the two made with no wind maximum present overshadowed the one that probably did show the maximum. In this case it is not the balloon data per se which is at fault but rather an insufficient number of measurements (samples) of the mesoscale feature of interest.

In summary, Pittsburgh and Crown wind shear profiles differed in two important ways. First, Pittsburgh profiles were much more variable. This result was expected since there was much less data. Second, the level of maximum shear was generally found 1 to 3 km above the level of maximum wind speed measured "at" Pittsburgh. Balloon

tracking difficulties are the most likely cause of this problem. The only similarities between Pittsburgh and Crown shear profiles were found during case 1 when the jet axis was near or to the south of both sites. In these regimes, wind shear maxima were found in the lowest 5 km of measurement at both locations, although the shear values were apparently greater at Pittsburgh.

4.3.2 Frequency Statistics

Frequency histograms and cumulative relative frequency diagrams make comparison of Crown and Pittsburgh data easier. We will focus here on data from the second case study and simply note that case 1 data showed the same features but with lesser magnitudes. Further, the most observations acquired from Pittsburgh occurred when the jet axis was nearest, thus we will further focus on the data comprising the largest Pittsburgh sample size in order to make comparisons as unbiased as possible.

Figures 4.20 and 4.21 show cumulative frequency diagrams and frequency histograms for Crown and Pittsburgh. The first critical difference is the number of observations that comprise each data set. This is the largest Pittsburgh data set and yet it makes up only 10 percent of the Crown data base.

Extreme shear values, larger than 20 ms^{-1}/500m, were recorded with both the radiosondes and the radar, but the mean shear at Pittsburgh was larger than that at Crown by 20

CUMULATIVE RELATIVE FREQUENCIES
CASE 2   UNDER JET   CROWN, PA

MEAN   =   4.6060
MEDIAN   =   4.1602
MINIMUM =   0.1077
MAXIMUM = 20.3140
NUMOBS   =   3553

WIND SHEAR ((M/S)/500M)

FREQUENCY HISTOGRAM
CASE 2   UNDER JET   CROWN, PA
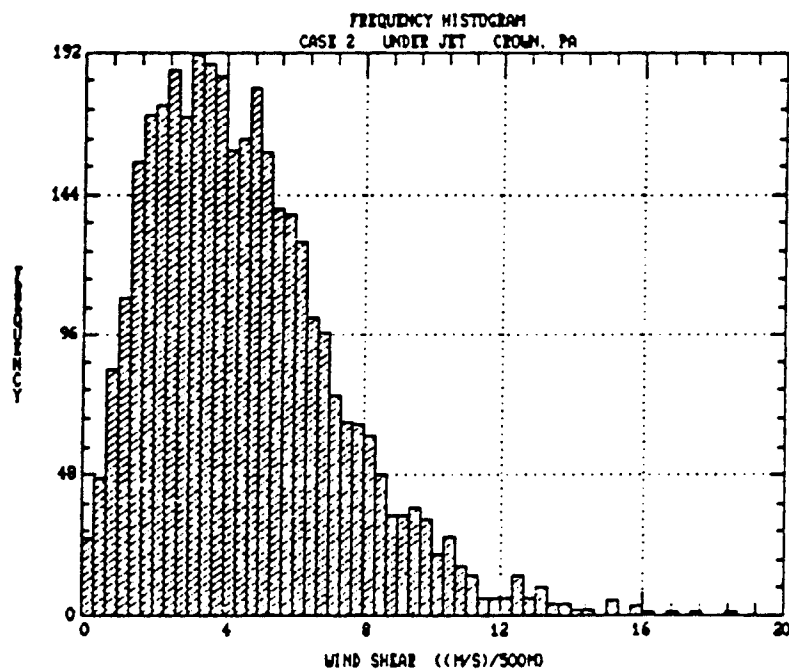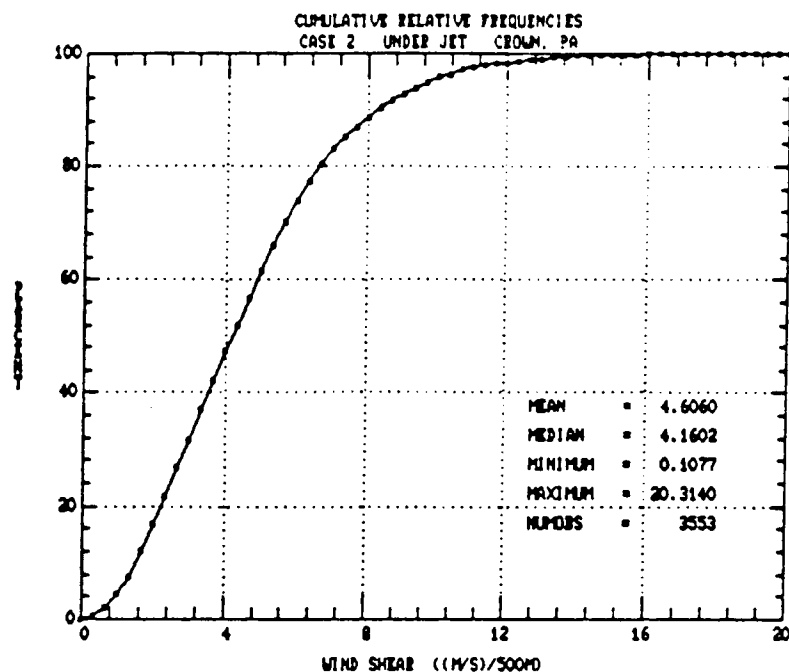
WIND SHEAR ((M/S)/500M)

Figure 4.20.   Cumulative relative frequency diagram and
frequency histogram of wind shear for Crown
during case 2, within 100 km of the jet axis.

CUMULATIVE RELATIVE FREQUENCIES
CASE 2   UNDER JET   PITTSBURGH

MEAN   = 5.5010
MEDIAN = 4.7745
MINIMUM = 0.3869
MAXIMUM = 22.0090
NUMOBS =   354

WIND SHEAR ((M/S)/500M)

FREQUENCY HISTOGRAM
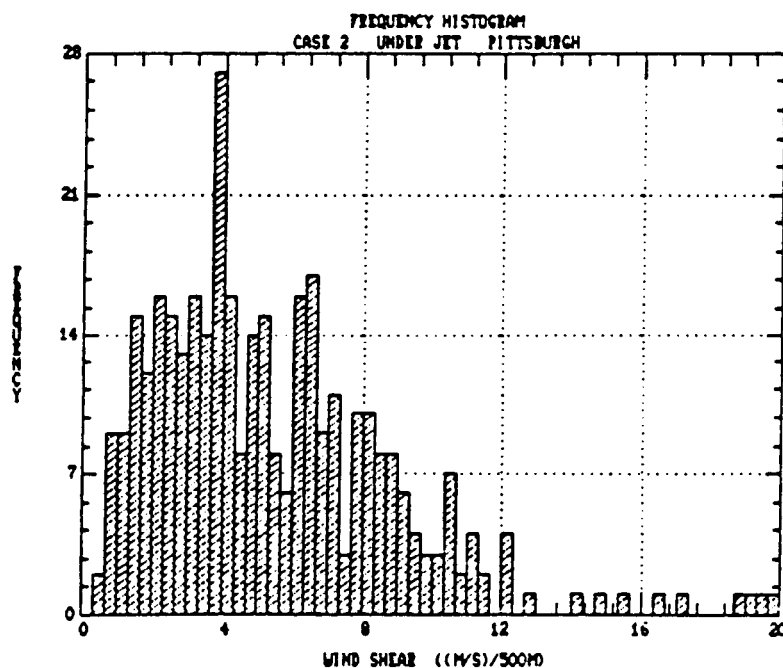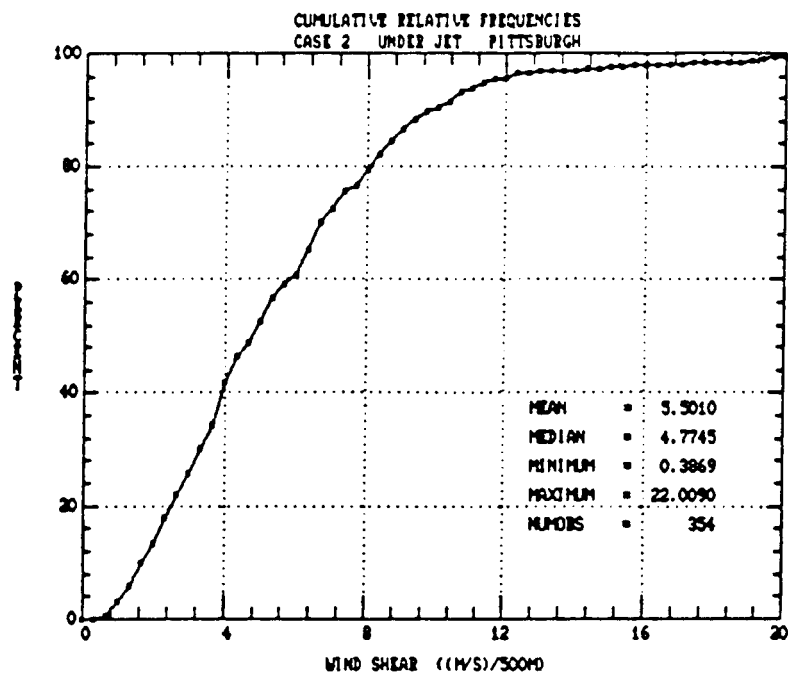CASE 2   UNDER JET   PITTSBURGH

WIND SHEAR ((M/S)/500M)

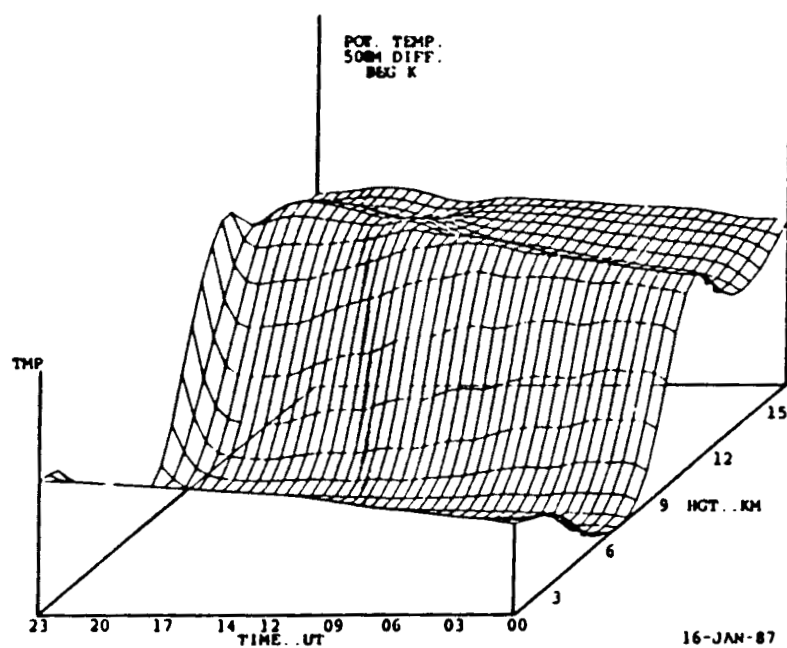Figure 4.21.   As in figure 4.20 but for Pittsburgh.

percent. This large discrepancy was due mainly to the radiosonde's overestimation of shear at upper levels, as can be seen by comparing figures 4.16 (case 2) and 4.19. The median shears also showed a rather large discrepancy, consistent with the other observations.

The frequency histograms nicely illustrate all the differences discussed above. The difference in ordinate scaling along with the general smoothness of the histograms illustrate the smaller Pittsburgh data base size. The greater relative frequency of high-shear observations at Pittsburgh can also be seen. These findings will be brought up again in a later section in the discussion of the relationship between clear air turbulence and wind shear.

## 4.4   Richardson Number Observations at Crown, Pennsylvania

The Richardson number has long been associated with turbulence. In theory turbulence is created when the Richardson number falls below a critical value of 0.25. However, it has been argued (Colson, 1966; Kennedy and Shapiro, 1980) that the magnitude of the Richardson number is largely dependent on the resolution of the data used to compute it. The results of testing the validity of this argument are given in this section.

Figure 4.22 shows surface plots of potential temperature gradient, wind shear and Richardson number for 16 January 1987. Observations of figures such as these indicated that Richardson number values were strongly

POT. TEMP.
500M DIFF.
DEG K

TMP

TIME..UT

23   20   17   14 12   09   06   03   00

15

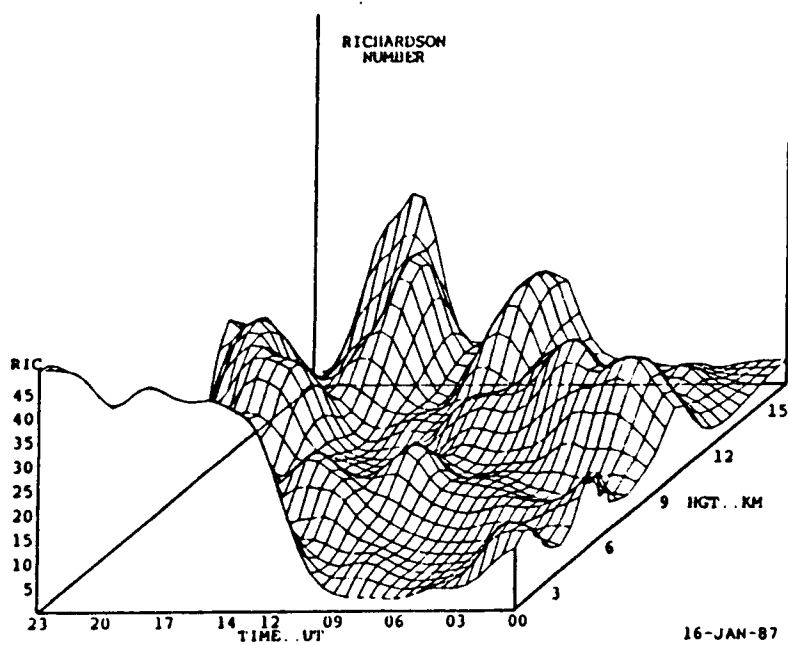12

9   HGT..KM

6

3

16-JAN-87

(a)

Figure 4.22.   Surface plots of (a) potential temperature
gradient, (b) wind shear and (c) Richardson
number above Crown on 16 January 1987.
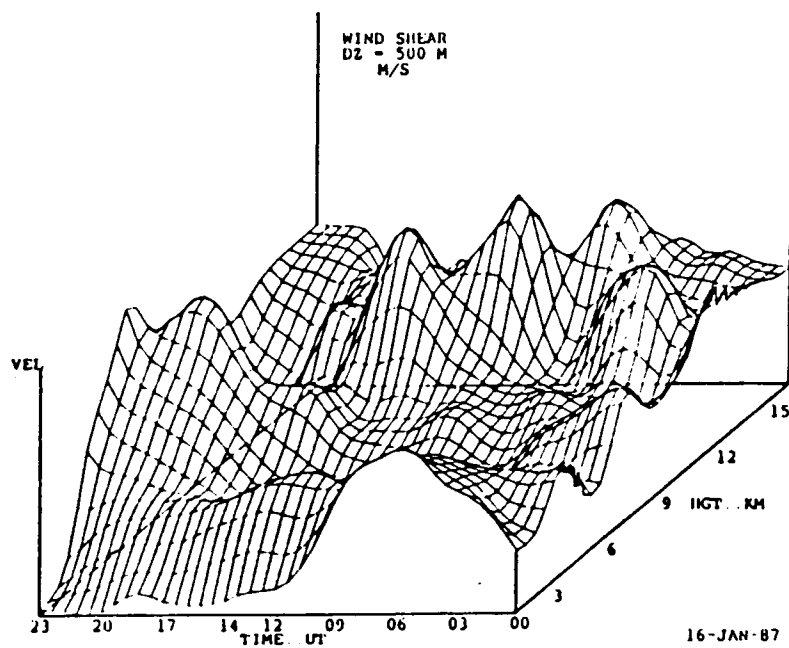
(b)

(c)

Figure 4.22 (continued).

dependent upon values of the wind shear. Measurements of
the interpolated potential temperature indicated only slow
variations in potential temperature gradients with time.
Note also the inverse relationship between wind shear and
Richardson number. Given the sensitivity of the Richardson
number to the shear, we felt that comparison of Richardson
number statistics between sites was unnecessary. Wind shear
comparisons would serve the same purpose. Richardson
numbers were thus computed only for the Crown measurements.
The results of those evaluations are presented in the same
format as the wind shear data.

4.4.1 Mean and Standard Deviation Profiles

As expected, Richardson numbers showed huge variations
in magnitude. When shears were exceedingly small,
Richardson numbers of over 10,000 were computed. Values of
this magnitude would render mean and standard deviation
profiles useless if they were included. Thus, profiles were
computed by arbitrarily setting a maximum value equal to 50.

Only data from the second case are shown because all
the structural and statistical features of case 1 data were
evident in this data set. The only exception was that
during case 2 the jet stream was never located 100 to 300 km
to the north of Crown. Case 1 data were thus used to fill
this gap.

In figures 4.23 through 4.27 mean and standard
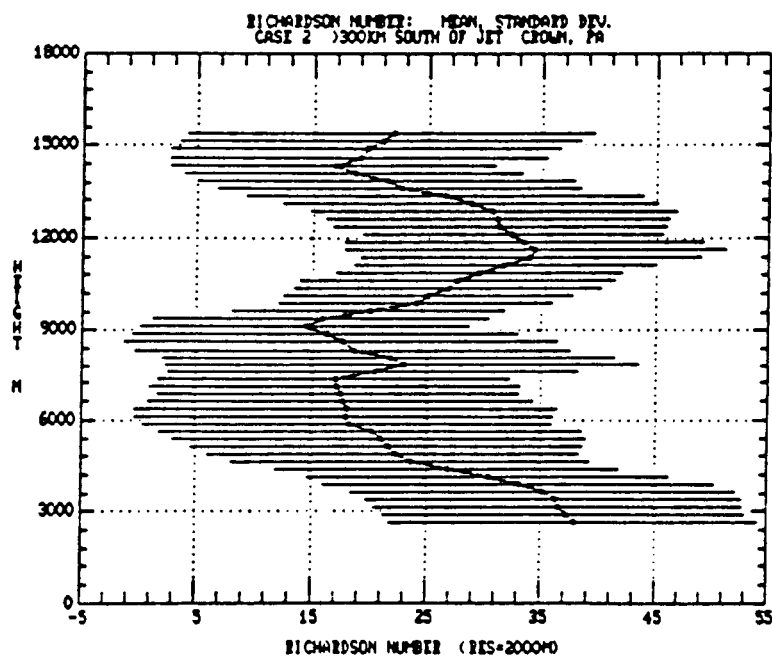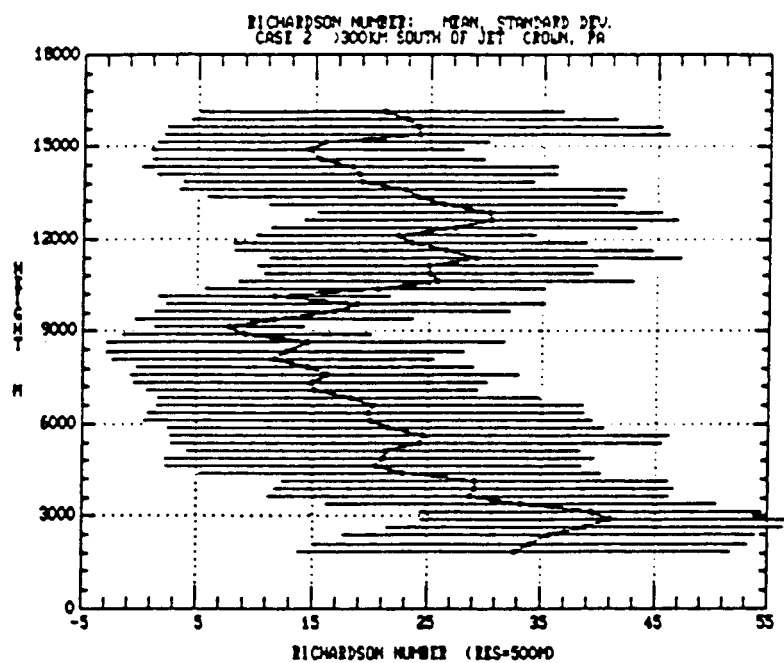deviation profiles of the Richardson number are shown for

Figure 4.23.   Crown mean and standard deviation profiles
of Richardson number during case 2, far to the
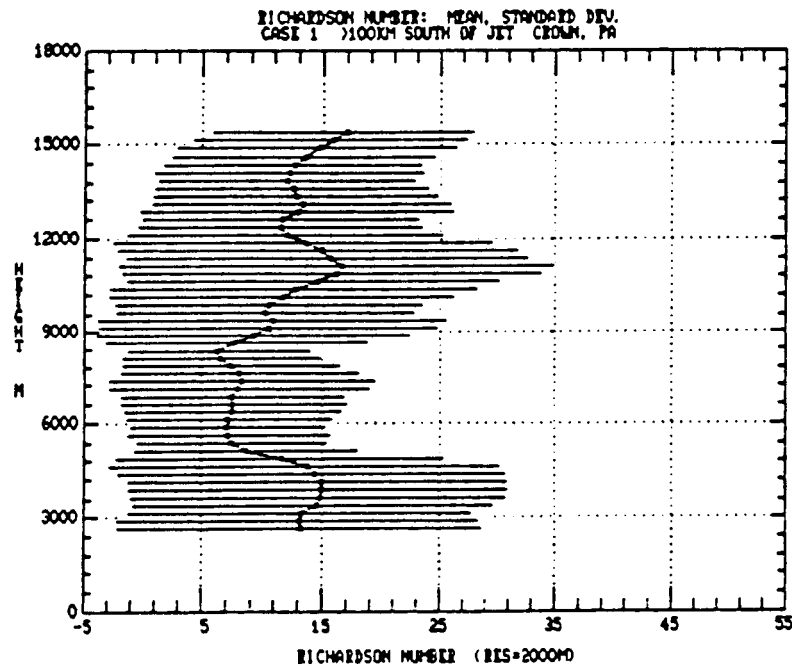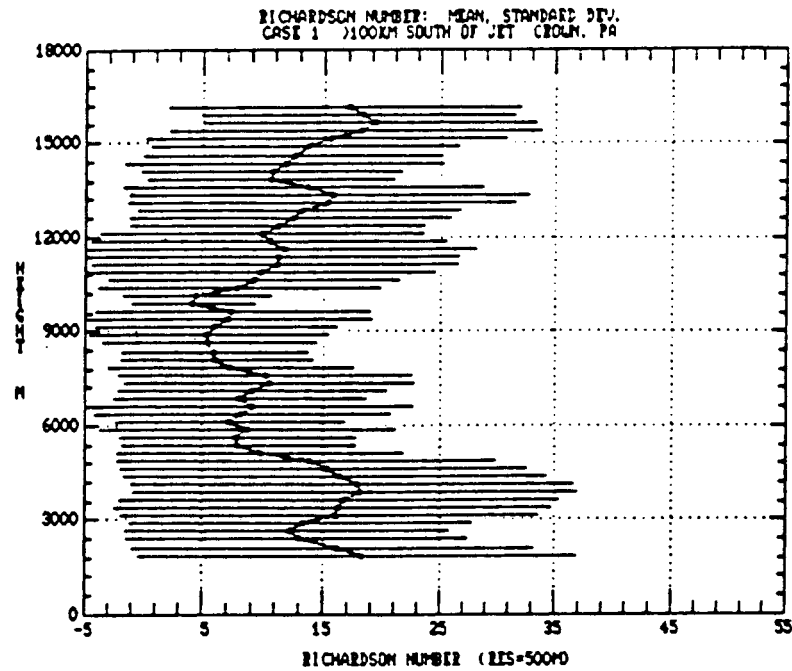south of the jet axis: 500- and 2000-meter
resolution.

Figure 4.24.   As in figure 4.23 but during case 1, 100 to
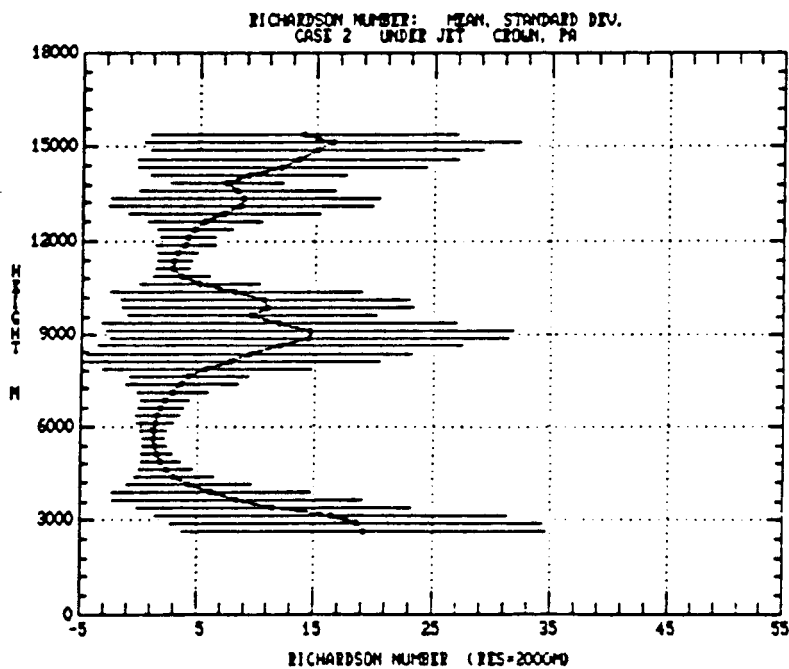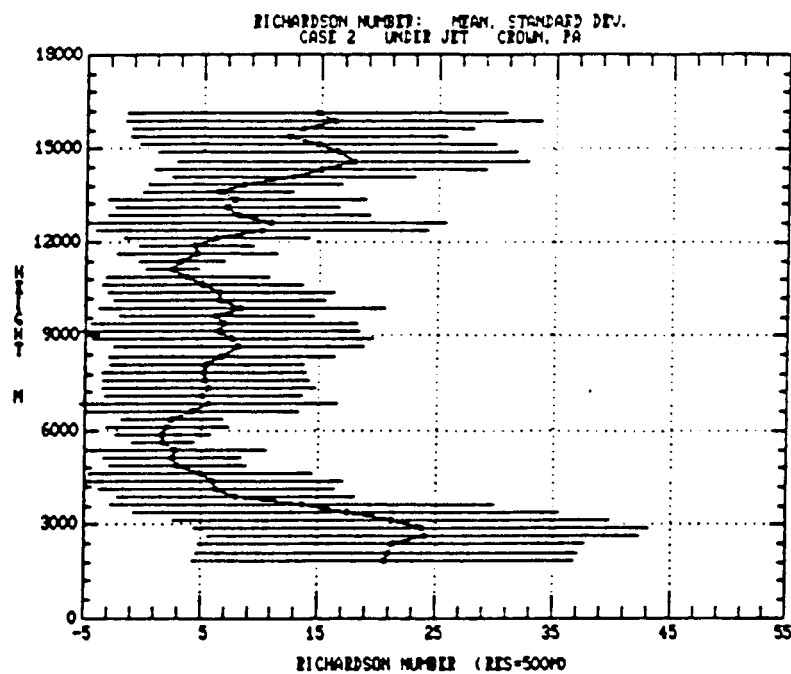300 km south of the jet axis.

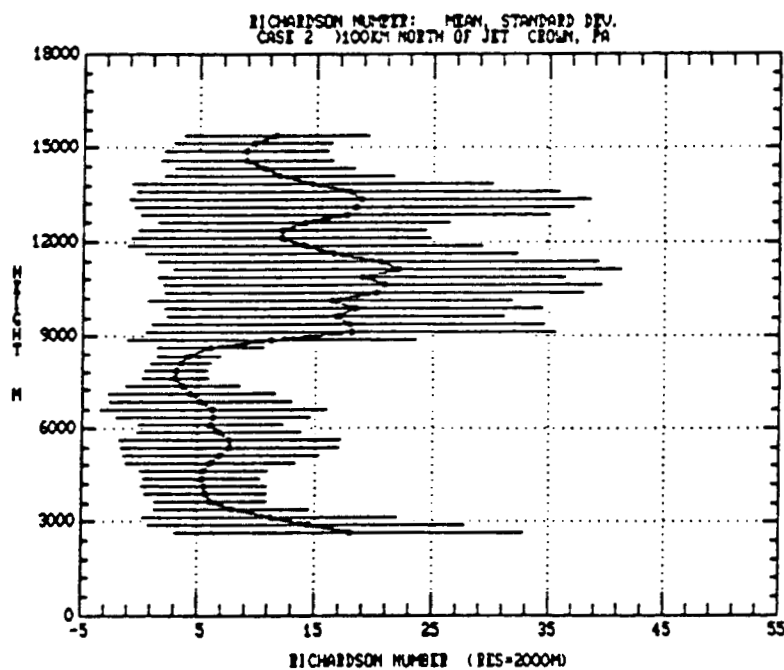Figure 4.25. As in figure 4.23 but within 100 km of the jet axis.
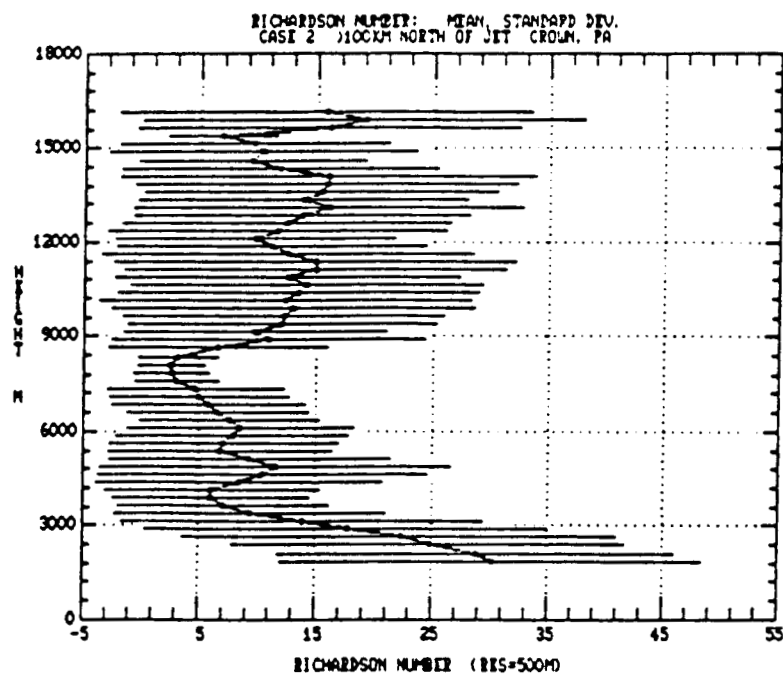
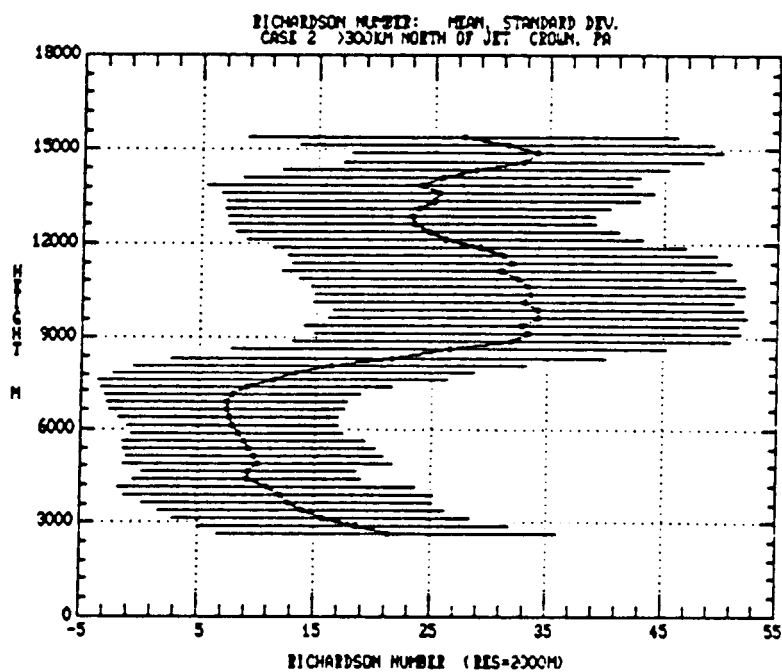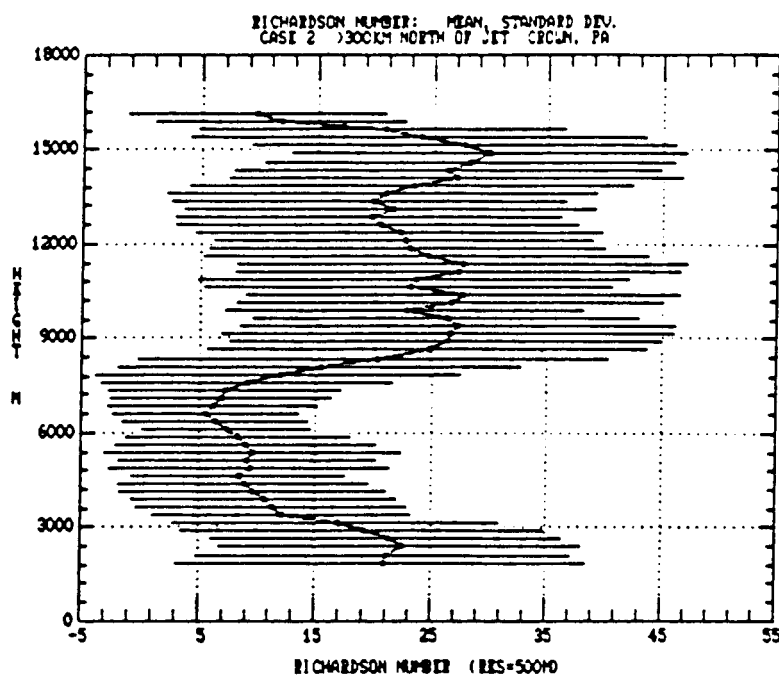Figure 4.26.   As in figure 4.23 but 100 to 300 km north of the jet axis.

Figure 4.27. As in figure 4.23 but far to the north of the jet axis.

vertical resolutions of 500 and 2000 m. Let us examine the differences in profile structure as they relate to jet stream position before comparisons are made between values computed with different resolutions.

Comparisons of appropriate mean wind shear profiles with 500-meter resolution Richardson number profiles revealed the same inverse relationship between shear and Ri as was evident in figures 4.22b,c. Figure 4.28 shows a direct comparison of shear and Ri for the first case study when the jet stream was located far to the north of Crown. Notice the minimum in Ri at the same altitude as the shear maximum. Further comparison shows that the Ri maximum at 9 km corresponds to the wind speed maximum shown in figure 4.8 (top plot). A comparison between wind speed and Ri is not intended, but it has been shown that Richardson numbers are increased at the level of maximum wind, where shears are decreased. Recall from section 4.1 the decreased profiler performance at this level.

By comparing figures 4.23 through 4.27, one can see that the Richardson number generally decreased at all levels as the jet stream approached the radar. In all regimes there were local maxima of Ri of varying depth which seemed to be associated with the level of maximum wind speed. The maxima tended to be located above the absolute minimum of each profile. These were found between 6 and 10 km, corresponding to the maximum shear zones. The depth of the layers containing high Ri values increased as the distance
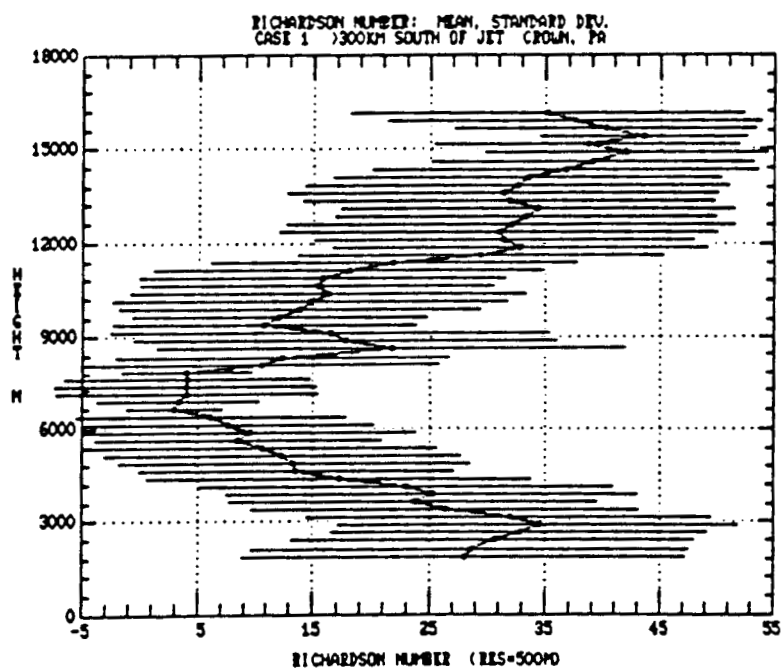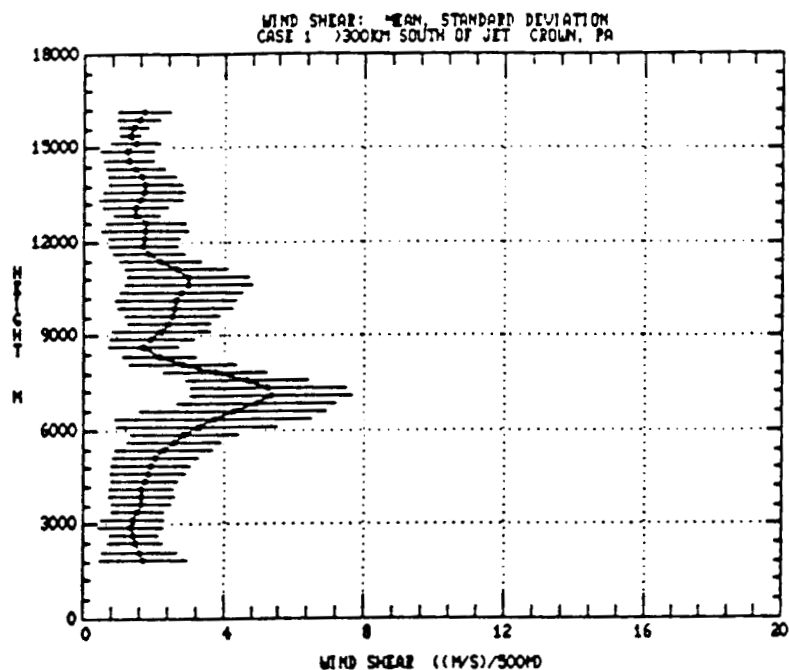
Figure 4.28. Crown mean and standard deviation profiles of wind shear and Richardson number during case 1, far to the south of the jet axis.

from the jet axis increased. The altitude of minimum Ri generally decreased as the jet stream moved from north of the site to south of the site.

Minimum mean Ri values approached 1 in fairly shallow layers (less than 1 or 2 km deep) when the jet axis was within 100 km of the site. Kennedy and Shapiro (1980) determined a critical Ri of slightly less than 1 for data with resolution comparable to our higher resolution observations, thus in at least these layers turbulence generation was probably likely.

An important result was the critical dependence of the inferred Ri on the data resolution. There was an increase in variability (noise) of the mean profiles as resolution was improved. Thus, the general large-scale patterns were easier to find with 2000-meter data; the increase in Ri at the level of maximum wind was better defined with the low-resolution data (Compare figures 4.35 and 4.36.).

From the frequency diagrams it is clear that a 230-percent increase in observationally critical Ri values (Ri less than about 0.7) were calculated for the higher resolution data when the jet stream was within 100 km of the site. This means that determination of critical Ri is strongly dependent upon data resolution. Pilot reports of turbulence, to be detailed in the next section, were found in some cases to correspond with Ri values much larger than 1. Thus we believe that in order to achieve experimental results which will be consistent with a theoretically

critical Ri value of 0.25, much better spatial (vertical) resolution will be required than the 300- or 900-meter currently available with the VHF wind profilers.

4.4.2 Frequency Statistics

Frequency histograms facilitate easy comparisons between data of different resolution. Figures 4.29 and 4.30 show the histograms for case 1 and case 2 data when the jet stream was within 100 km of Crown. Note the 230-percent increase in observationally critical Ri values for the higher resolution data, found in the first column of each histogram. Also note that the shapes of the frequency distributions are similar, all plots show a peak frequency between Ri values of about 1 and 3, regardless of resolution. Mean and median values of 500-meter data were nearly equal to those of the lower resolution data, thus the only difference was in the number of small values of Ri computed. Note also that the histograms of the stronger second case peaked at lower values and the frequency of occurrence of high Ri decreased more rapidly. The mean Ri of case 1 was approximately 13, for case 2 a mean value 8 was found.

The peak frequency shifted to higher Ri values as distance from the jet stream increased, while the number of critical Ri observations dramatically decreased. During times when the jet stream was 100 to 300 km from the site, there was a 300-percent increase in critical Ri's for the better resolution data. When the jet stream was far away
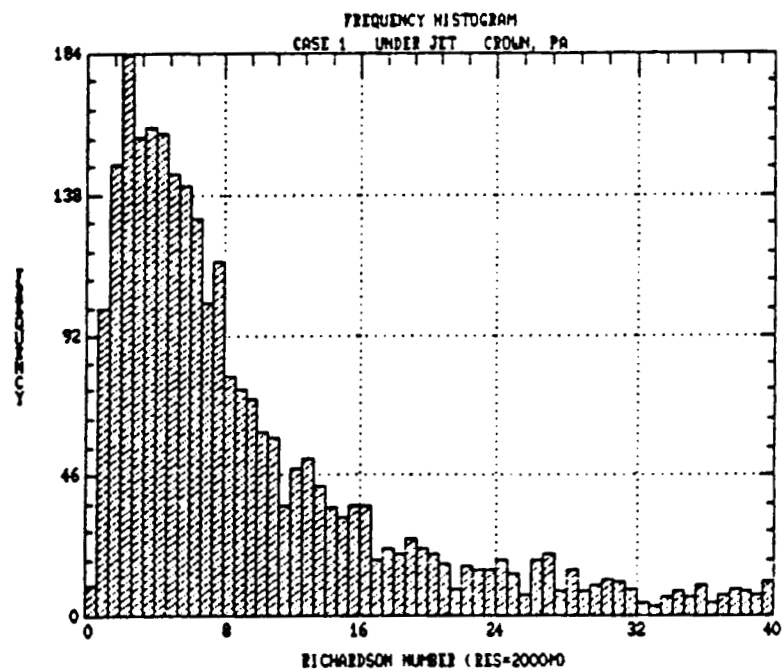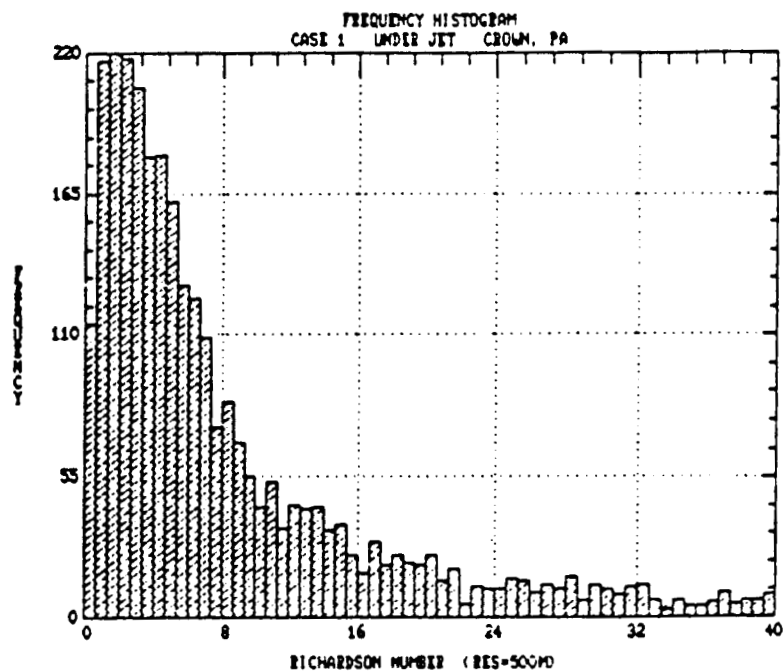
Figure 4.29. Frequency histograms of Richardson number for Crown during case 1, within 100 km of the jet axis: 500- and 2000-meter resolution.
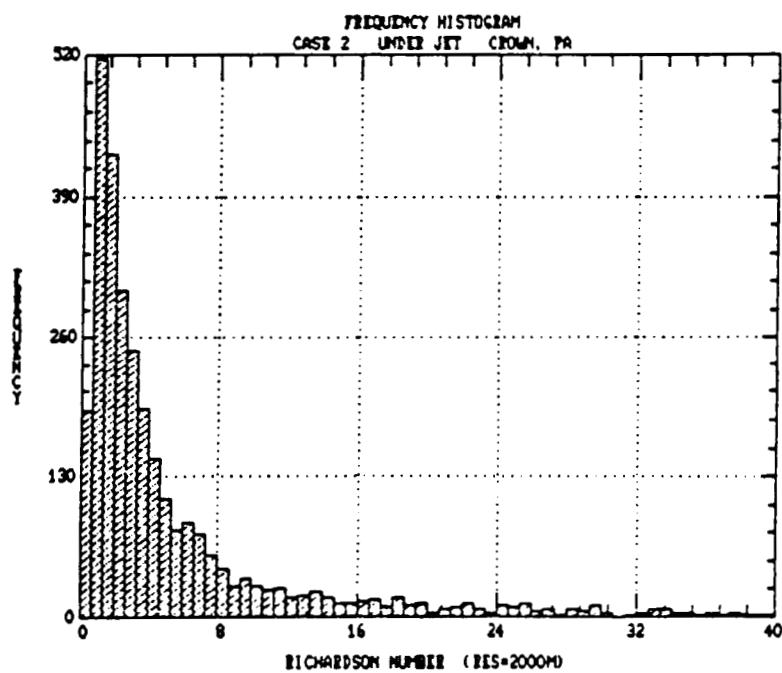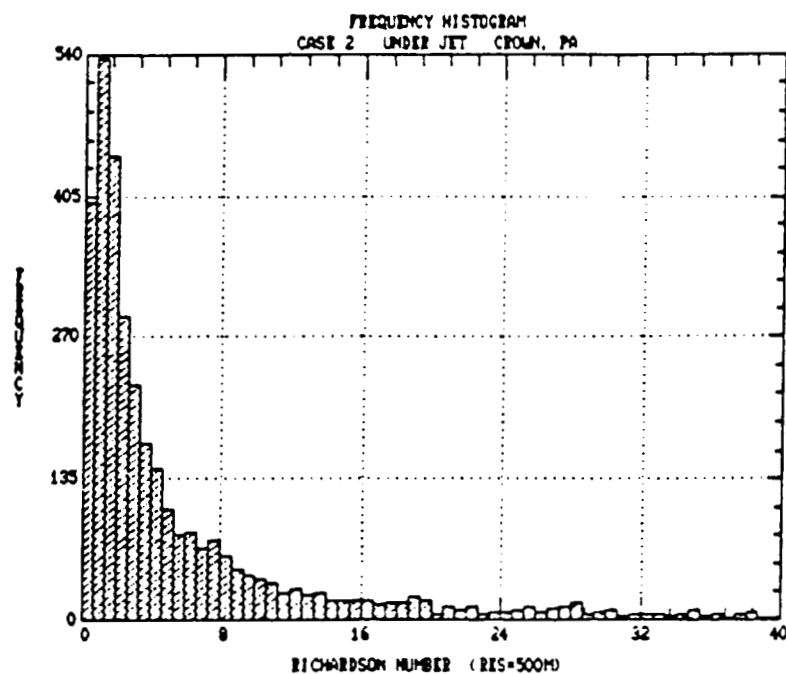
Figure 4.30. As in figure 4.29 but during case 2.

there were almost no critical Ri's at either resolution.

Scatterplots of Richardson number parameters, the temperature contribution (numerator) versus the shear contribution (denominator), provided valuable information that could not be extracted from the other plots. Aspects of temperature structure and the number of theoretically critical observations could be obtained. Figure 4.31 was computed from case 2 data when the jet stream was within 100 km of Crown. It is included because the maximum number of critical Ri observations occurred in this case.

From the scatterplots we can easily see the occurrence of maximum wind shears in regions of low static stability. It is generally believed that wind shears are usually maximum in the vicinity of upper-tropospheric fronts, where high static stability is found. But in this study this was not found in more than half of the data sets. Figure 4.22a shows a minimum in the potential temperature gradient at 6 km, the level of maximum shear, on the average. Other temperature plots showed similar structure.

We believe that in this case the interpolated sounding procedure failed to adequately resolve the details of the internal front(s) above Crown. Vertical resolution of the temperature sounding was 50 mb throughout the layer between 1000 and 100 mb. This translates to 1000-meter resolution at 6 km MSL. It is also possible that the frontal structure above Crown could have been absent, or weaker downwind of the radiosonde stations in the regions from which the

SCATTERPLOT OF Ri PARAMETERS (RES=500M)
CASE 2   UNDER JET   CROWN, PA

SCATTERPLOT OF Ri PARAMETERS (RES=2000M)
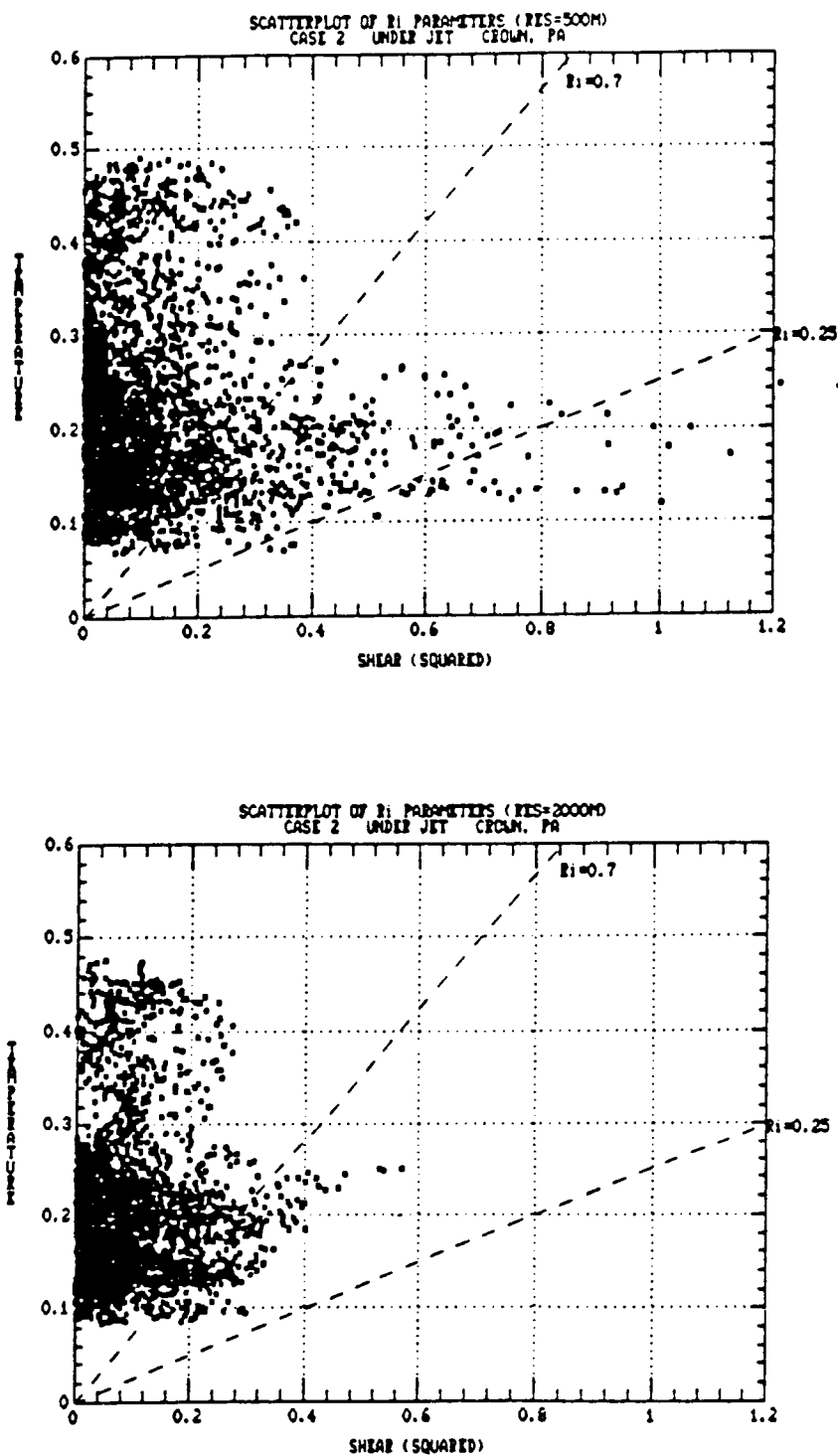CASE 2   UNDER JET   CROWN, PA

Figure 4.31.   Scatterplots of Richardson number parameters for Crown during case 2, within 100 km of the jet axis: 500- and 2000-meter resolution. Units of the values on the axes are $10^{-3}s^{-2}$.

interpolated soundings were deduced.

Notice the difference in the number of critical Ri values (to the right of the "Ri=0.7" line) and, especially in the theoretically critical values (to the right and below the "Ri=0.25" line) caused by the resolution difference. Nearly 40 values less than 0.25 were found with the higher-resolution data as compared to none for 2000-meter data. The data points were more densely packed to the left, low-shear side, as distance from the jet stream increased.

Fairall and Markson (1985) plotted preferred values of radiosonde-derived Ri parameters on a graph scaled similarly to these scatterplots. With some imagination, agreement between the quantities derived from the radar in this study and those from radiosondes can be seen when comparing graphs. Analysis of the scatterplots indicated that there was a lack of data at intermediate values of static stability. Preferred values were found at low static stabilities and again at very high stabilities. Figure 4.22a reveals the reason for this occurrence. Notice that there is a "leveling off" of the temperature gradient in regions of low and high static stability (low and high altitudes). A steep slope is found in the temperature gradient at mid-levels. Thus, a layer only one or two km deep is moderately stable.

We are not the first to note that Richardson number measurements are highly resolution-dependent. Measurements by Kennedy and Shapiro (1980) showed an average Ri value of

0.71 in turbulent zones. They had expected values closer to the critical value of 0.25 and deduced that underestimation of wind shear from the aircraft caused the discrepancy. Aircraft measurements of shear are also uncertain and quite noisy. We believe that the use of wind shear values, instead of Ri values which are dependent upon the square of the shear, are likely to be more practical when one is attempting to develop relationships between measured parameters and the presence or likelihood of clear air turbulence. Colson and Panofsky (1965) also had found vertical shear to be the best indicator of clear air turbulence.

4.5 Pilot Reports of Clear Air Turbulence in Relation to Crown Wind Shear Values

Clear air turbulence is an expensive and sometimes life-threatening occurrence that affects the entire aviation industry. The causes and favored locations for CAT are known (section 1.3). The various CAT detection methods which exist are only marginally satisfactory.

Balloon measurements of wind shear have been shown to be inadequate because of poor height resolution. Aircraft detection of CAT is flawless, but when one is in it, it is already too late! Radars can detect turbulence in two ways. First, changes in the refractive index structure of the atmosphere, which are caused by turbulence, are revealed in the returned power profiles (analysis of the returned power for these purposes is one topic being studied by Michael T.

Moss in his dissertation research). A second method is simply the measurement of wind speed and direction and subsequent computation of wind shear.

Pilot reports of turbulence were assembled for the 416-hour period comprising both cases. Any pilot reports of light-to-moderate or stronger turbulence found within a 3-by-7 degrees of latitude box centered on Crown were logged. The box was oriented lengthwise, parallel to the mean wind direction, as determined by the hourly profiler observations.

Approximately 400 pilot reports were logged during the entire period and numerically classified from 1 to 6, in order of increasing severity. The altitudes of the aircraft, the turbulence strength and the wind shear were compared. For both cases there was excellent correlation between profiler-derived shear values and pilot reports of turbulence. Figure 4.32 (top) shows a coded scatterplot of all reports of turbulence during the second case study.

The observations of Colson (1969) are supported by this plot since a vigorous short wave passed above Crown at about the half-way point of case 2. The straight flow from the west and southwest was replaced by curved flow. At the same time the jet stream was pushed well to the south of the site after which it quickly returned north to its original position. The resulting curvature in the flow, along with strong horizontal wind shear, led to the dramatic increase in reported turbulence at all levels between the surface and
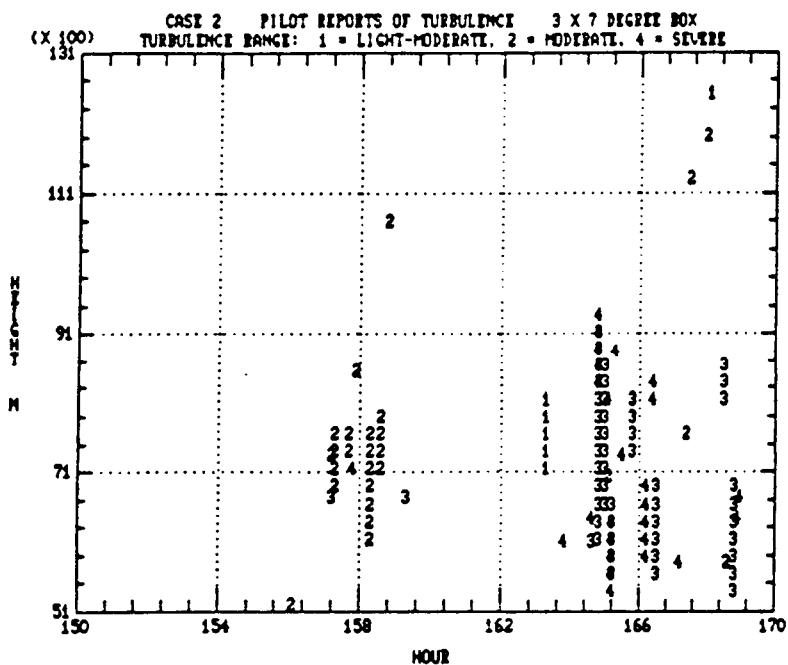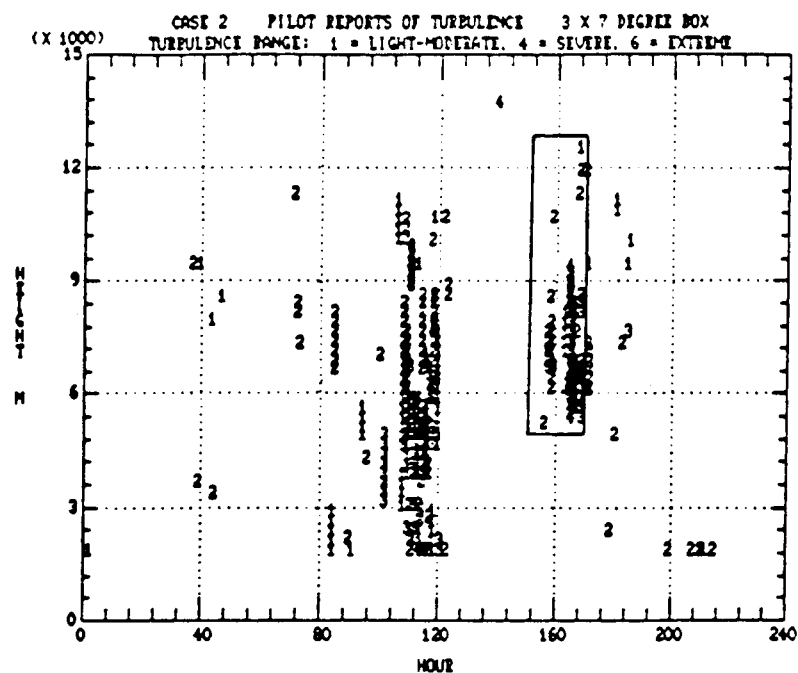
Figure 4.32. Pilot reports of turbulence during case 2. The bottom plot is a blowup of the boxed area of the top plot.

12 km. There were two reports of extreme turbulence during this time with one pilot reporting the worst turbulence he had ever seen in 20 years of flying and another (presumably the copilot) reporting, "Passengers in the aisles, pilot very upset."

An increase in reported turbulence near the end of the period was again the result of curvature and increased horizontal shear. At this time a long-wave trough was pushing over Crown from the west and the jet stream was making its final retreat to the south and east.

Figure 4.32 (bottom) shows a blowup of the second concentrated area of turbulence. Please note the different height scaling from the previous plot. Note (by comparing with figure 2.2d, page 31) that the reports were maximized in the region below the level of maximum wind. This observation is somewhat biased, however, because fewer aircraft fly at altitudes above the maximum wind level. The "vertical alignment" of the turbulence occured when pilots reported turbulence in a deep layer. If a pilot reported moderate turbulence during ascent from 15 to 20 thousand feet, a column of twos would be generated similar to the one depicted just after hour 158.

These observations suggest that a change in the flow pattern was apparently needed to trigger CAT. If the flow was straight there were almost no reports of turbulence, even if the maximum wind speeds approached 95 ms^{-1}.

Observations indicated that vertical shears were maximized
at times just before upper-level waves passed over the site.

Figure 4.33 shows the relationship between shear and Ri
at times when turbulence was reported. Notice that the
majority of observations occurred when shears were greater
than 4 ms^{-1}/500m and Richardson numbers were less than about
2. Notice also that Ri values never reached the
theoretically critical value of 0.25 until shears became
greater than 5 ms^{-1}/500m, but with even greater shears the
Richardson number often was greater than 1.

During 21 January, 1987, as a long wave trough
approached Crown, reports of turbulence rapidly increased,
as figure 4.32 (bottom) illustrates. Correlations between
the profiler-derived shears and reported turbulence were
excellent. Figures 4.34 through 4.36 show surface plots of
shear, high-resolution Ri, and low-resolution Ri plots for
this date. Regions in space and time where a turbulence
report was made are marked on the shear plots. Solid black
markings indicate moderate-to-severe or severe turbulence
and dotted sectors denote regions of light-to-moderate or
moderate turbulence.

The increase in shear that developed as the long wave
approached is shown (the maximum value in this smoothed plot
is about 9 ms^{-1}/500m) to be the primary region of
turbulence. Notice also the two turbulent sectors above the
level of maximum wind that correspond to a secondary shear
maximum.
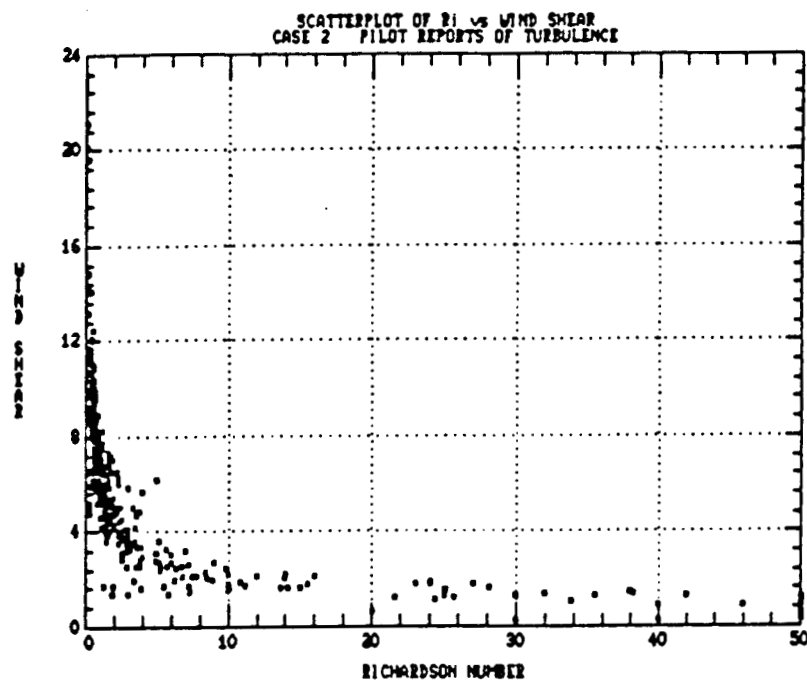
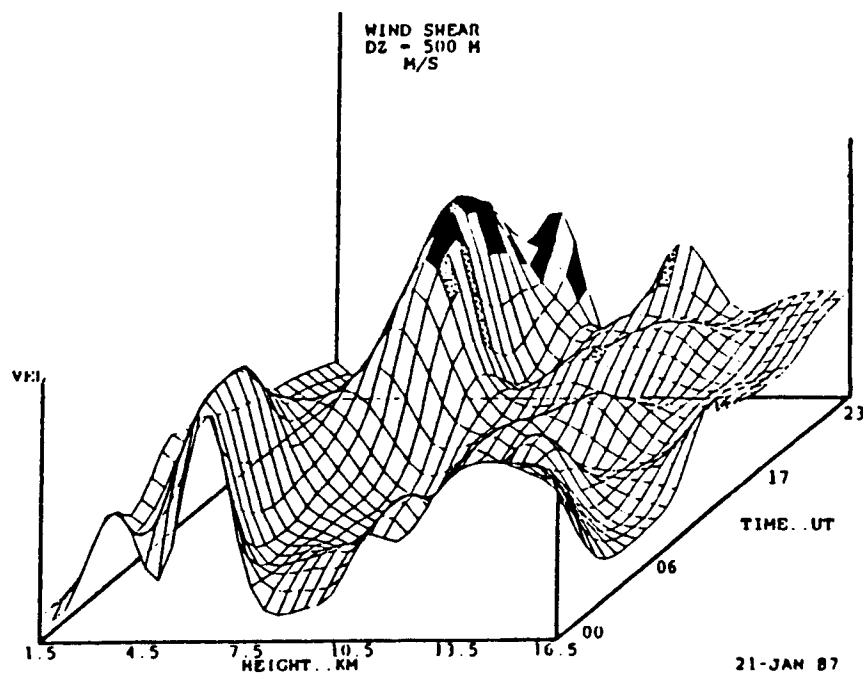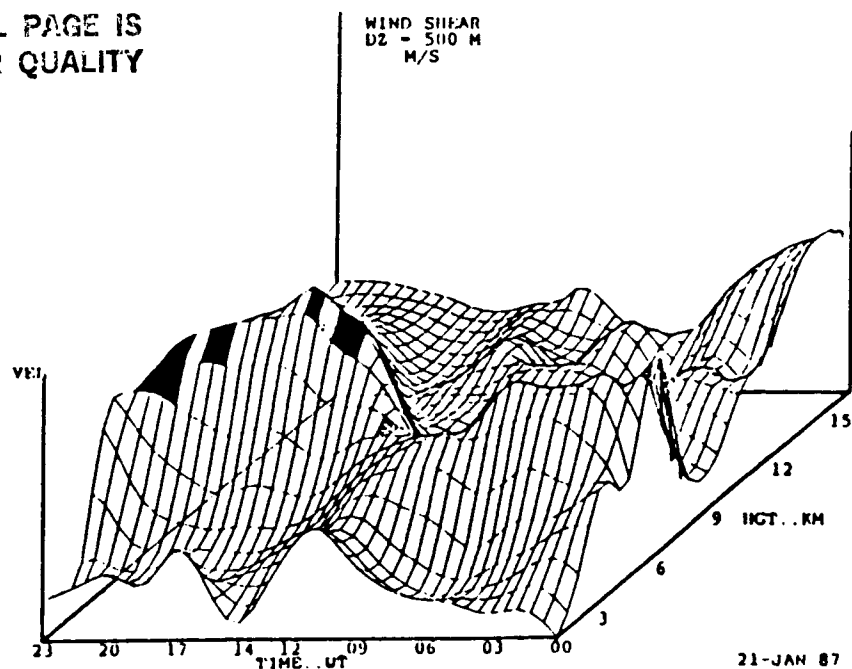Figure 4.33. Scatterplot of wind shear versus Richardson number during episodes of turbulence.

Figure 4.34.   Surface plots of wind shear above Crown
during 21 January 1987. The bottom figure is
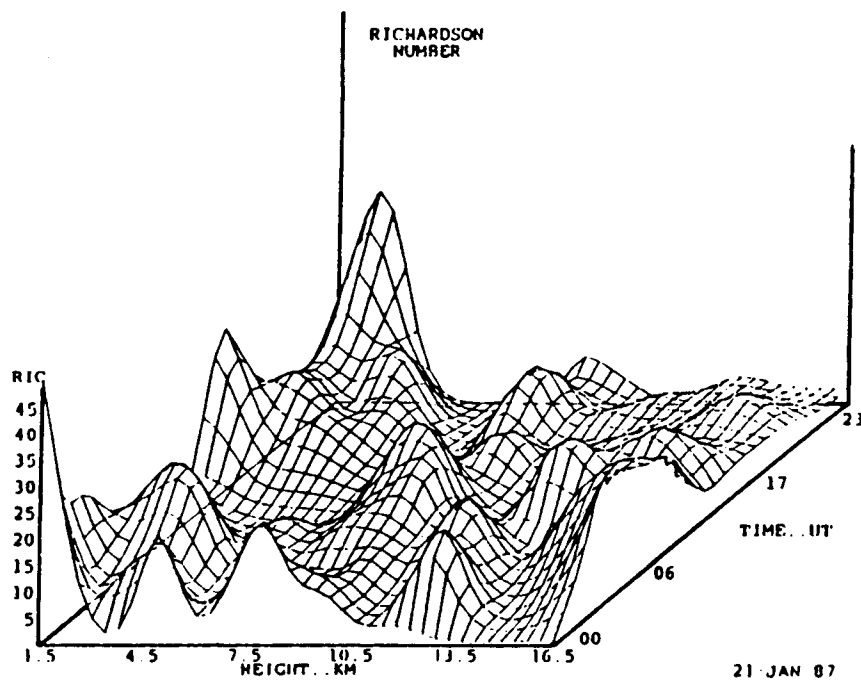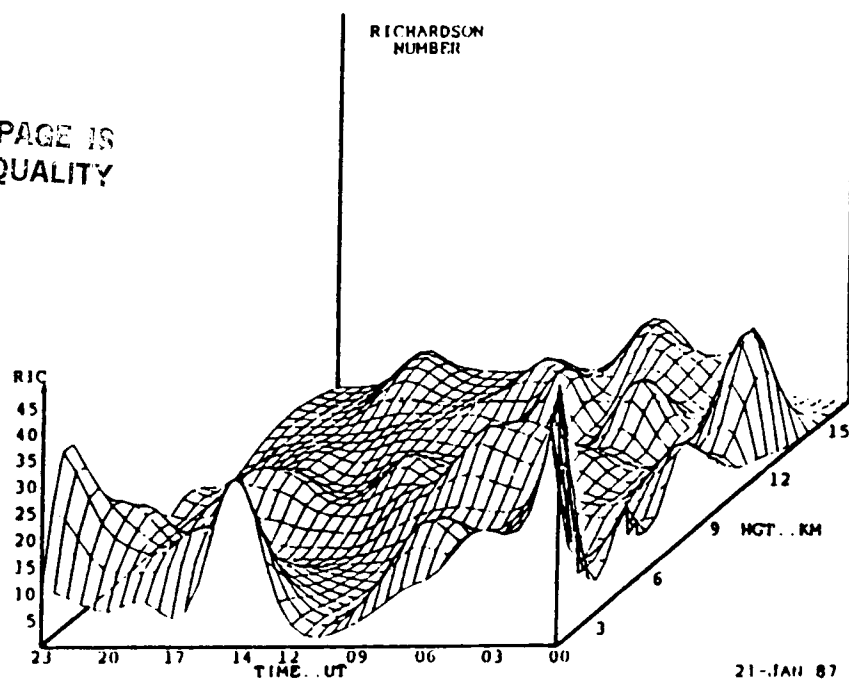a 90-degree rotation of the top figure.

Figure 4.35.   As in figure 4.34 but for 500-meter resolution
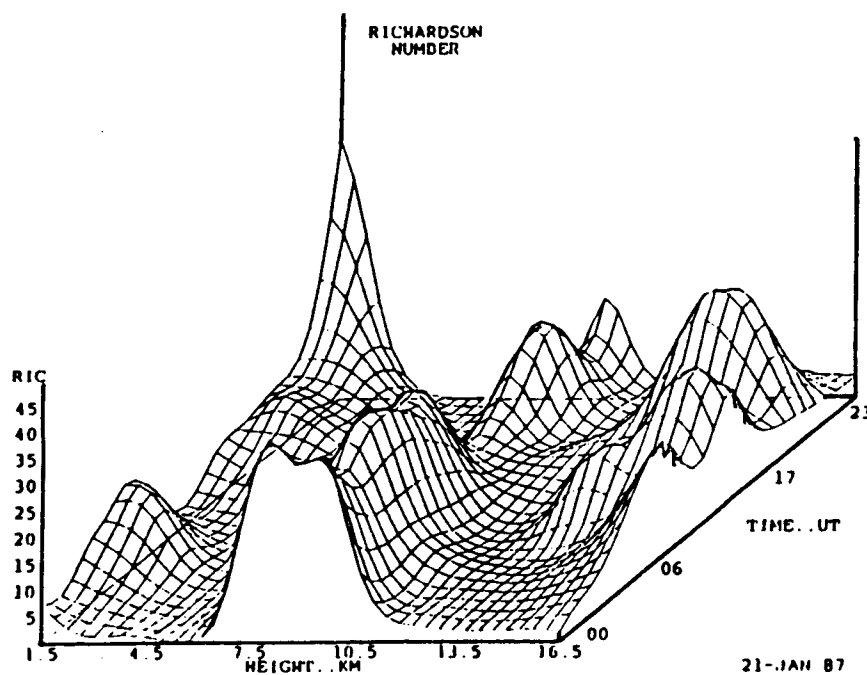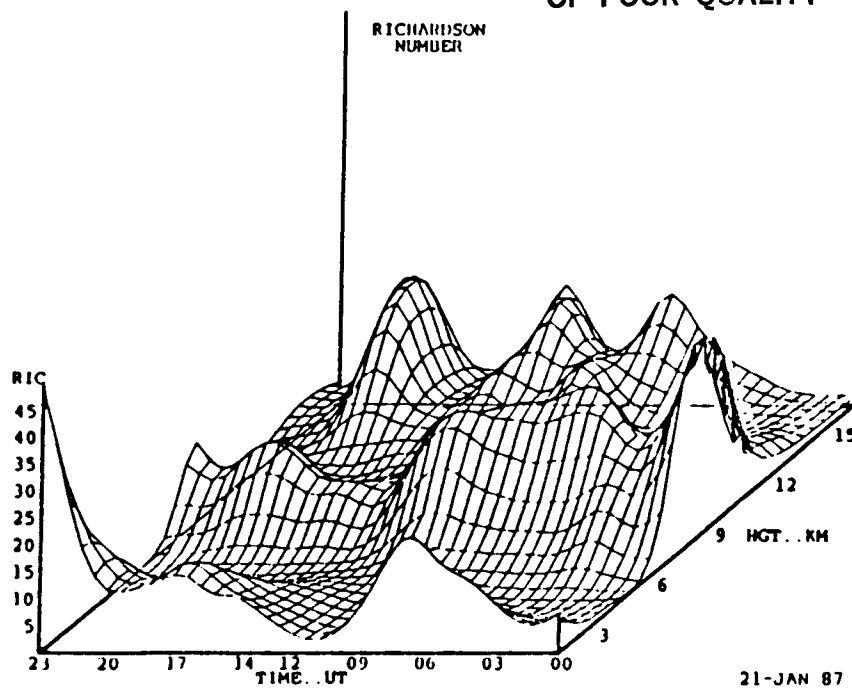   Richardson number.

Figure 4.36. As in figure 4.34 but for 2000-meter
resolution Richardson number.

The Richardson number plots show the previously discussed inverse relationship with shear. Note that the "valleys" of Ri correspond to the "peaks" in the shear plots. It is also evident that the low-resolution Ri plots more clearly show the large-scale features, such as the Ri increase at the level of maximum wind. Notice the increase in smoothness of the low-resolution plots and recall that the same smoothing was found in the mean profiles.

4.6 Energy Spectra of Hourly Data

Time series of the measurements of wind speed at 9870 and 6120 m MSL were further analyzed for each case. When each of the missing hours in case 2 was encountered, interpolation was performed to preserve temporal continuity. The upper level corresponded to the observed level of maximum wind during times when the jet stream was within 100 km of Crown, the lower altitude was chosen to represent the level of maximum shear. These heights were thus chosen to see if the energy distributions at these two levels would show any noticeable differences or other interesting features.

Figure 4.37 shows the wind speed versus time at these levels for each case. Note that while winds showed a gradual increase and then decrease during case 1, data from the second case showed two prolonged periods of strong winds (at 9870 m) that were surrounded by rapid and significant velocity dropoffs.
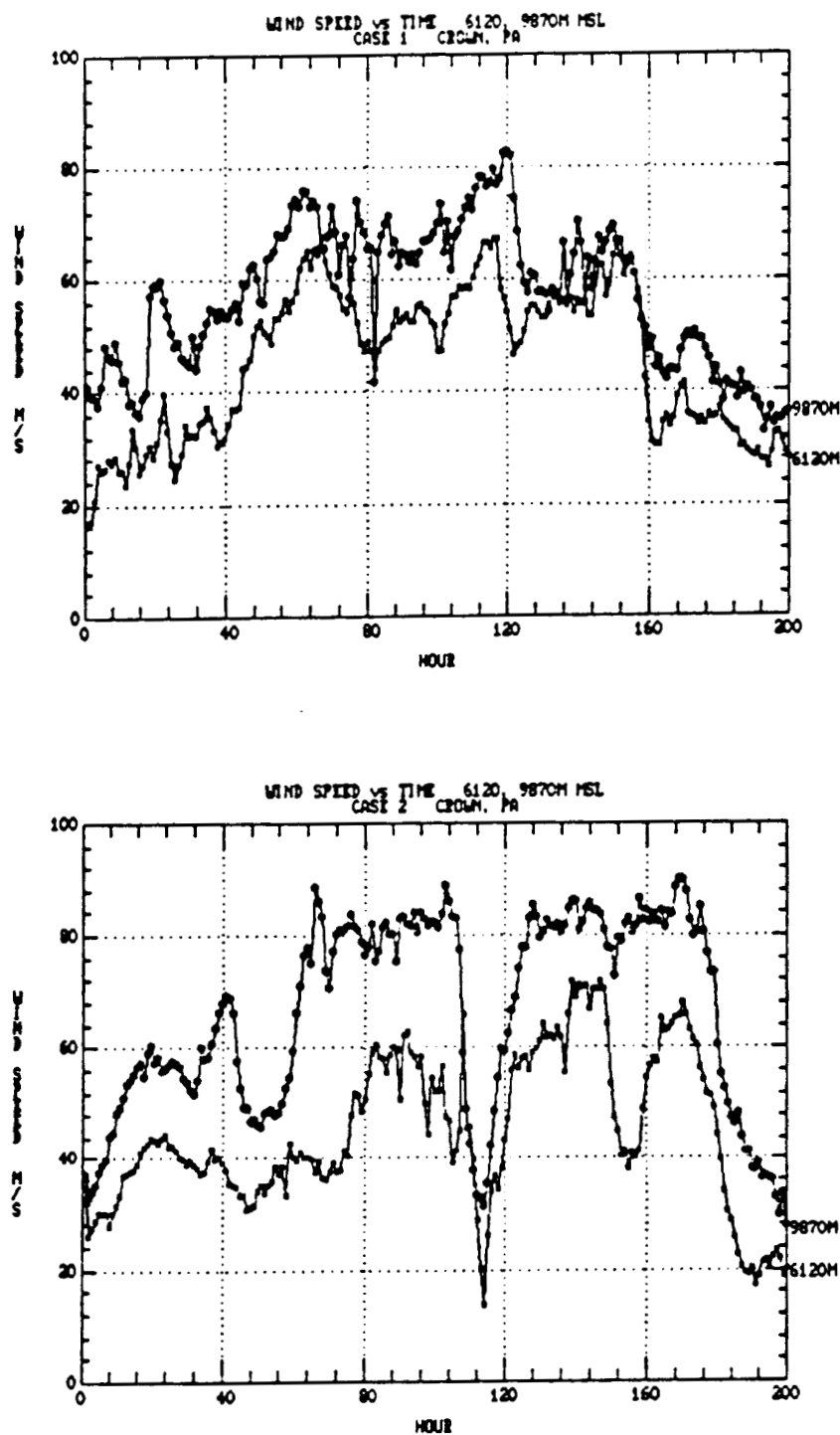
Figure 4.37. Wind speed versus time at 6120, 9870 m MSL
above Crown during cases 1 and 2,
respectively. Note that the first and last 8
hours of case 2 data were omitted for easier
comparison with data from the first case.

Spectrum analysis is useful because it shows how the variance of a quantity is distributed over different scales, frequencies, or eddy sizes. In this case, the variance of the wind speed was decomposed into contributions over a range of frequencies. Spectra of this type can afford considerable insight into important aspects of mid-atmospheric dynamics such as vertical coupling processes, instability mechanisms and the global circulation (Balsley and Carter, 1982).

From an observational point of view the mesoscale spectrum of motions provides the "noise" background against which all atmospheric wind measurements are interpreted. To observe representative synoptic-scale winds for input to numerical weather prediction models, it is essential to understand this noise background (Gage and Nastrom, 1985).

Figures 4.38 and 4.39 are power spectra obtained from hourly observations at the two chosen heights. Because Doppler radars measure the radial component of the wind, some assumptions must be made in order to infer horizontal winds, one of which is that the magnitude of the vertical velocity is negligible when compared to horizontal velocity. When spectra are computed for frequencies greater than about 10^{-4} Hz, vertical power spectral densities have been shown to be sufficiently close to oblique power spectral densities that the effect of vertical motions on the oblique spectrum must be taken into account (Balsley and Carter, 1982). Note that the time scale of the spectra ranges from 2 to 200
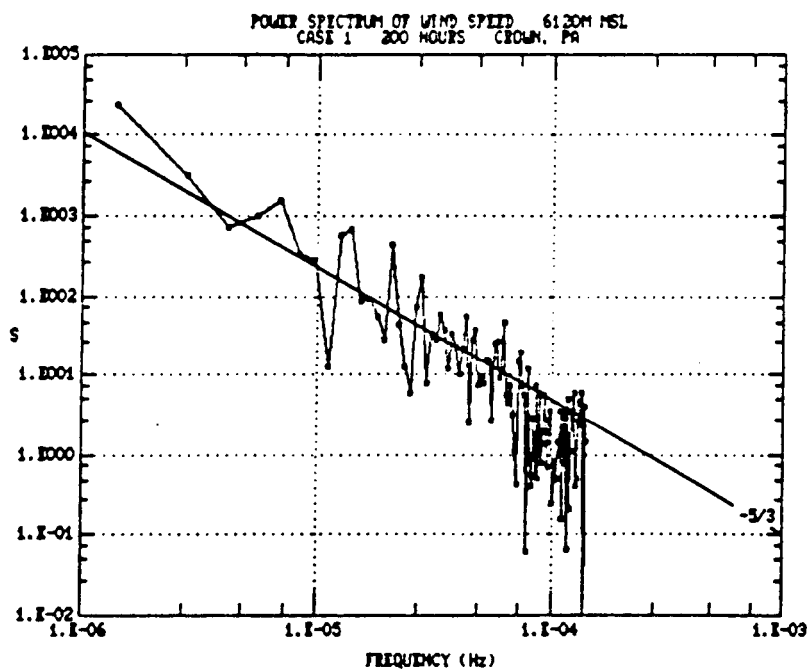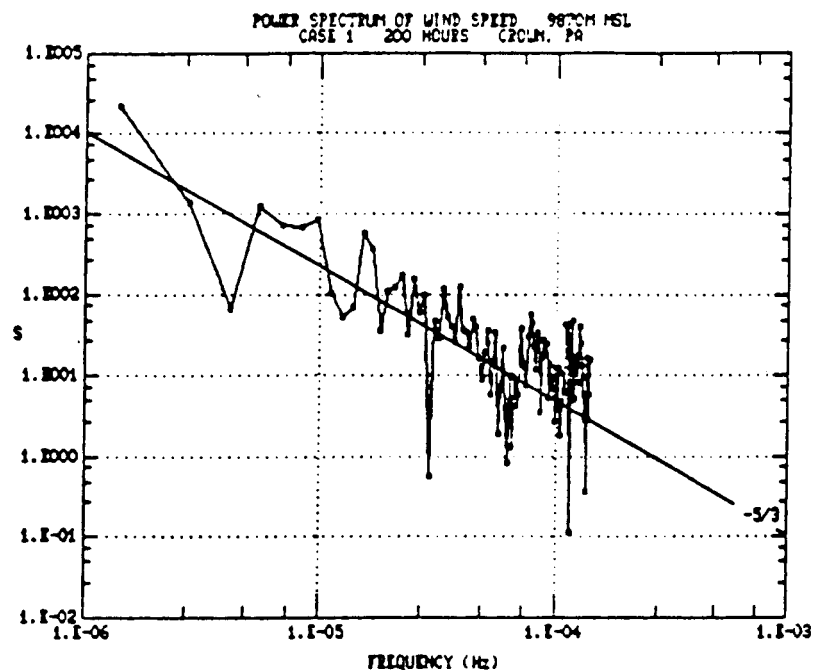
Figure 4.38. Power spectra of hourly wind speed at 9870 and 6120 m MSL during case 1 at Crown.
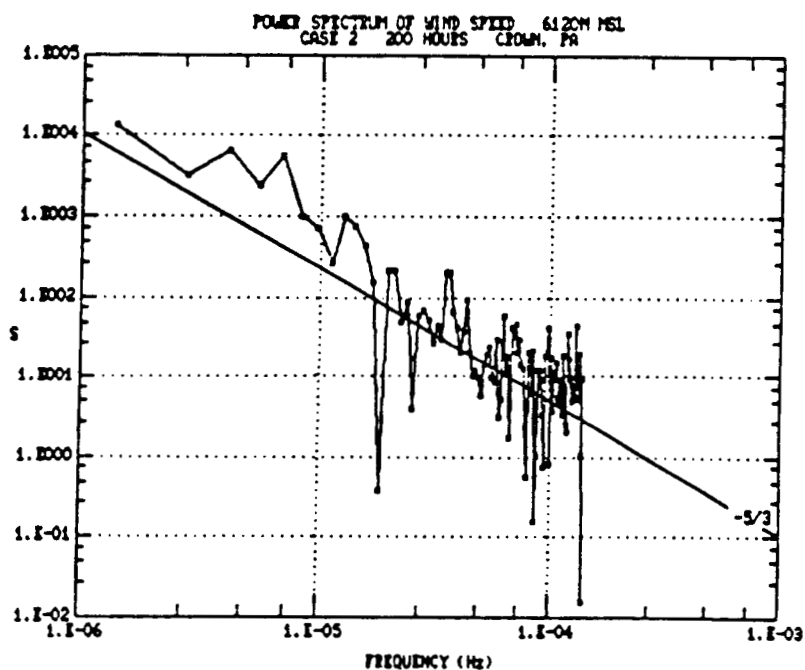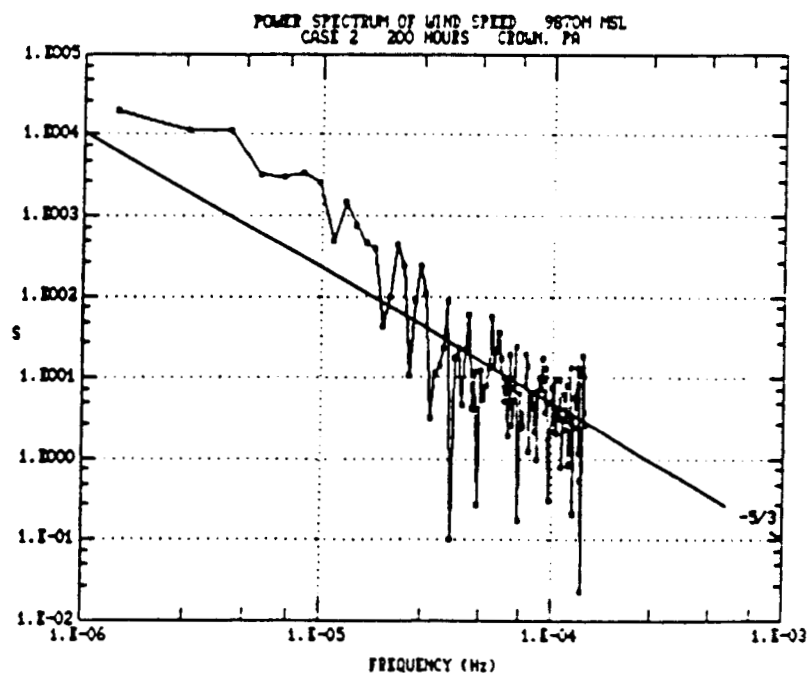
Figure 4.39. As in figure 4.38 but during case 2.

hours, thus we are examining turbulence at the meso- and synoptic scales.

Reports in the literature to date (see e.g. Panofsky and Dutton, 1984, fig. 8.2) have concentrated on microscale turbulence (periods of seconds). However, there have been several papers dealing with spectra obtained from "low-frequency" profiler data. Results from our study appear to agree quite well with other observations.

Balsley and Carter examined spectra over periods from 3 minutes to 8 days. They found a nearly straight-line fall off (log-log coordinates) of spectral density with decreasing period. Comparison between the straight line corresponding to a -5/3 power law dependence and the observed spectral slope was good over most of the frequency range. At frequencies greater than about 10^{-4} Hz there was a decrease in the absolute value of the spectral slope. It was determined, as stated above, that vertical motion contributed to this decrease. When corrections were made for vertical motions, the slope approached -5/3 for all frequencies down to the Brunt-Vaisala frequency.

The - 5/3 power law relation held for the data presented here for periods greater than about 3 hours, and then there was a leveling-off similar to that which Balsley and Carter reported. Based upon the findings of Balsley and Carter, it appears that contamination by vertical motions caused this decrease in slope. Figures 4.40 and 4.41 are the power spectra plotted in log-area preserving form (i.e.,
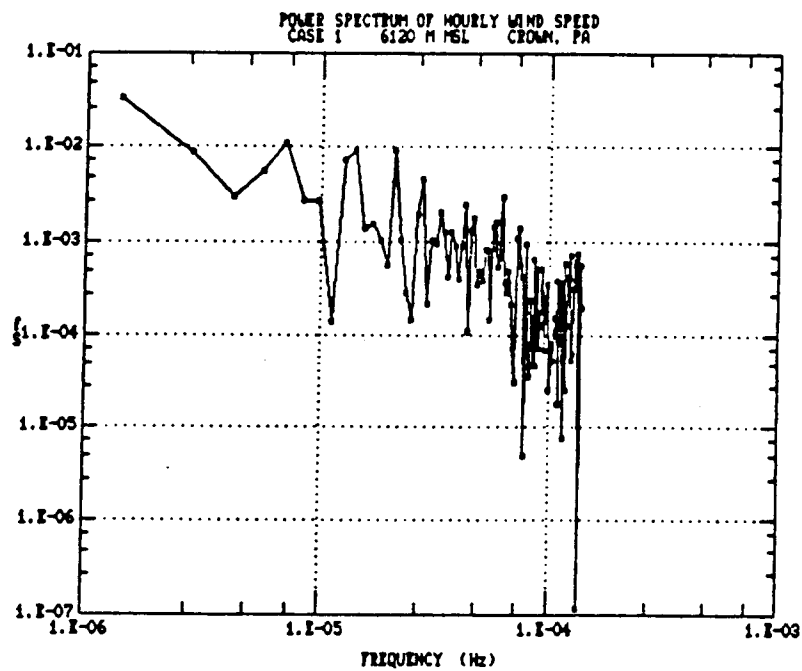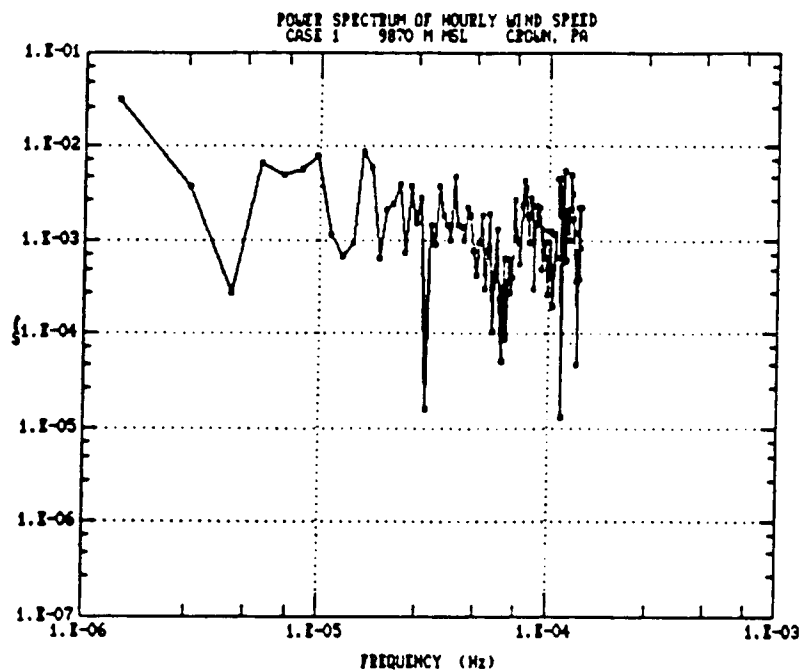
Figure 4.40.   As in figure 4.38 but the spectral density is
multiplied by the frequency.
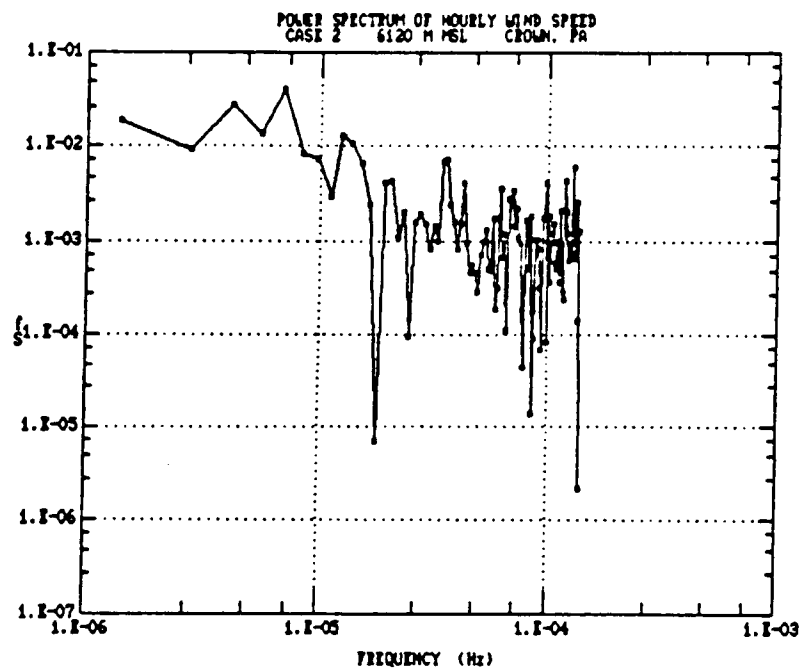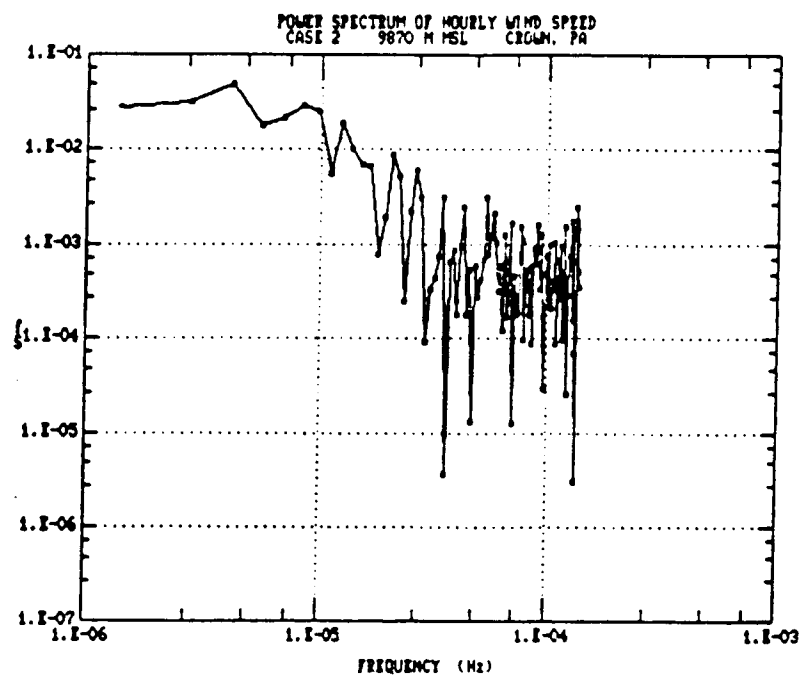
Figure 4.41.   As in figure 4.39 but the spectral density is multiplied by the frequency.

fS(f) vs. log(f)). Low-frequency peaks were found in these plots, as well as the decrease in slope at higher frequencies, especially evident in case 2 data. These peaks indicate dominant time scales on the order of three days. It was hoped that the upper-air maps would show wave features with similar time scales, but this did not appear to be the case. However, low-amplitude short waves of scales smaller than the resolution of the radiosonde network could have been present.

Gage (1979) suggested that the observed slope in the mesoscale energy spectrum is produced by two-dimensional turbulence, transferring energy upscale from inititially three-dimensional small scale sources such as convection, shearing instability and orography. The 3-d turbulence decomposes into a mixture of internal gravity waves and a quasi-two-dimensional non-linear flow which Lilly (1983) calls "stratified turbulence."

5.0 SUMMARY OF RESULTS

In section 4.1 we examined the performance of the 50 MHz wind profiler at Crown, Pennsylvania. Mean wind speed profiles obtained by the profiler during two jet stream occurrences were examined in the next section, and then compared to speed profiles obtained by Pittsburgh radiosondes during the same two jet stream passages. In section 4.3 wind shear statistics were examined. Section 4.4 included a comparison study between Richardson number values derived from data spaced at 500-meter intervals in the vertical to those obtained from data with a vertical resolution of 2000 meters. Richardson numbers were then compared to shear values. Pilot reports of turbulence were correlated with profiler-derived shears in the next section. Section 4.6 illustrated power spectra derived from hourly profiler data. The results obtained from these studies are summarized below.

5.1 Results and Conclusions

Radiosonde observations provided at best only 10 percent as much good data as the Crown profiler. There was a significant loss of balloon data at altitudes above 10 km during strong winds. At the altitudes of interest, gaps in the data were of the order of days for the Pittsburgh radiosonde and hours for the Crown profiler.

Cosmic interference was determined to be the major cause of 50-MHz profiler outages at high altitudes. The only jet stream-related data dropouts were due to a reduction in backscattered power resulting from the decrease in shear found at the level of maximum wind. Location relative to the jet stream and jet stream strength appeared to have little effect on profiler performance.

Observations of wind speed and wind shear indicated that radiosonde tracking difficulties during strong wind events such as jet stream passages lead to an overestimation of wind shear above the level of maximum wind. Profiler observations detected a level of maximum shear below the wind speed maximum, with lesser, but still significant, shears above.

Magnitudes of the measured shears increased as the jet stream approached the radar. Shear profiles computed from balloon data were very noisy, due to the small data sample size and probable tracking errors. Wind speed magnitudes determined by radar and radiosonde at the level of maximum wind were in good agreement, when the balloon data was available.

Richardson number estimates proved to be extremely resolution-dependent. This resolution dependence is responsible for an increase in the number of "critical" Ri observations as resolution is improved. Thus the magnitude of a "critical" Ri appears to be strongly dependent upon the data resolution. A critical value of about 1 was found for

500-meter resolution data, but there were many exceptions. Because of the dependence of Ri on the square of the shear, it was felt that the use of radar-derived shear statistics, and not Richardson number, would be best suited for applications to pilot reports of turbulence.

The relationships found between flow patterns and clear air turbulence were excellent. When flow was straight there were almost no pilot reports of turbulence, even during times when the maximum wind speed was nearly 100 ms^{-1}. But in the vicinity of curved flow, induced by both short- and long-waves, there were huge increases in the number of turbulence reports. The relationship between wind shear and reported turbulence was equally good. A critical shear value of about 5 ms^{-1}/500m was found for many of the turbulent reports. We believe that the consistency of profiler data, that is, the lack of meteorologically induced data dropouts and errors, will facilitate definition of critical shear values in the study of clear air turbulence.

Power spectra of the profiler wind speed observations obeyed a - 5/3 power law at frequencies above about 10^{-4} Hz. Area-conserving spectral plots indicated leveling off at low frequencies (synoptic scale) consistent with other observations (e.g., Lilly, 1983; Nastrom and Gage, 1985).

The observed slope is thought to be produced by two-dimensional turbulence (Gage, 1979), or "stratified turbulence" (Lilly, 1983), which developed from the decomposition of small scale, three-dimensional turbulence.

The most likely source of this small scale turbulence is shearing instability.

5.2   Suggestions For Future Research

The potential for future research is enormous. Several options exist, all of which have practical applications. The use of profiler networks will not be discussed, although an even greater potential for research exists with multiple-profiler derived data.

Comparison of profiler data with model-derived quantities such as divergence and vorticity has already begun at Penn State (Carlson, 1987). If further comparisons are required between balloon and profiler data, there should be a larger radiosonde database. This would reduce any bias in the data because of sample size. With a sufficiently large radiosonde data base, several-hour averaged profiler data (e.g., 5, 7, 9 or 11 hours), centered on radiosonde launch times, could be compared to balloon data. This would make the sample sizes relatively equal.

The further investigation of critical shear values in relation to clear air turbulence should be pursued. This research would require a data base large enough to include more pilot reports of turbulence above the level of maximum wind, more observations during times when the flow is curved, an assessment on the accuracy of pilot reports, and a determination of an optimum "radius of influence"; that is how far can profiler-observed conditions be extrapolated to

flow outside the sounding volume. The "radius of influence" problem is not trivial. As the radius is decreased, the correlation between turbulence reports and shear can be expected to increase, but the number of reports will also decrease. Two radii of influence were tested in this study. Both a 3-by-7 degrees of latitude box aligned with the mean wind and a 1-degree radius circle were tested. There appeared to be better agreement with the smaller radius of influence, but the data base was so depleted that the results became questionable.

The recent addition of a third beam to the Penn State wind profilers has made vertical velocity measurements possible. The effect of upward or downward motion on horizontal wind measurements can now be determined directly. Precipitation fall velocity distributions have already been computed by G. Forbes. Power spectra of vertical velocity can also be computed.

Further study of energy spectra is encouraged, based upon the agreement of the results obtained in this study with other published reports. Individual case studies can then be grouped into a climatology of frequency (or wavenumber) spectra, similar to that already done by Nastrom and Gage, 1985.

Measurement of the mesoscale variability of the jet stream is only one of the practical applications of wind profilers. The potential for the detection of clear air turbulence patches by determining critical wind shear values

should stimulate substantial further profiler-based
research.

BIBLIOGRAPHY

Augustine, J. A. and E. J. Zipser, 1987: The use of wind profilers in a mesoscale experiment. _Bull. Am. Meteor. Soc._, _68_, 4-17.

Balsley, B. B. and D. A. Carter, 1982: The spectrum of atmospheric velocity fluctuations at 8 km and 86 km. _Geophys. Res. Lett._, _9_, 465-468.

Balsley, B. B. and K. S. Gage, 1982: On the use of radars for operational wind profiling. _Bull. Am. Meteor. Soc._, _63_, 1009-1018.

Balsley, B. and V. L. Peterson, 1981: Doppler-radar measurements of clear air atmospheric turbulence at 1290 MHz. _J. Appl. Meteor._, _20_, 266-274.

Carlson, C. A., 1987: Kinematic quantities derived from VHF wind profilers. The Pennsylvania State University, Department of Meteorology, M. S. Thesis.

Campbell, S. D. and S. H. Olson, 1987: Recognizing low-altitude wind shear hazards from Doppler weather radar: an artificial intelligence approach. _J. Atmos. Ocean. Tech._, _4_, 5-18.

Colson, D., 1966: Nature and intensity of clear air turbulence. _National Air Meeting on Clear Air Turbulence_, Society of Automotive Engineers, New York, 1-4.

Colson, D., 1969: Clear air turbulence and upper level meteorological patterns. _Clear Air Turbulence and Its Detection_, Plenum Press, New York, 542 pp.

Colson, D. and H. A. Panofsky, 1965: An index of clear air turbulence. _Quart. J. Roy. Meteor. Soc._, _91_, 507-513.

Doviak, R. J., 1984: _Doppler Radar and Weather Observations_, Academic Press, Inc., Orlando, 458 pp.

Dutton, J. A., 1976: _The Ceaseless Wind_, McGraw-Hill, Inc., New York, 579 pp.

Dutton, J. A. and H. A. Panofsky, 1970: Clear air turbulence: a mystery may be unfolding. _Science_, _167_, 937-944.

Emanuel, K., 1984: Fronts and frontogenesis: other types of fronts. Lecture notes, 18 June.

Fairall, C. W. and R. Markson, 1985: Aircraft measurements of temperature and velocity microturbulence in the stably stratified free troposphere. Preprint Vol. Seventh Symposium on Turbulence and Diffusion, Nov. 12-15, 1985. Boulder, CO.

Frisch, A. S., B. L. Weber, R. G. Strauch, D. A. Merritt and K. P. Morgan, 1986: The altitude coverage of the Colorado wind profilers at 50, 405 and 915 MHz. J. Atmos. Ocean. Tech., 3, 680-692.

Gage, K. S., 1979: Evidence for a $k^{-5/3}$ law inertial range in mesoscale two-dimensional turbulence. J. Atmos. Sci., 36, 1950-1954.

Gage, K. S., 1983: Jet stream related observations by MST radars. Handbook for MAP Vol. 9, 12-21, SCOTSTEP Secretariat, University of Illinois, Urbana.

Gage, K. S. and B. B. Balsley, 1978: Doppler radar probing of the clear atmosphere. Bull. Am. Meteor. Soc., 59, 1074-1093.

Gage, K. S. and W. L. Clark, 1978: Mesoscale variability of jet stream winds observed by the Sunset VHF Doppler radar. J. Appl. Meteor., 17, 1412-1416.

Gage, K. S. and G. D. Nastrom, 1985: Evidence for coexisting spectra of stratified turbulence and internal waves in mesoscale atmospheric velocity fields. Seventh Symposium on Turbulence and Diffusion, 176-179, American Meteorological Society, Boston.

Gage, K. S. and G. D. Nastrom, 1986: Theoretical interpretation of atmospheric wavenumber spectra of wind and temperature observed by commercial aircraft during GASP. J. Atmos. Sci., 43, 729-740.

Haltiner, G. J. and R. T. Williams, 1980: Numerical Prediction and Dynamic Meteorology, John Wiley and Sons, New York, 477 pp.

Keller, J. L., 1981: Prediction and monitoring of clear-air turbulence: an evaluation of the applicability of the rawinsonde system. J. Appl. Meteor., 20, 686-692.

Kennedy, P. J. and M. A. Shapiro, 1975: The energy budget in a clear air turbulence zone as observed by aircraft. Mon. Wea. Rev., 103, 650-654.

Kennedy, P. J. and M. A. Shapiro, 1980: Further encounters with clear air turbulence in research aircraft. J. Atmos. Sci., 37, 986-993.

Larsen, M. F., 1983: The MST radar technique: a tool for investigations of turbulence spectra. _Handbook for MAP Vol. 9_, 250-255, SCOTSTEP Secretariat, University of Illinois, Urbana.

Lederer, J., 1966: Economic aspects of flight in turbulence. _National Air Meeting on Clear Air Turbulence_, Society of Automotive Engineers, New York, 35-39.

Lilly, D. K., 1983: Mesoscale variability of the atmosphere. _Mesoscale Meteorology- Theories, Observations and Models_, 13-24, D. K. Lilly and T. Gal-Chen, eds. D. Reidel Publishing Company, Dordrecht, Holland, 781 pp.

Lindzen, R. S., 1974: Stability of a Helmholtz velocity profile in a continuously stratified, infinite Boussinesq fluid- applications to clear-air turbulence. _J. Atmos. Sci._, _31_, 1507-1514.

Miller, A. L., 1985: A skew T for McAlevy's Fort, PA. The Pennsylvania State University, Research Paper.

Moore, R. L. and T. N. Krishnamurti, 1966: A theory of generation of clear air turbulence. _National Air Meeting on Clear Air turbulence_, Society of Automotive Engineers, New York, 13-27.

Munn, R. E., 1966: _Descriptive Micrometeorology_, Academic Press, New York, 245 pp.

Nastrom, G. D. and K. S. Gage, 1985: A climatology of atmospheric wavenumber spectra of wind and temperature observed by commercial aircraft. _J. Atmos. Sci._, _42_, 950-960.

Nastrom, G. D., K. S. Gage and W. L. Ecklund, 1986: Variability of turbulence, 4-20 km, in Colorado and Alaska from MST radar observations. _J. Geophys. Res._, _91_, 6722-6734.

Palmen, E. and C. W. Newton, 1969: _Atmospheric Circulation Systems: Their Structure and Interpretation_, Academic Press, New York, 603 pp.

Panofsky, H. A. and J. A. Dutton, 1984: _Atmospheric Turbulence_, John Wiley and Sons, New York, 397 pp.

Reiter, E. R., 1963: _Jet Stream Meteorology_, University of Chicago Press, Chicago, 515 pp.

Reiter, E. R., 1966: Clear air turbulence: problems and solutions (a state-of-the-art report). National Air Meeting on Clear Air Turbulence, Society of Automotive Engineers, New York, 5-12.

Röttger, J., 1983: Interpretation of radar returns from clear air- discrimination against clutter. Handbook for MAP Vol. 9, 114-119, SCOTSTEP Secretariat, University of Illinois, Urbana.

Ruster, R. and P. Czechowsky, 1980: VHF radar measurements during a jetstream passage. Radio Sci., 15, 363-369.

Shapiro, M. A., T. Hample and D. W. Van deKamp, 1984: Radar wind profiler observations of fronts and jet streams. Mon. Wea. Rev., 112, 1263-1266.

Strauch, R. G., K. B. Earnshaw, D. A. Merritt, K. P. Moran and D. W. Van deKamp, 1983: Performance of the Colorado wind-profiling network. Handbook for MAP Vol. 14, 38-48, SCOTSTEP Secretariat, University of Illinois, Urbana.

The Microwave Engineers' Handbook and Buyers Guide, 1965. T. S. Saad, ed., Horizon House, Dedham, MA, 392 pp.

Thomson, D. W., C. W. Fairall and R. M. Peters, 1983: Network ST radar and related measurements at Penn State University: a progress report. Handbook for MAP Vol. 14, 350-355, SCOTSTEP Secretariat, University of Illinois, Urbana.

Uccellini, L. W., K. F. Brill, R. A. Petersen, D. Keyser, R. Aune, P. J. Kocin and M. desJardins, 1986: A report on the upper-level wind conditions preceding and during the shuttle Challenger (STS 51L) explosion. Bull. Am. Meteor. Soc., 67, 1248-1265.

VanZandt, T. E., K. S. Gage and J. M. Warnock, 1981: An improved model for the calculation of C_n^2 and E in the free atmosphere from background profiles of wind, temperature and humidity. Preprint Vol.: 20th Conference on Radar Meteorology, Boston, 129-135.

Weinstock, J., 1980: A theory of gaps in the turbulence spectra of stably stratified shear flows. J. Atmos. Sci., 37, 1542-1549.

Woods, J. A., 1972: Satellite radiance gradients and clear air turbulence. The Pennsylvania State University, Department of Meteorology, Ph.D. Thesis, 79 pp.